virucidal nanomaterials against influenza

Thèse N° 9114

Présentée le 8 mars 2019

à la Faculté des sciences et techniques de l'ingénieur
Laboratoire des nanomatériaux supramoléculaires et interfaces - Chaire Constellium
Programme doctoral en science et génie des matériaux

pour l'obtention du grade de Docteur ès Sciences

par

Özgün KOCABIYIK

Acceptée sur proposition du jury

Prof. A. Fontcuberta i Morral, présidente du jury
Prof. F. Stellacci, directeur de thèse
Prof. M. Prato, rapporteur
Prof. L. Liz-Marzan, rapporteur
Prof. J. Fellay, rapporteur

2019

ÉCOLE POLYTECHNIQUE
FÉDÉRALE DE LAUSANNE

Acknowledgments

First of all, I am grateful to Francesco. He always believed in me, contributed to my career development so much. He has been like a father to all of us, rather than a boss. I feel very lucky to have him as my advisor.

When I was doing my master at EPFL, I learned a lot about colloids from Javier Reguera, organic chemistry from Stephen Schrettl and Caroline Sugnaux. The knowledge I gained from them helped me very much during my phd thesis.

Thanks to Valeria Cagno, I almost became a virologist. It was great that we always worked in harmony together. I also would like to thank to Caroline Tapparel for advises and for accepting me in her lab. Thanks to Ronan Le Goffic, who performed the in-vivo experiments, my thesis became much more prestigious. Special thanks to Nicholas Dorma who brought me a lot of luck from Italy and introduced me to the world of virology. It was also a great pleasure to work with Matteo, Rosie and Matej in the bio-lab. I will miss our interesting discussions about nano-bio world. Besides my colleagues, I am grateful to Sam and Nikea, they changed the fate of my project.

I spent more than seven years in Lausanne. Thanks to my friends and colleagues, I skipped adult lifestyle during these years. We had very cheerful days together, great Sat and Zelig evenings and delicious BBQs. During my first years, it was great to be with my friends from university in Lausanne: Gozde, Gorkem and Mete. I am missing those days so much. Big thanks to Anna Dalmau, Louis, Gian-Luca and Andi for after-work drinks and great company. Riccardo, Ghil, Hale, Jose, Guiseppe, Andreana, Jessica and Thibault made me forget that my family was far away… We always had great discussions and fresh lab gossips with our morning coffee team in sunmil: Elif, Ahmet, Ula, Pelin, Evi and Nikos. I will miss you guys!

Lastly, I am grateful to my parents and my sister. I feel very strong because of the huge support they give me…

Abstract

Influenza affects millions of people in all parts of the world. The fact that influenza virus can spread through air increases the chance of influenza outbreaks. There are 3 to 5 million severe cases of influenza resulting in 290,000 to 650,000 deaths every year. Not as common as outbreaks, but in the 20th century four influenza pandemics appeared: Spanish influenza (1918, 50 million deaths), Asian influenza (1957, 2 million deaths), Hong Kong influenza (1968, 1 million deaths) and swine influenza pandemic (2009, 150,000 to 500,000 deaths). World health organization (WHO) emphasizes that influenza is the only pathogen that has a reasonable chance of causing a new pandemic in the near future. It is unlikely that current influenza vaccines and therapeutics will be sufficient to prevent a coming pandemic.

Presented within this thesis is a novel approach to irreversibly inhibit influenza virus with non-toxic and highly effective nanomaterials. These nanomaterials are designed so to bear glycan end-groups that bind to the influenza virus with high-affinity. Their design is such that binding determines a chain of events that leads to the irreversible loss of viral infectivity (*i.e.* virucidal mechanism). There are two key elements in the design of these materials. The first is the correct glycan sequence, terminating with sialic acid, needed to bind with high affinity to the influenza virus attachment ligand that is hemagglutinin. The second is a certain hydrophobic content in the drug, needed to impart the irreversibility in the antiviral effect. We show that when both elements are present, a virucidal non-toxic drug can be achieved either with gold nanoparticles or with cyclodextrins.

With these materials several human influenza strains of type A and B were inhibited with virucidal mechanism. Furthermore, ex-vivo and in-vivo antiviral activity of the nanomaterials with cyclodextrin core was investigated against a very aggressive influenza A strain. Ex-vivo studies clearly demonstrated that the mechanism of inhibition is virucidal. In the in-vivo studies, nanomaterials prevented the mice to

loose weight and body temperature; significantly reduced the virus concentration in the lungs and in the nose. These materials can be further developed to target animal strains of the influenza virus. This is particularly important since influenza pandemics usually appear when humans are infected with a new animal strain such as avian and swine influenza.

Keywords: influenza, nanomaterials, virucidal, irreversible inhibition

Résumé

La grippe touche des millions de personnes à travers la planète. Le fait que la grippe puisse se propager par l'air augmente les risques d'épidémie. Chaque année, ce sont plus de 3 à 5 millions de cas sévères de grippe qui sont reportés, causant de 290 000 à 650 000 morts. Au cours du 20ème siècle, pas moins de quatre épidémies majeures de grippe ont eu lieu : la grippe espagnole (1918, 50 millions de morts), la grippe asiatique (1957, 2 millions de morts), la grippe Hong-Kongaise (1968, 1 million de morts), et la grippe porcine (2009, 150 000 à 500 000 morts). L'Organisation Mondiale de la Santé (OMS) souligne que la grippe est le seul pathogène qui a des chances de causer de nouvelles épidémies dans l'avenir. Il est improbable que les vaccins actuels contre la grippe ainsi que les thérapeutiques établies suffisent pour empêcher une prochaine épidémie.

Dans cette thèse, une nouvelle approche pour inhiber irréversiblement le virus de la grippe par le biais de nanomatériaux efficaces et non toxiques. Ces nanomatériaux sont conçus pour porter des terminaisons à base de glycane, qui se fixent au virus de la grippe avec une excellente affinité. De part leur structure, cette étape de fixation engendre par la suite une chaîne d'évènement qui conduit à une perte irréversible de l'infectiosité virale (i.e. mécanisme virucide). Deux éléments sont clés dans la conception de ces nanomatériaux. D'une part, il est nécessaire de synthétiser une séquence de glycane, particulière se terminant par de l'acide sialique, nécessaire pour se fixer avec une grande affinité à l'hémagglutinine, ligand d'attache du virus grippaire. D'autre part, un contenu hydrophobe au sein du médicament est nécessaire afin d'assurer l'irréversibilité de l'effet antiviral. Nous démontrons que, lorsque les deux éléments sont réunis, un médicament virucide non-toxique peut être obtenu soit grâce à des nanoparticules d'or ou bien par le biais de cyclodextrine.

A l'aide de ces nanomatériaux, plusieurs souches de grippe humaine de type A et B sont inhibées par un mécanisme virucide. L'activité antiviral *in-vivo* et *ex-vivo* des

nanomatériaux avec cyclodextrine est étudié contre une souche de type A particulièrement agressive. Les études *ex-vivo* démontrent clairement que le mécanisme d'inhibition est virucide. Lors des études *in-vivo*, les nanomatériaux permettent d'empêcher une perte de poids ainsi que de température corporelle à une population de souris, tandis que la concentration en virus est largement réduite dans leurs poumons et leur nez. Ces matériaux peuvent être adaptés pour cibler des souches animales du virus de la grippe. Ceci est particulièrement important car les épidémies de grippe apparaissent lorsque les humains sont infectés par de nouvelles souches animales tels que la grippe aviaire ou porcine.

Mots-clefs : Grippe, Nanomatériaux, virucide, inhibition irréversible.

List of Abbreviations

C6	6-hexadecenoic acid
C11	11-dodecenoic acid
C14	14-pentadecenoic acid
C15	16-mercaptohexadecanoic acid
EC_{50}	Half maximal effective concentration
EC_{90}	Ninety percent effective concentration
EC_{99}	Ninety-nine percent effective concentration
HA	Hemagglutinin
HSPG	Heparan sulfate proteoglycan
ICC	Immuno cytochemical
MUA	11-mercapto undecanoic acid
MUS	11-mercaptoundecane sulfonate
NMR	Nuclear magnetic resonance spectroscopy
NM	Nanomaterial
NP	Nanoparticle
OT	1-octanethiol
PEG8	1-mercapto-3,6,9,12,15,18,21,24-octaoxaheptacosan-27-oic acid
PEG4	1-mercapto-3,6,9,12-tetraoxapentadecan-15-oic acid
SA	Sialic acid
TEM	Transmission electron microscopy
TGA	Thermogravimetric analysis
6'SLN	6-Sialyl-N-acetyllactoseamine
β-CD	Beta cyclodextrin

Table of Contents

CHAPTER 1

Scope of the Thesis and the Extended Synopsis

Viruses are our selfish life partners. Moderately selfish ones reproduce a few billion copies, make us a little sick and leave our bodies in a few days. Occasionally they come back, and the cycle continues. Markedly selfish ones alter our genes, travel with us from Europe to America and meet new hosts, make us very sick and eventually kill us. The immune system is our superhero that protects us against viruses. However, when our superhero is late or the danger is severe, we end up taking antiviral drugs.

Current antiviral drugs are virustatics that are designed to suppress the viral replication process. They interfere with one step in the viral replication process and prevent the virus from reaching high concentrations. Virucides (virucidal drugs) that inactivate the virus particle with limited host toxicity are not currently used to treat viral infections. Indeed, these types of drugs that fight against bacteria have been in therapeutic use for many years. For instance, Penicillin is a bactericide, which leads to lysis of the bacteria. It is well known that Penicillin has saved millions of lives since the early 20th century.

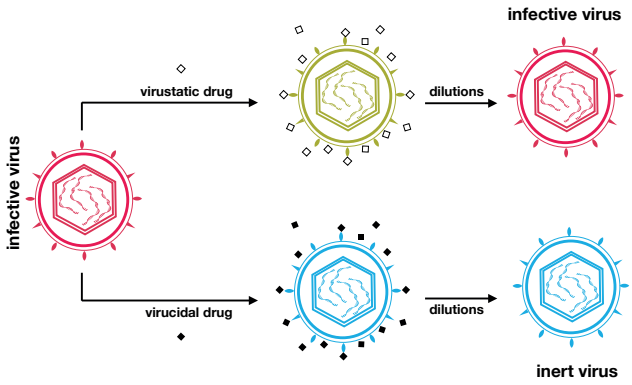

Figure 1.1: Virucidal drugs permanently inactivate the virus. The difference between the virucidal and virustatic inhibition mechanism is clearly observed upon dilution of the virus-drug complex

There is a need for broad-spectrum antiviral drugs that inhibit viruses with virucidal mechanism despite viral mutations (figure 1.1). This type of drugs is particularly important to fight against viral mutations as well as emerging viruses. It was previously demonstrated that MUS-OT NPs inhibit HSPG dependent viruses with virucidal inhibition mechanism. Sulfonate end-groups target conserved HSPG binding points of the virus, whereas the rigid hydrophobic spacers initiate deformations in the viral proteins. MUS-OT NPs successfully inhibited several HSPG binding viruses such as Herpes Simplex Virus 1 and 2 (HSV-1, HSV-2), Human Papilloma Virus (HPV), respiratory syndical virus (RSV) and lentivirus.

The objective of this thesis is translating the concept described above to the sialic acid targeting viruses. Unlike HSPG dependent viruses, sialic acid targeting viruses make distinctive interactions with the host-cell glycoproteins. Each virus prefers a different glycan arrangement involving sialic acid, for high affinity binding. Therefore, sialic acid alone may not be sufficient to target these viruses. A material design specific to the virus has to be done.

In the family of sialic acid targeting viruses, influenza affects the highest number of people in the world. People from all ages in the developed and developing world; even animals such as birds and pigs are affected by influenza. More importantly, influenza virus occasionally leads to pandemics.

Over the last 100 years influenza virus A H1N1 subtype caused two pandemics. The first one is Spanish influenza which caused 50 millions deaths in 1918 and the second one is 2009 swine influenza pandemic which caused around half million deaths. Despite the fact that influenza is a rapidly mutating virus, these two H1N1 strains targeted the same glycans on the host-cell receptors to start the infection.

Human upper respiratory track tissues are rich with glycans terminating with -2,6 linked sialic acids. Even though influenza virus rapidly mutates, sialic acid binding pockets of the hemagglutinin (HA) does not significantly change. If this part of the virus would mutate, the chance for successful infection would decrease. Therefore, the glycan array studies show that the majority of human influenza viruses bind to

glycans terminating with 6-Sialyl-N-acetyllactoseamine (6'SLN). 6'SLN trisaccharide was grafted onto nanomaterials (gold or β-cyclodextrin core) bearing a rigid spacer ligand (figure 1.2). Antiviral and virucidal activity of the modified nanomaterials against human influenza A and B viruses was then investigated. The nanomaterials with the gold core were synthesized in order to conduct structure-activity relationship. In the case of nanomaterials based on cyclodextrin scaffolds, the focus was complex biological assays since organic materials have a greater potential to become a drug. Ultimately, this thesis demonstrates how to design nanomaterials that irreversibly inhibit influenza and what is potential of nanomaterials to become a drug.

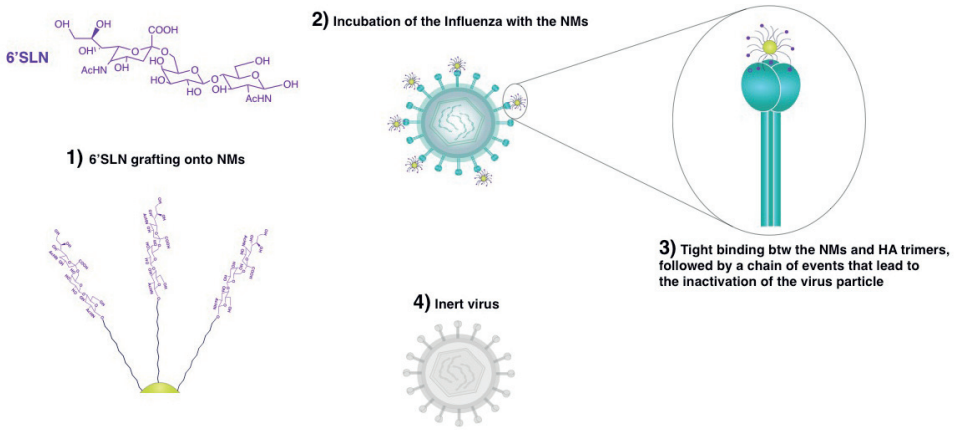

Figure 1.2: 6'SLN is the trisaccharide that binds to human influenza virus with high affinity. In order to irreversibly inhibit the influenza virus, Nanomaterials (NMs) based on gold or cyclodextrin scaffolds were modified with 6'SLN molecules. The tight binding between the HA trimers and NMs, followed by a chain of events lead virus to loose infectivity.

The thesis is divided into six chapters:

Chapter 2 starts with a brief introduction to viruses and antiviral drugs. The mechanism of inhibition of conventional drugs as well as the virucidal drugs is described. The chapter continues with the concepts of non-covalent interactions and multivalent interactions that are important for the virus-host interactions. The last topic of chapter 1 is antiviral materials that mimic the virus-host interactions. A detailed summary of previous antiviral materials targeting HSPG or sialic acid

dependent viruses is given. Possible mechanism of inhibition of these materials, virustatic or virucidal, is also discussed.

Chapter 3 is about influenza virus and how to design antiviral materials that irreversibly inhibit influenza virus. The characteristics, classifications as well as potential dangers of the influenza virus are described in detail. Following the background information on the influenza virus, previous glycan array studies on the influenza virus that demonstrates the glycan sequences providing high-affinity binding to influenza is discussed. Accordingly, 6-Sialyl-N-acetyllactoseamine (6'SLN) provides the high affinity binding to the majority of the human influenza viruses. Lastly, designing virucidal nanomaterials against human influenza virus in the light of glycan array studies is described.

In chapter 4, the experimental work on the 6'SLN coated gold nanoparticles that irreversibly inhibit influenza is described. It was shown that the density of the 6'SLN end-groups as well as the chemical structure of the spacer ligand is important on the inhibitory activity. In these studies, the optimum density of 6'SLN trisaccharide providing high-affinity binding is determined. The ideal spacer ligand that contributes to both binding and virucidal activity is also suggested.

Gold NPs showed virucidal activity against influenza A virus H1N1 and H3N2 strains as well as against influenza B virus. Apart from the virucidal activity, gold NPs are found to be non-toxic to cells and highly specific to influenza virus. There was no inhibitory activity against HSV-2 and enterovirus 68. In the beginning of this chapter, synthesis and experimental procedures are summarized. The methods to conduct NP characterization are also involved. Additional data on the characterization of NPs can be found in the **appendix A**.

Chapter 5 is about virucidal nanomaterials against influenza bearing a cyclodextrin core. Biodegradability of a material is very important for pharmaceutical applications. Therefore, the gold core was replaced with β-cyclodextrin so that the nanomaterials would have the potential to become a drug.

In this part, the importance of the spacer length on the inhibitory activity was investigated. It was found that sufficiently long spacer ligand is important for end-group flexibility. 6'SLN modified β-cyclodextrins without spacer ligands poorly inhibited influenza virus. On the other hand, 6'SLN modified β-cyclodextrins bearing a spacer ligand, showed a strong antiviral activity against human influenza strains. The mechanism of inhibition was determined to be virucidal, as it was the case for gold NPs.

The virucidal activity was also demonstrated with more complex biological assays such as ex-vivo and in-vivo. In the ex-vivo experiments, modified β-cyclodextrins reduced the virus concentration by several log units relative to non-treated controls. In the ex-vivo experiments modified β-cyclodextrins prevented the mice to loose weight and body temperature; significantly reduced the virus concentration in the lungs and in the nose. The experimental procedures as well as NMR characterization of cyclodextrin derivatives are given in the beginning of the chapter. The additional data on the characterization of modified β-cyclodextrins can be found in **appendix B**.

Chapter 6 summarizes the important conclusions of this thesis and what additional studies can be done in the near future. This thesis only covers human influenza strains and excludes avian influenza strains. However, avian influenza virus potentially leads to pandemics. Targeting the avian influenza strains such as H5N1 is suggested as the most straightforward yet important future study.

Overall, this thesis demonstrates that it is possible to design highly specific materials that irreversibly inhibit viruses. The concepts demonstrated here could be an inspiration to new studies that aim to irreversibly inhibit other HSPG or sialic acid targeting viruses.

CHAPTER 2

Antiviral Materials

Viruses are infectious organisms that use the machinery of the host-cells to replicate. The interaction of the viral ligands with the host-cell receptors is the first step of the viral replication process. This step involves many non-covalent interactions and plays a crucial role in the success of the viral replication process. Multivalent antiviral materials that mimic the interaction between the viruses and the host-cell receptors are the main topic of this chapter. The inhibition mechanisms and design principles will be discussed with several examples from literature. To give a background information, the chapter begins with a brief description of the whole viral replication cycle that ends up with the invasion of the host. It continues with antiviral therapeutics: their mechanism of action, advantages and limitations. Non-covalent interactions in the biological systems and the concept of multivalency are then introduced before the antiviral materials are discussed in detail.

2.1. Viruses and viral diseases

Viruses are infectious organisms that have evolved to replicate using the machinery of the living cells. They carry a genetic material, DNA or RNA, which starts the replication process inside the host-cell. The genetic material is protected by the capsid proteins. and in certain cases additionally with an envelope. The size of the viruses varies from a few nanometers to hundreds of nanometers, and enveloped viruses are usually larger in comparison to the non-enveloped viruses.

Although, the study of viruses has made great contributions to many research fields such as macromolecules, medicine and genetics, the main reason why viruses are

investigated is that they can be the source of diseases in humans, animals as well as plants (figure 2.1). Diseases start because the viruses lead to malfunctioning of certain cells as well as organs. Some well-known examples of the virus caused diseases are human immunodeficiency syndrome by HIV; chronic hepatitis and liver carcinoma by Hepatits B; enteric infection by poliovirus; smallpox by variola virus.

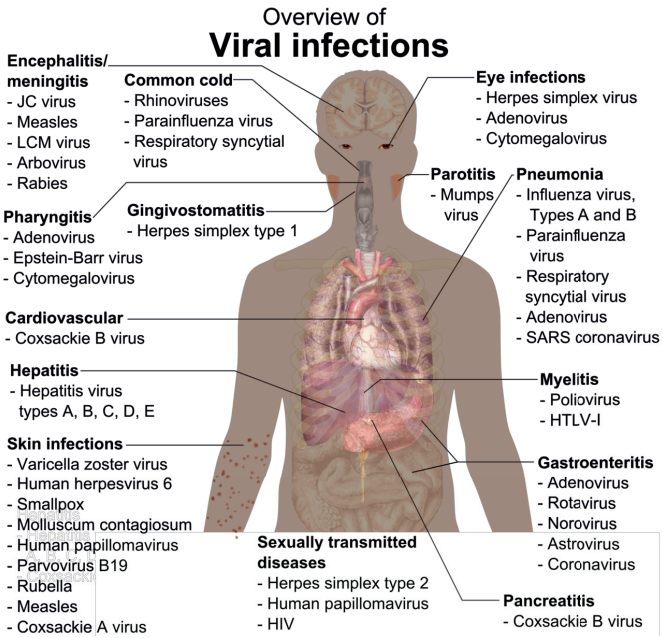

Figure 2.1: The summary of viral diseases that appear in humans. Copyright: Häggström, Mikael (2014)

The immune system protects humans and animals against viral diseases. During the course of a viral infection, foreign proteins (antigens) are recognized by B-cell (humoral) immunity and T-cell (cell-mediated) immunity. B-cell immunity detects and clears the virus particles, whereas T-cell immunity detects infected cells and induces apoptosis. However, the immune system alone is not sufficient to fight against severe viral infections. Vaccination provides protection against viral infections whereas antiviral drugs cure the viral infections.

2.2. How viruses invade the host?

The first step of the viral replication process is the attachment of the viral ligands onto the host-cell glycoproteins through non-covalent interactions. Majority of the viruses

have two attachment receptors on the host-cell surface: primary-receptor and entry-receptor. These receptors can be proteins, carbohydrates and lipids.[1] As a primary binding point, viruses commonly target either heparan sulfate proteoglycans (HSPG) or sialic acid moieties on the host-cell surface. For example, Herpes Simplex Virus (HSV), Human Papillomavirus (HPV), Human Immunodeficiency Virus (HIV) targets HSPGs; Rotavirus, influenza virus and enterovirus target sialiated glycans.

Once the virus binds to the primary-receptors, the interaction with the entry-receptors starts. In general, high affinity interactions (nM-μM) between the viral attachment proteins and its corresponding receptor lead to conformational changes in the viral proteins.[1] For instance, binding of HIV-1 to CD4 and CCR5 lead to conformational changes. The conformational changes on the viral proteins may facilitate the entry process.[2] Conversely, low affinity interactions (μM-mM) do not lead to any significant conformational changes.

Viruses enter into the host-cell via two main entry-routes: endocytic or non-endocytic. As a general rule, non-enveloped viruses are uptaken via endocytic route whereas enveloped viruses enter via membrane fusion. Exceptionally, some viruses with an envelope, such as influenza virus, can enter the host via endocytic route as well. Once the virus enters into the host-cell, cellular enzymes disassemble the capsid so that the genetic material is released to start the viral reproduction. Majority of the RNA viruses copy their genetic material in the cyctoplasm whereas DNA viruses in the nucleus. Following the transcription or translation of the genome, the viral proteins are synthesized and different parts of the virus assemble. Finally, the progeny virus leaves the host in order to infect new cells.

2.3. Conventional Antiviral Drugs and their mechanism of action

Antivirals are the most common type of medication to cure viral infections. They can be in the form of a small molecule (smaller than 900 Dalton and with a size in the order of 1 nm) or larger such as peptides, proteins and polysaccharides.[3–7] Most of the current antivirals are small molecules and suppress the viral reproduction, interfering one step in the viral replication process (figure 2.2). A viral replication process

involves seven steps that are: 1) virus attachment to the host-cell glycoproteins 2) entry via fusion or endocytosis 3) uncoating of the capsid, 4) transcription/translation of the genetic material 5) virion synthesis and assembly 6) release of the mature virus particle.

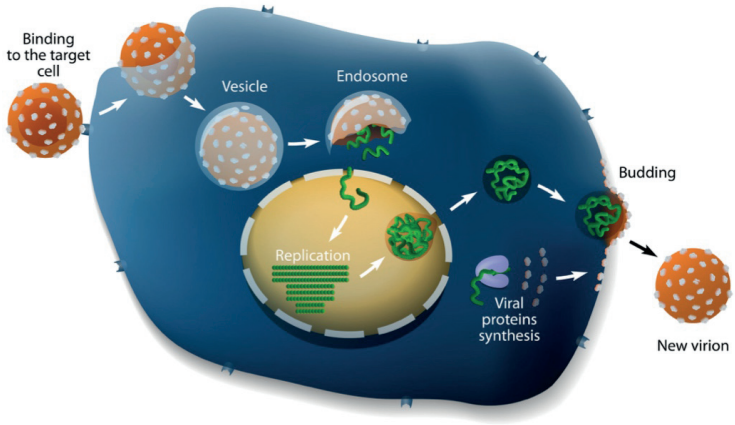

Figure 2.2: Illustration demonstrating the replication cycle of a virus particle. Viruses use the machinery of the host-cell in order copy the viral components. Once the replication process is complete, the virus progeny leaves the cell in order to infect new cells. Graphic copyright: designua.

For instance, Zanamivir, a neuraminidase inhibitor against influenza, targets the exit step so that the virus progeny cannot leave the host-cell to infect new cells. Azidothymidine (AZT) targets the transcription step of HIV virus, preventing the virus from synthesizing the viral genetic material. Antiviral drugs can function inside the cell (intra-cellular) or outside of the cell (extra-cellular) depending on which step of viral replication it targets.

In-vitro antiviral assays are the first step of investigating the efficacy of an antiviral drug. *Dose-response assays* are conducted by incubating a fix virus concentration with a varying dose of the antiviral. The antiviral concentration required inhibiting half (EC_{50}), 90% (EC_{90}) and 99% (EC_{99}) of the virus are determined with dose-response assays. The virus concentration to conduct the experiment is determined by multiplicity of infection (MOI) calculations, which is the ratio of virus particles to the number of cells. For longer infection durations (24h to 72h) smaller MOI values (0.05

to 0.1); for shorter infection durations (8h to 24h), larger MOI values (0.5 to 1) is convenient. There are several quantitative methods that can be followed to read-out a dose-response experiment. Plaque assay, focus-forming assay and end point dilution assays are some of the widely used methods to evaluate the results of a cell-based antiviral assay. Once the in-vitro antiviral assays are successful, the efficacy of the drug in tissues (ex-vivo) and in animals (in-vivo) is then tested.

2.4. Virucides: a sub-category of antiviral drugs

Virucides (virucidal drugs) are a sub-category of antivirals. Unlike traditional antivirals that suppress one step in viral replication process, virucidals deactivate or destroy the virus particle. Therefore, virucides irreversibly inhibit the virus particle. At first glance, virucidal drugs seem to be similar to the entry or fusion inhibitors. However, most of the entry/fusion inhibitors are *virustatic* and reversibly inhibit the virus.

Virucidal drugs deform the virus particles to different extent. They can alter the conformation of the viral proteins, which in turn lead viruses to loose infectivity. On the other extreme, virus particle can completely be destroyed. Although virucidal drugs are efficient to inactivate the virus particle, they are in general toxic to the host. Therefore, virucidals are currently used as disinfectants.[8] Bleach, acids and virkon are efficient virucides, but also highly toxic to the host.

Even tough virucidal drugs do not yet exist, drugs that irreversibly inhibit bacteria (bactericides) are very common. Penicilin, for example, is a bactericide, which leads the bacteria to lyse. It has been used as a medication to treat bacterial infections and do not have serious toxicity on the host.

Similarly, the ideal antiviral drug would be a virucidal drug that has limited host toxicity. Therefore, there is an ongoing research to synthesize non-toxic virucidal drugs.[9–11] For example, a protein called Cyanovirin-A is under investigation due to its virucidal activity on viruses such as HIV, HSV, RSV and enteric viruses.[11,12]

Cyanovirin-A interacts with the glycoproteins on the viral surface and on average 10,000 times more toxic to the virus in comparison to the host-cells.

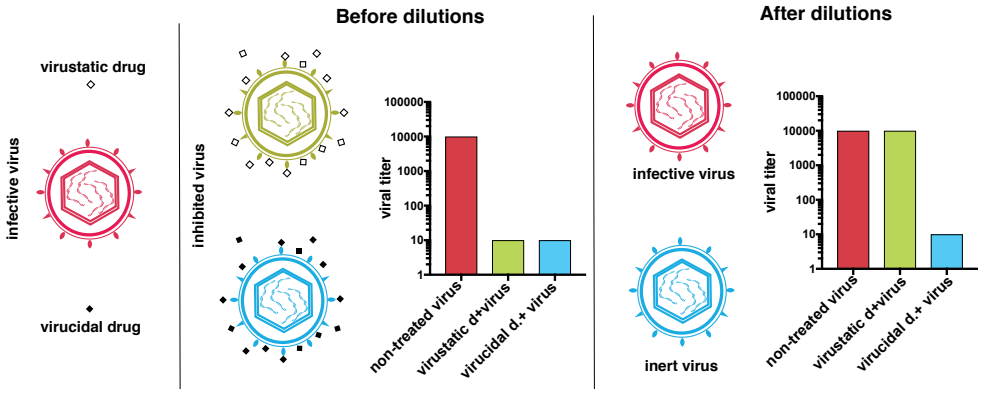

Figure 2.3: In order to find out if an antiviral drug is virucidal, virus-drug complex undergoes several dilutions following an incubation period. If the mechanism of inhibition is virucidal (irreversible inhibition), the virus is no more infective. If the mechanism is virustatic (reversible inhibition), the virus regains the ability to infect.

Dose-response assays do not show if a drug is virucidal or virustatic. In order to determine if the mechanism of inhibition is virucidal (irreversible), *virucidal assays* are conducted.[9,10] Before conducting the virucidal assay, *dose-response* assay should be conducted in order to determine the EC_{99} concentration of the antiviral drug. Virus and the antiviral are then incubated for a period of time, at the EC_{99} concentration of the antiviral. As a control, non-treated virus is incubated as well. Then the serial dilutions of the inoculum are conducted and transferred onto cells in a similar way to dose-response assays. Finally, the titer of the treated virus is compared to the non-

treated virus. A significant difference (at least 1 log unit) between the titers of the treated and non-treated virus indicates a virucidal effect. The bigger the difference, the stronger the virucidal effect is. If the inhibition mechanism is merely *virustatic*, then the infective virus reappears (figure 2.3). It is important to note that virucidal assays should always be conducted together with the toxicity assays. If the drug is toxic to host-cells while being virucidal, the results of the virucidal assay may not be reliable.

The reasoning behind this assay is that interaction between a drug and the virus is not possible upon significant dilutions since a large entropic penalty is paid for binding. If the infectivity of the virus disappears after dilutions, the virus probably became inert once incubated with the drug.

2.5. Non-covalent interactions in the biological systems

Non-covalent bonds are a type of chemical interaction that can be formed intermolecular or intra-molecular. Unlike covalent bonds, non-covalent bonds are not formed by electron sharing but the momentary charges form the bond. Therefore, they are in general weaker in comparison to ionic, covalent and metallic bonds.

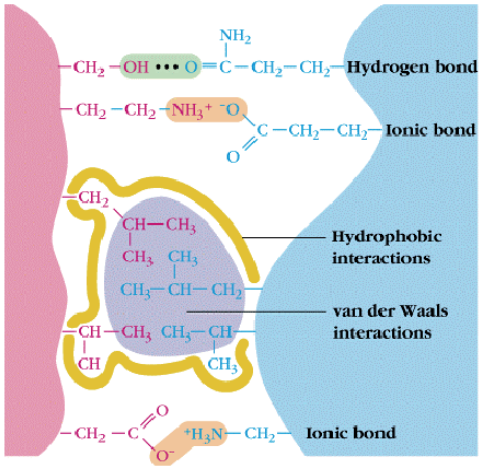

Figure 2.4: Examples of different non-covalent interactions between molecules. The interaction between biological macromolecules usually involves several types of non-covalent interactions. Graphic reproduced from Kim et al.[13]

Van der Waals forces, electrostatic effect (involves hydrogen bonding and ionic bonding), π-effect, and hydrophobic effect are different categories of non-covalent interactions (figure 2.4). A weak yet reversible bonding is formed by non-covalent interactions. Reversible nature of non-covalent interactions makes them important in the biological processes.[14] Non-covalent interactions hold two helices of DNA together; mediate protein folding and cell-to-cell communications; enable pathogens

to start the infection process. Multiple types of non-covalent bonds are simultaneously involved in the interaction between the biological macromolecules.

A non-covalent interaction involves the dynamic equilibrium of binding and unbinding reactions. Binding reaction is governed by the association constant (K_a) whereas its inverse, unbinding reaction, is governed by dissociation constant (K_d). Dissociation constant (K_d) is typically used to describe binding affinity in a non-covalent interaction. In a reaction where A_xB_y complex separates into x subunits of A and y subunits of B (equation1), the dissociation constant is described with the equation 2. Smaller K_d values represent a higher binding affinity (stronger interaction) whereas larger K_d values represent a weaker binding affinity. There are several methods to measure the K_d such as surface plasmon resonance (SPR), gel-shift assays, ELISA and spectroscopic assays.

$$A_x + B_y \rightleftharpoons A_xB_y \quad (1)$$

$$K_d = \frac{[A]^x[B]^y}{[A_xB_y]} \quad (2)$$

The weak nature of the secondary bonds is compensated by multivalent interactions.[15,16] Simultaneous binding of the multiple points enhances the non-covalent interactions by reducing the dissociation constant.[17] For instance, several binding sites are involved in the interaction between a viral ligand and the cell receptors. Once a ligand binds to the receptor, the binding chance of the next ligand increases due to spatial proximity. Dissociation then slows down as it involves multiple groups. The interaction between a multivalent ligand and a multivalent

receptor is considered “multivalent”. On the other hand the interaction between a monovalent ligand and multivalent receptor is not multivalent but “monovalent” (figure 2.5).[16] Multivalent interactions may involve identical or different groups.[16] Homo-multivalent interactions involve the identical binding groups, whereas hetero-multivalent interactions involve non-identical binding groups. The term

"multivalency" is often replaced with "polyvalency" when the binding sites are numerous (>>10).[16] Indeed, many biological interactions are polyvalent.

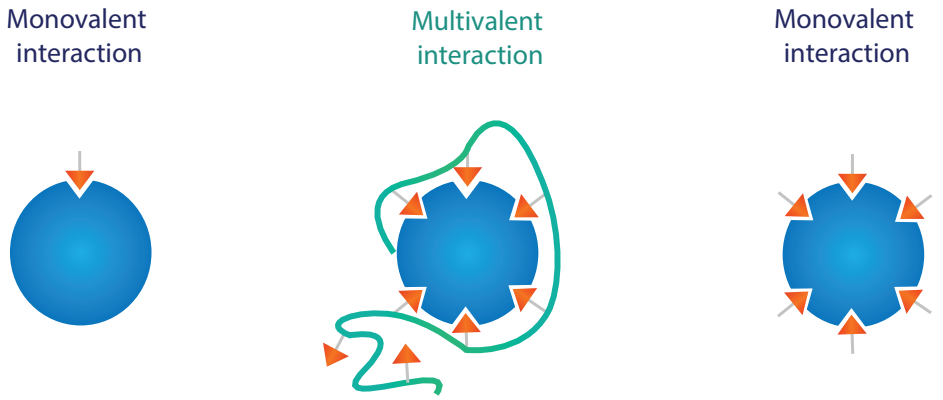

Figure 2.5: Illustration showing the monovalent and multivalent interactions. Both of the interacting substances should have multiple interacting points for a multivalent interaction.

2.6. Antiviral Materials

Most of the conventional small-molecule antiviral drugs are virus specific. When a new virus or mutation of an existing virus appears, antiviral drugs in the therapeutic use are usually not sufficient. Furthermore, small-molecule antiviral drugs interfere in the cellular functioning since most of them act intracellular.

In the recent years, antiviral materials have widely been studied as an alternative to the conventional small-molecule antivirals. These materials can be designed to target the conserved parts of the viral proteins. Therefore they are potentially resistant to viral mutations. Moreover, they do not necessarily interfere with the natural processes in the cell as they target the virus extra-cellular.

Antiviral materials in this chapter involve any kind of organic or inorganic biocompatible multivalent material inhibiting viruses. However, non-therapeutic antiviral materials are excluded.

As it was mentioned previously, the first step of the viral replication process is the attachment of the viral ligands to the host-cell receptors. Multivalent interactions between the ligands and the receptors prolong the binding event. Prolonged times of binding increase the chance of cell-entry. Antiviral materials, in general, are multivalent entry-inhibitors mimicking the interaction between the glycoproteins and the viruses. Therefore they are commonly functionalized with sulfonate or sialic acid groups since most of the viruses primarily attach to HSPG or sialic acid moieties that are abundant on the host-cell surface (figure 2.6). In some studies, the materials are modified with other molecules that bind to viral proteins with high affinity.

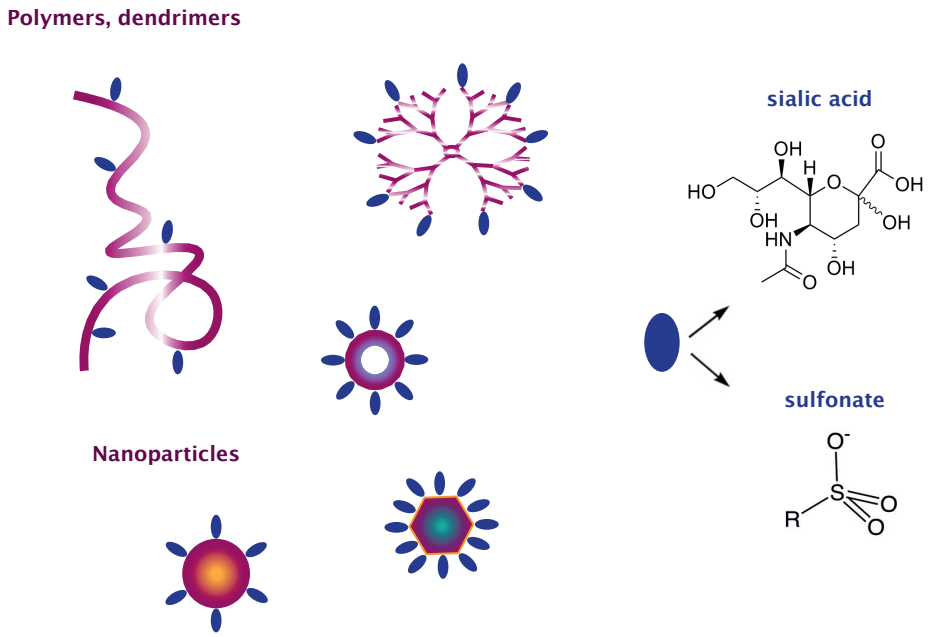

Figure 2.6: Inorganic or organic scaffolds are modified with ligands bearing sialic acid or sulfonate end group in order to target sialic acid and HSPG dependent viruses, respectively. Materials coated with other end-groups that bind viruses with high affinity were also investigated.

Unless specially designed, most of the antiviral materials are virustatic. The inhibitory activity is reversible and usually lost upon dilutions. However, most of the previous studies on the antiviral materials do not involve virucidal assays. Indeed, the half inhibitory concentration (EC_{50}) of antiviral materials is usually a good indication of mechanism of inhibition. High EC_{50} values (μM to mM) is an indication of virustatic

activity. On the other hand, lower EC_{50} values (nM to µM) may result from virucidal activity.

The importance of the virucidal inhibition mechanism is more pronounced in the ex-vivo and in-vivo experiments. Ex-vivo and in-vivo experiments are natural virucidal assays since the virus-material complex undergo dilutions in the tissues. Therefore, a material, that was demonstrated to be virucidal with in-vitro virucidal assay, has a higher chance for in-vivo success. It is unlikely that a virustatic material has an antiviral activity at micromolar concentrations in-vitro, will have a strong ex-vivo or in-vivo activity. Upon dilution of the inoculum in the host, the antiviral effect will probably disappear.

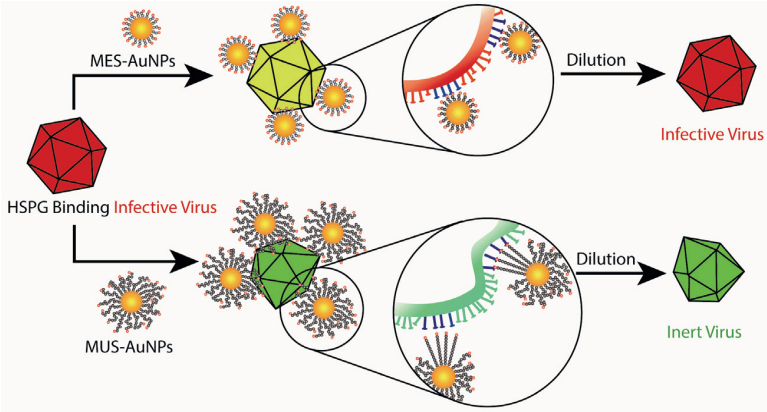

Figure 2.7: Illustration demonstrating the virucidal activity of the MUS coated gold NPs.[18]

Cagno et al. claimed that the rigidity originates from core and linker generate local forces that lead to irreversible viral deformations.[18] According to this study, virucidal activity can be introduced by sufficiently long, rigid ligands (figure 2.7). Therefore, antiviral materials having a rigid core and spacer ligand are more likely to be virucidal than soft, flexible materials.

In summary, it is possible to estimate if a material is virucidal or virustatic by considering at the chemical structure as well as the inhibitory activity against viruses.

Antiviral materials with inorganic core

Inorganic nanoparticles are widely used in biomedicine as imaging tools, cancer therapeutics and drug delivery vehicles.[19,20] They are typically formed of a biocompatible inorganic core and an organic shell. Inorganic core provides properties such as defined size and shape, increased uptake by cells and contrasting agent. On the other hand, organic shell provides colloidal stability in the aqueous medium and can be designed for targeting specific biomolecules.

Antiviral properties of several inorganic nanoparticles were previously investigated.[21–25] All these studies showed that inorganic nanoparticles coated with sulfonate bearing ligands inhibit HSPG-dependent viruses. Di Gianvincenzo et al. showed that gold nanoparticles modified with 11-mercaptoundecane sulfonate (MUS) inhibit HIV virus at nanomolar concentrations.[23] Regarding the structure of the nanoparticles and inhibiting concentration, the mechanism of inhibition is likely to be virucidal. However, the study does not involve any virucidal assay. Similarly, antiviral properties of (2-mercaptoethane sulfonate) MES coated silver nanoparticles on the HSV-1 was investigated.[21] The inhibiting concentration was found to be much higher indicating a virustatic effect. Comparing these two studies, both viruses are HSPG-dependent and the core material as well as the size of the NPs is similar. However, the spacer length is different. MES has two carbons whereas MUS has eleven carbons.

It is possible that longer spacer length enhances the virucidal activity, as Cagno et al. studied it in detail (figure 7).[18] Antiviral activity of MES and MUS coated gold NPs against HSV-2 were compared and the latter found to be virucidal. MUS coated NPs were demonstrated to be broad-spectrum virucides against HSPG-dependent viruses while being non-toxic to cells. The results were supported with TEM studies, which showed that more than 80% of the viruses were deformed (stage 4 in figure 2.8) after 90 minutes incubation period with MUS coated NPs. On the other hand less than 10% of the viruses incubated with MES NPs were deformed.

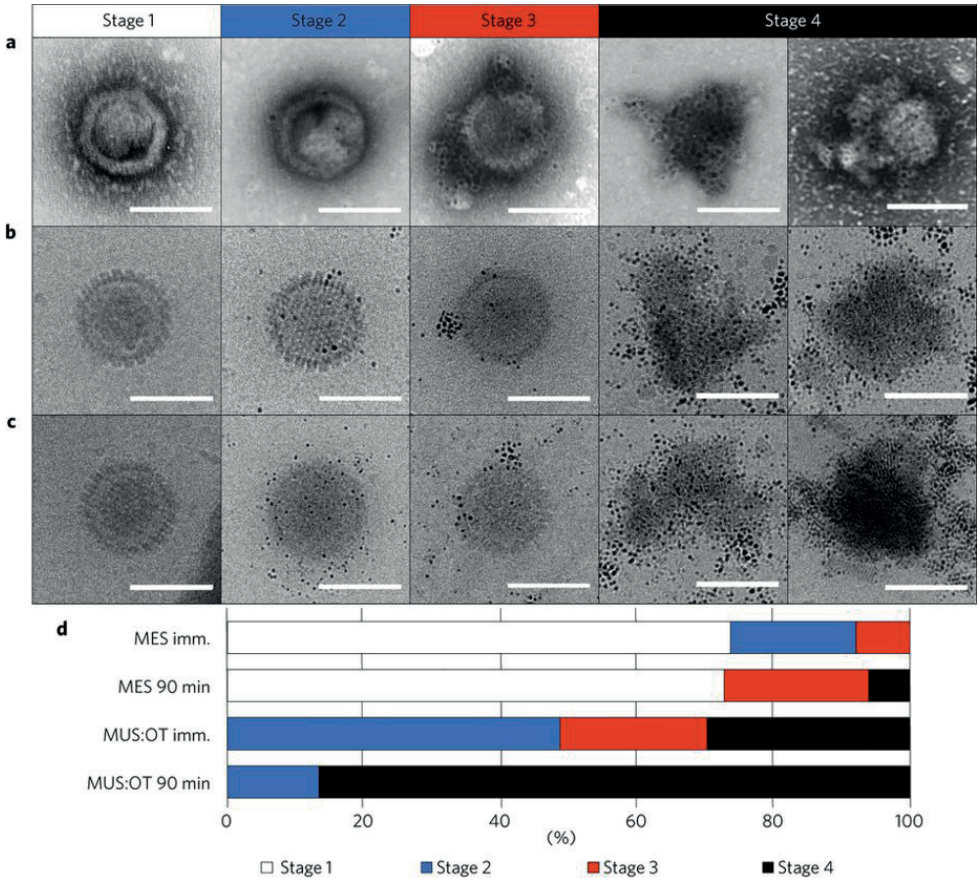

Figure 2.8: TEM images showing the virucidal activity of MUS coated gold NPs against HSV-2 virus. TEM studies demonstrated that more than 80% of the viruses treated with MUS coated gold NPs were deformed (stage 4) after 90 minutes of incubation.[18] On the other hand less than 10% of the virus particles were deformed after 90 minutes of incubation with MES coated NPs.

Apart from inorganic NPs coated with sulfonated ligands, peptides conjugated to inorganic NPs were studied as antiviral materials. Peptide triazole is a known inhibitor of HIV-1. Bastian et al. prepared gold NPs-peptide triazole conjugates in order to target HIV-1.[26] Gold NPs were found to be enhancing the inhibitory activity of peptide triazole. Another approach is to block receptors on the cell-surface using NPs.[27] Bowman et al. coated gold NPs with molecules binding to CCR5, a known entry receptor of HIV-1. Resulting NPs inhibited the fusion of HIV-1 into cells.

Similarly, sialic acid coated inorganic NPs were tested against influenza that is a sialic acid dependent virus. Papp. et. al. demonstrated the antiviral activity of sialic

acid modified gold NPs against A virus/X-31 strain.[28] As an alternative strategy to target influenza virus, Lin et al modified silver NPs with Zanamivir and inhibited H1N1 replication as well as virus-induced apoptosis.[29]

Antiviral materials with organic core

Biodegradability is the major problem with inorganic NPs. Hydrolysis or enzymatic pathways cannot degrade the majority of inorganic nanoparticles. Therefore, after a treatment using inorganic NPs, bio-elimination is the only way to clear the NPs from body. Certain inorganic NPs, such as iron oxide NPs, are degradable. However, excess amount of iron after degradation may cause problems. The main advantage of the organic materials over the inorganic ones is that they are degraded and eliminated from the body effectively.[30–33] Therefore, organic scaffolds such as dendrimers and polymers were modified in order to target viruses.

Antiviral activity of sulfonated polylysine dendrimers as potential topical microbicides against HSPG-dependent viruses were investigated.[34,35] The dendrimers successfully inhibited HSV-2 and HIV-1. In addition to in-vitro studies, the inhibiting activity of the dendrimers was demonstrated with ex-vivo studies. Similarly, Poly(lactic-co-glycoic acid) (PLGA) nanoparticles modified with sulfonated carbosilane dendrons were demonstrated to be antiviral against HIV in-vitro.[36] Dendritic polyglycerol sulfate nanogels (100-200 nm) inhibited the entry of HSV-1 to the cells.[37] Antiviral activity of many polymers, natural or synthetic, bearing sulfate groups were investigated particularly against HIV virus.[38] These materials were envisioned to be vaginal creams in order to prevent HIV transmission and the research proceeded until the clinical trials. However, all the materials under investigation failed at one stage of the clinical trials. As discussed earlier, these polymers are likely to inhibit the viruses with virustatic mechanism. Therefore, the limited in-vivo efficacy is not surprising.

Apart from the nanomaterials coated with sulfonate groups, other nanomaterials with different functional groups were tested against HSPG dependent viruses. Carbon nanodots with boronic acid and amine functional groups were found to be effective

entry-inhibitors against HSV-1.[39] Phosphonate coated polylysine dendrimers were designed to target HIV-1 virus.[40] These dendrimers were further decorated with hydrophobic alkyl chains in order to enhance binding via hydrophobic interactions. Different from other organic materials, they can potentially be virucidal because of their hydrophobic content.

Several sialic acid modified antiviral materials were designed against influenza since it affects millions of people in the world. Reuter et al. synthesized sialic acid decorated polymeric materials in various architectures such as lineer polymer, comb-branched polymer and dendrons; tested them against different strains of influenza A virus. Only high molecular weight (>100 kDa) branched architectures were found to be inhibiting one strain of influenza virus, X-31, at micromolar concentrations of sialic acid.[41] Similarly, Sumati et al. demonstrated that inhibitory activity of linear polysialoside against influenza X-31 is stronger relative to its dendritic analogs.[42] Papp et al synthesized sialic acid decorated glycoarchitectures of different sizes and inhibited X-31 strain at millimolar concentrations.[43]

It is known that, human influenza virus preferentially binds α2,6-linked SA on the glycoproteins. More recently, multivalent materials bearing α2,6-sialylactose were demonstrated to inhibit influenza virus at low micromolar concentrations. Tang et al. synthesized brush polymers bearing α2,6-sialylactose which inhibited influenza A PR8 strain at micromolar concentrations of sialic acid unit.[44] Kwon et al. decorated PAMAM dendrimers with α2,6-sialylactose (6'SL) and inhibited several strains of influenza such as influenza A PR8, CAL 09 and NWS 33.[45] The density of the trisaccharides on the dendrimers was demonstrated to be important for the inhibitory activity (figure 2.9). Even though the dendrimers had also showed in-vivo inhibitory activity, the material concentrations at which the experiment was conducted were very high (in the milligram range).

Different from sialic acid modified materials, a peptide-nanoparticle conjugate (non-carbohydrate based material) was also tested against influenza virus X-31 strain and inhibited the virus at nanomolar concentrations in-vitro.[46]

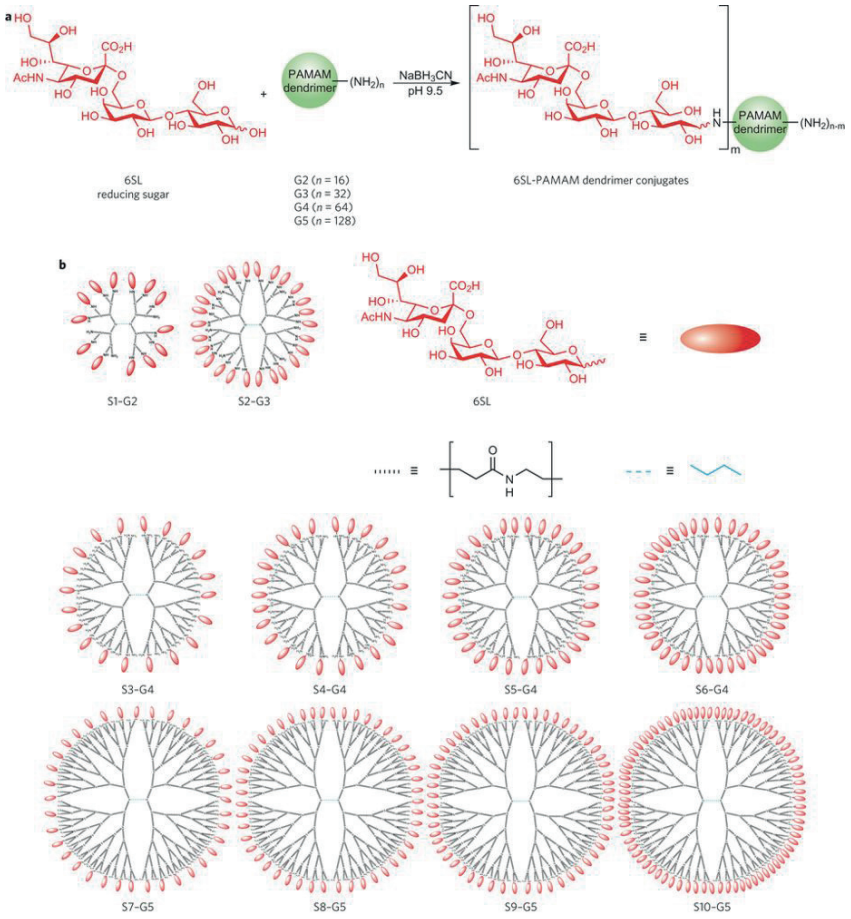

Figure 2.9: Dendrimers with a varying density of 6'SL trisaccharides. Dendrimers with a lower density of 6'SL trisaccharides were demonstrated to be more potent to inhibit influenza virus.[45]

In summary, antiviral properties of many materials were investigated against HSPG and sialic acid dependent viruses. Majority of the materials showed a strong in-vitro inhibitory activity. Unfortunately, most of the studies did not involve ex-vivo and in-vivo experiments. It is still possible to estimate if the mechanism of inhibition is virucidal, regarding the structure and the antiviral activity of these materials. Except a few of them, most of the antiviral materials appear to be virustatic. However, virucidal assays and ex-vivo experiments should be conducted in order to make a conclusion.

CHAPTER 3

Designing Virucidal Materials Against Influenza

Influenza is an airborne virus that affects millions of people every year. High mutation rate of the virus limits the efficacy of the drugs and vaccines. Therefore, there is a huge research effort on the novel antivirals against influenza that resist virus mutations. This chapter is a brief introduction to the influenza virus, current therapeutics and how to design antiviral materials against influenza. The chapter starts with the interaction of influenza virus with the host-cells and its replication cycle. Current therapeutics and vaccines under development is then discussed in detail. The chapter continues with a description of the previous glycan array studies conducted on the influenza virus. The last topic of this chapter demonstrates how to design antiviral materials against influenza with the help of glycan array studies and protein crystal structures.

3.1. Influenza virus: a member of sialic acid targeting viruses

Sialic acid is a monosaccharide that is widely expressed in animal tissues. There are more than 50 types of sialic acids, all derived from neuraminic acid. In animal tissues, two most abundant sialic acids are N-acetylneuraminic acid (Neu5Ac) and N-glycolylneuraminic acid (Neu5Gc) (figure 3.1 a).[47] Sialic acid can be linked to the next sugar from different points (figure 3.1 b). The linkage point is very important since it determines the proteins that sialic acid interacts with. A regular animal cell contains millions of sialic acids on its surface that have crucial roles such as keeping

water at the cell surface; providing adhesion between cells and conducting neural transmission.[48,49] A number of viruses also evolved to target sialic acid moieties on the host-cell surface, perhaps due to abundancy of the sialic acid moieties on the host-cell glycoproteins.[50]

As mentioned previously, the primary receptor for many viruses is either heparan sulfates or sialic acids on the host-cell surface. The family of sialic acid targeting viruses is smaller in comparison to HSPG targeting viruses. Members of this family do not share any genetic or structural similarity. They can be an RNA or a DNA virus; they can have an envelope or not; the attachment ligands can be spike like or canyon like. Certain types of rotavirus and adenovirus, enterovirus, reovirus and influenza virus are some examples of sialic acid targeting viruses.

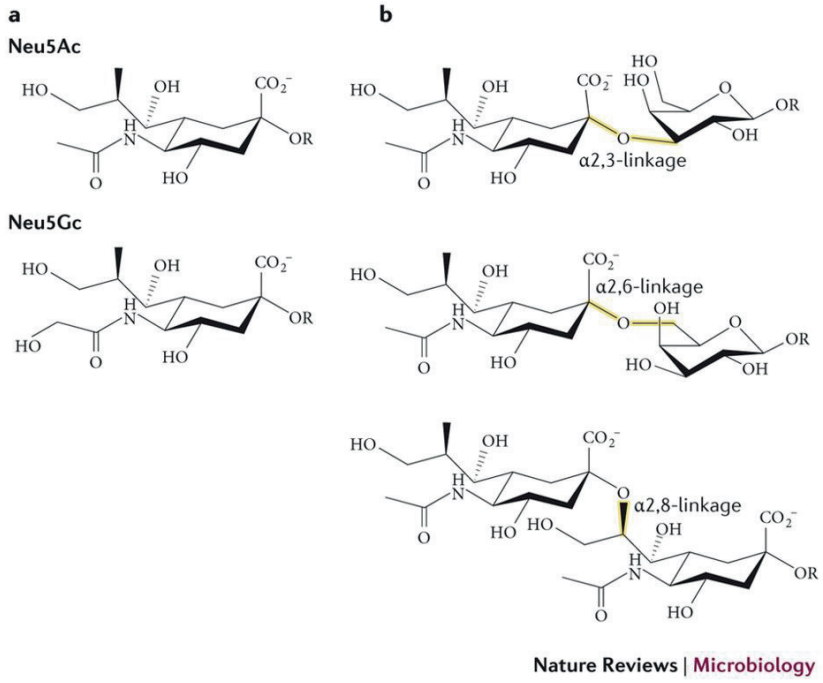

Figure 3.1: Two most abundant types of sialic acid, Neu5Ac and Neu5Gc, on the animal tissues (a). Sialic acid can be bonded to the next sugar from the point of α2,3, α2,6 and α2,8 (b). Different binding points enables sialic acids to make specific interactions with the proteins.

In the family of sialic acid targeting viruses, rotavirus and influenza affect the highest number of people around the world.[51,52] Rotavirus causes inflammation of stomach and intestines. It is particularly dangerous for children, as it is the main cause of fatal diarrhea in young children. Developing countries are affected more by the rotavirus. However, in developed countries rotavirus outbreaks occasionally appears as well. In 2013, rotavirus caused 215,000 deaths worldwide.

Rotavirus related diseases are mostly limited to children in developing countries. On the other hand, influenza virus affects people from all the age groups, both in developed and developing countries. It also affects animals such as birds, ducks and pigs.[53] More importantly, mixture of animal and human strains may lead to influenza pandemics that can end up in millions of deaths.[54] Therefore, influenza virus is the first sialic acid binding virus that is targeted in this project.

3.2. Structure, Properties and Classification of the Influenza Virus

Influenza virus is a member of Orthomyxoviridae family and typically 80-120 nm in diameter. The shape of the virus is in general spherical, and occasionally filamentous. It is an enveloped virus with two main glycoproteins on the surface, hemagglutinin (HA) and neuraminidase (NA) (figure 3.3). The core of the virus contains negative single strand ribonucleic acid (-)ssRNA, which is protected by the viral proteins called capsid.

Influenza is categorized into three as influenza A,B, C and D. Influenza A and C viruses affect both humans and animals whereas type B is exclusive to humans and type D is exclusive to animals. Among the different types, Influenza A virus circulates the most. Therefore the mutation rate of the influenza A virus is very high. Influenza A subtypes are described with H and N letters followed by a number. These numbers represent the genes, which produce the surface proteins. H stands for Hemagglutinin whereas N stands for Neuraminidase that is two important glycoproteins on the envelope. Currently 18 known subtypes of hemagglutinin and 11 known subtypes of neuraminidase exist. This means 198 subtypes of influenza may exist. Three most common A subtypes are H1N1, H3N2 and H5N1. Influenza A

subtypes undergo further mutations resulting in different strains such as H1N1 Spanish Flu 1918 or H1N1 California 2009.

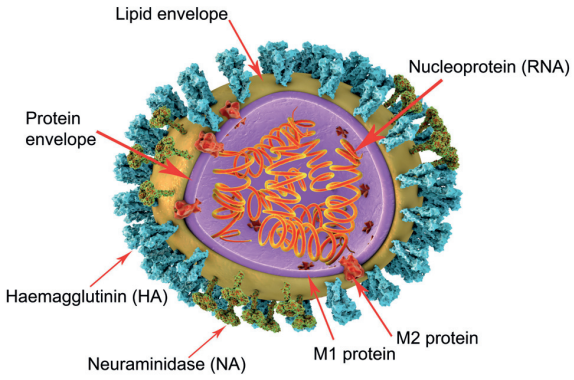

Figure 3.2: Main components of an influenza virus particle. Influenza is an enveloped virus with two important glycoproteins, hemagglutinin and neuraminidase, located on the envelope. The genetic material (RNA), which is protected M1 and capsid proteins, is at the core of the virus. (image copyright: 123RF Stock Photo)

3.3. Replication cycle of the Influenza Virus

Influenza virus is replicated in the living-cells, following a typical viral replication process consisted of 9 steps. The first step of viral replication is the attachment of the hemagglutinin proteins to the sialic acid moieties on the host-cell glycoproteins (step 1). The virus particle is then uptaken into cells by endocytosis (step 2). M2 protein is responsible to form channels between the endosome and the viral envelop. Through this channel, protons travel from the endosome to the interior part of the virus so that the internal pH is reduced (step 3). Reduction in the internal pH leads the viral proteins to disassemble and eventually (-)ssRNA and RNA-dependent RNA polymerase is released (step 4). RNA-dependent RNA polymerase enables the (-)ssRNA to synthesize (+)ss RNA in the nucleus (step 6). (+)ss RNA mediates the synthesis of different viral components such as viral proteins and (-)ssRNA (step 7). Viral components are assembled to form the new virus particle (step 8). The progeny

virus is cleaved from the cell surface by neuraminidase to further infect new cells (step 9).

3.4. The impact of influenza on the human health

Influenza is an infectious disease that has symptoms like muscle pain, fever and soar throat. Deaths directly resulting from influenza are rare although possible, particularly in young and old people, and more importantly in people with immunodeficiency. More often than deaths, influenza virus can lead to serious complications such as pneumonia or inflammation of the heart (figure 3.4).[55]

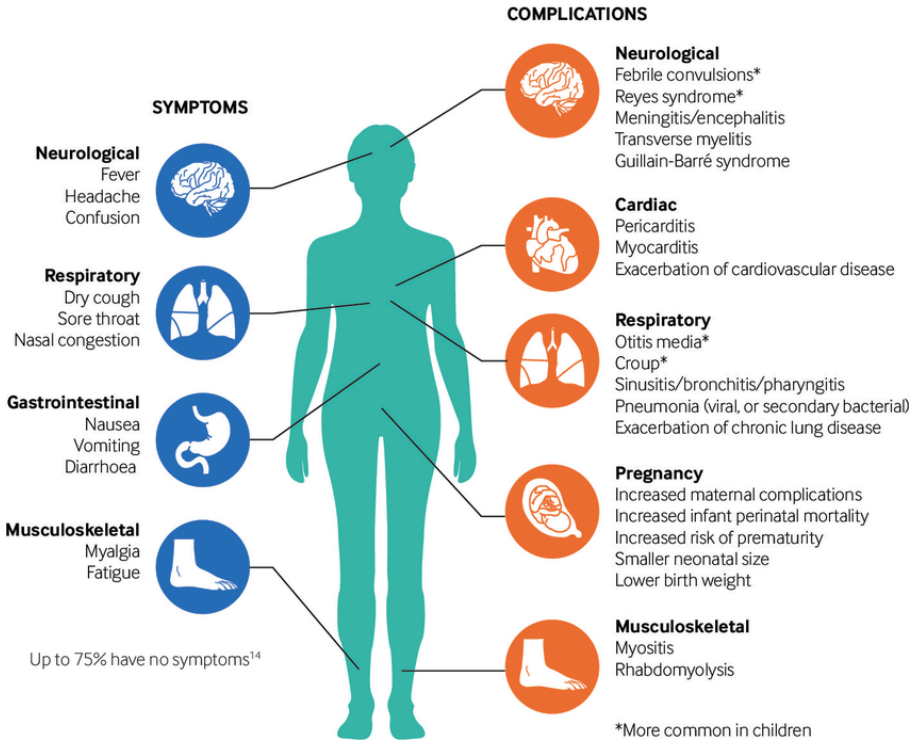

Figure 3.3: Influenza virus affects millions of people every year. The symptoms like fever, headache and sore throat appear after infection. Healing time varies between a few days to a few weeks. In case of prolonged times of infection, the virus can lead to serious complications such pneumonia and cardiovascular diseases. Graphic reproduced from Ghebrehewet et al.[56]

Humans are mostly affected by the influenza types composed of H1, H2, H3 and N1, N2 glycoproteins. These viruses are called human influenza viruses and typically replicate in the upper-respiratory track where the cells are rich with the receptors that H1,H2, H3 proteins preferentially binds to. On the other hand, humans can also be infected by animal strains such avian influenza H5N1. H5 preferentially binds to receptors that are located deep in lungs. Therefore it is less likely for humans to be infected with H5 strains, but once the infection is starts, it is usually fatal.

Unlike many other viruses, influenza virus can spread through air, forming aerosols. It can also be transmitted through saliva, blood and nasal secretions. The fact that influenza virus can spread through air increases the chance of influenza outbreaks. Influenza virus leads to 3 to 5 million severe cases; 250,000 to 500,000 deaths every year. Influenza pandemics are less common, still in the 20th century four influenza pandemics that are Spanish influenza (1918, 50 million deaths), Asian influenza (1957, 2 million deaths), Hong Kong influenza (1968, 1 million deaths), California (2009, 100,000-400,000 deaths) occurred.[54]

Influenza pandemics usually appear when humans who already carry the influenza virus is further infected with a new animal strain such as avian or swine influenza. The mixture of the human and animal strains leads to drastic changes in the HA and NA proteins, resulting in the antigenic shifts. The immune system can detect small changes, i.e. antigenic drifts, in the influenza surface proteins. Changes caused by antigenic shifts, on the other hand, cannot easily be recognized by the immune system resulting in the influenza pandemics.[57]

3.5. Prevention and treatment of influenza infections

One of the most effective ways to protect against influenza is vaccination. Influenza vaccines contain attenuated influenza strains of coming year predicted by WHO Global Influenza Surveillance Network. The traditional influenza vaccines (trivalent vaccines) provides protection against two influenza A strains (H1N1 and H2N3) and one influenza B strain. Vaccines are in general safe and effective. However allergic reactions and varying efficacy of vaccines are the drawbacks.

As an alternative to traditional vaccines, that contain the attenuated virus particle, novel vaccines were developed in the recent years. DNA vaccines, which contain the DNA sequence encoding the antigen, are promising influenza vaccines. DNA vaccines invoke both B and T cell responses, more stable than traditional vaccines, and easy to manufacture.[58] Broadly neutralizing antibodies (bNAbs), which recognize the conserved regions in the globular head or stem part of the HA and evoke an immune response, is another promising approach to generate new generation vaccines. Improved resistance to the viral mutations is the advantage of broadly neutralizing antibodies.[59,60]

For the high-risk population, antiviral drugs are used to treat influenza infections (figure 3.5). The most widespread drug type is Neuraminidase inhibitors. Zanamivir (nasal), oseltamivir (oral) and peramivir (intravenous) are neuraminidase inhibitors with a similar chemical structure. Neuraminidase inhibitors are effective on most of the influenza strains. However, certain influenza strains have started to show drug resistance.[61,62] Ion channel (M2 proteins) inhibitors, such as amantadine, were also developed.[63] However, these drugs have lost popularity since most of the influenza strains immediately developed drug resistance.

Drugs targeting the hemagglutinin protein are currently under development. Umifenovir and TBHQ are small molecule drugs that target hemagglutinin, inhibiting its fusion activity.[59] Several other drugs are also in the stage of clinical trials.[65] Two of these drugs, DAS 181 and Nitazoxanide, target the host. DAS 181 is a drug, which removes the sialic acids from glycoproteins on the upper respiratory track in order to prevent viral attachment to cells.[66] It is currently in clinical trial phase 2. Nitazoxanide is another drug in the clinical trial phase 3, which prevents hemagglutinin maturation.[67] The other drugs in clinical trials target the viral replication process. Favipiravir inhibits RNA dependent RNA polymerase and currently in clinical trial phase 3. Favipiravir work against influenza A (including avian strains), B and C.[68] Five different monoclonal antibodies targeting stem part of the influenza are currently under clinical trial.[69–72] Monoclonal antibodies prevent the virus from fusing into the host-cell. Even though many drugs are under clinical trials, it is very unlikely that one drug will treat all the influenza infections appearing next

10 years. Influenza is a rapidly mutating virus that already has several subtypes and strains. Therefore more and more therapeutics should be developed that resist viral mutations.

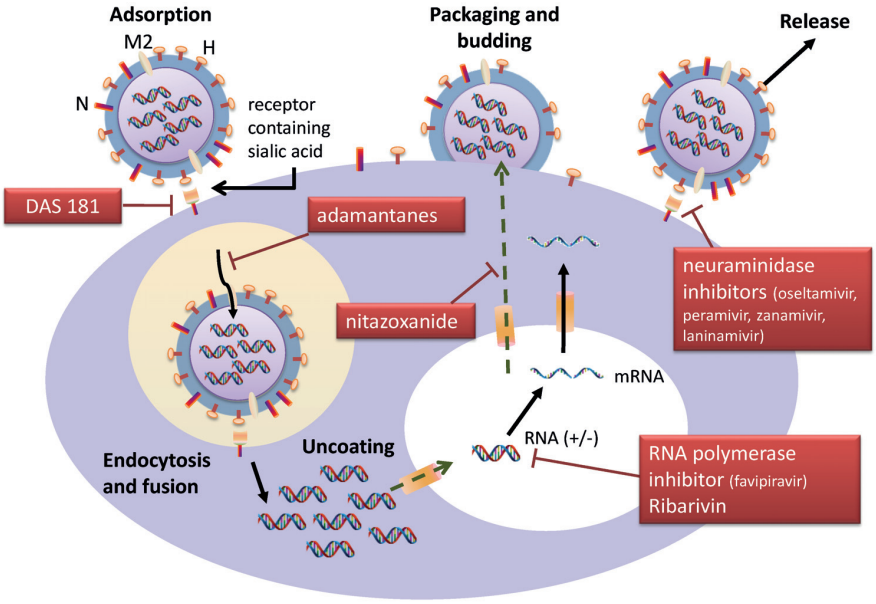

Figure 3.4: Antiviral drugs against influenza that are currently in the market or in the phase of clinical trials demonstrated together with their target step in the viral replication process. Graphic reproduced from Li at al.[64]

3.6. Previous glycan array studies on the influenza virus

Cells are decorated with glycoconjugates that are carbohydrates covalently linked to other molecules such as proteins, peptide and lipids. Glycoproteins, proteoglycans (heavily glycosylated proteins) and glycolipids are three major classes of glycoconjugates. Glycoconjugates have diverse functions such as providing intra and extra-cellular communications, labeling proteins for transport and recognizing extracellular signal molecules such as growth factors. Viruses interact with glycoconjugates in order to enter host-cells. Every virus has evolved to recognize a specific glycoconjugate presented on the host-cell surface. For instance, HIV interacts with heparin sulfate rich glycoconjugates whereas influenza A interacts with sialic acid rich glycoconjugates. Indeed, each virus prefers a certain glycoprotein with

specific glycan termini in the family of sialic acid binding viruses. For example, adenovirus 37 and reovirus are both sialic acid binding viruses. However, adenovirus 37 binds to the GD1a receptor whereas reovirus binds to the GM2 receptor, each terminate with a different glycan sequence.[49]

Cell-based infectivity assays can be used in order to reveal the interaction between a virus and sialylated glycan where sialyated glycans are blocked with lectins or cut by neuraminidases in the control experiment.[49] However, these cell-based assays do not provide any specific information about the glycan preference of a virus.

Glycan binding specifity of proteins, antibodies and microorganisms can be detected using glycan micro-arrays.[73,74] To conduct glycan micro-array studies, hundreds of glycan sequences are printed onto glass slides through a peptide bond (the glycan sequences are amine functionalized and the glass slides contain NHS-active carboxylic acid). The subject under investigation is labeled with a fluorescent dye and left for interaction with the glycan array. If there is an interaction between the subject and a glycan sequence, a strong fluorescence signal is observed for that specific glycan sequence. As a result, glycan sequences that bind to the subject with high affinity are determined (figure 3.6).

In the past, one limitation of the glycan array technology was the limited availability of glycans with amino linkers. Consortium for Functional Glycomics initiated a large scale research to modify hundreds of glycans with an amino linker.[75] Robot-produced glycan arrays that contain hundreds of glycan sequences were then prepared. The glycan binding specificity of several viruses, proteins and antibodies were determined in this platform. The diverse dataset produced by functional glycomics is currently open-access.

The dataset involves the results of many studies that were conducted to investigate the glycan binding patterns of influenza virus. Hemagglutinin was known to be binding to sialic acid moieties. However, the exact glycan sequence for different types and strains of influenza was not investigated in depth. Indeed, the amino acid sequence of hemagglutinin change in line with the high mutation rate of influenza. The glycan

array studies demonstrated the exact glycan sequences providing high affinity binding to the tens of different influenza strains.

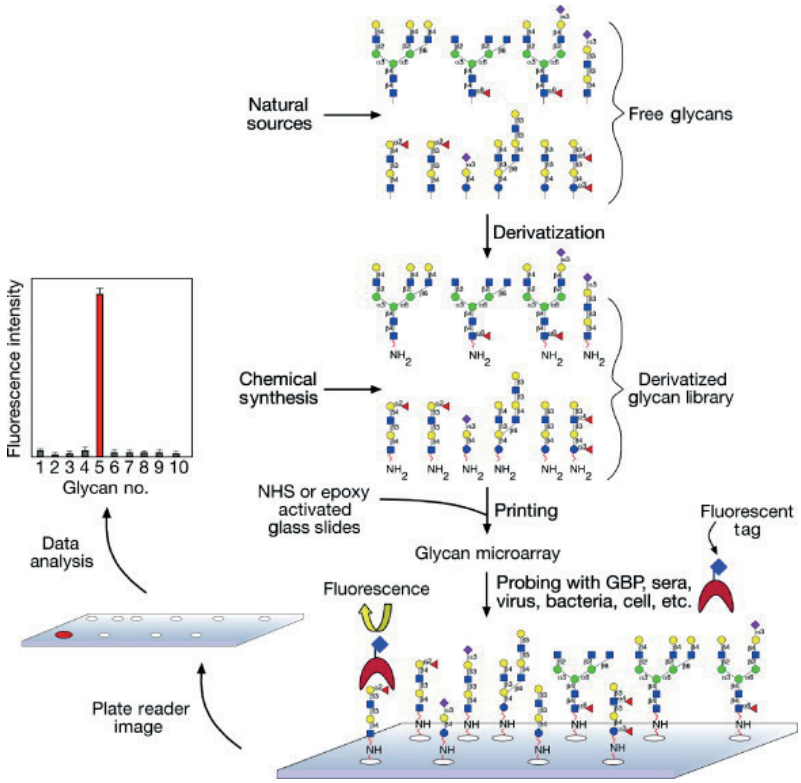

Figure 3.5: To fabricate glycan arrays, glycan sequences are modified with amino groups and printed onto NHS-active glass slides. The subject under investigation is tagged with a fluorescent dye. The strength of interaction between the subject and a specific glycan is determined by the fluorescence intensity. Graphic reproduced from Smith and Cummings.[74]

Every subtype or strain of influenza virus binds to slightly different glycan sequences with high affinity. However, there is a general trend: the majority of the influenza viruses that originates from humans bind to glycans terminating with 6-Sialyl-N-acetyllactoseamine (6'SLN) and the majority of influenza viruses that originates from avians bind to glycans terminating with 3-Sialyl-N-acetyllactoseamine (3'SLN). The glycan sequences forming the trisaccharides are the same, but the attachment point of sialic acid is different (figure 3.7 a). In general the glycans that terminate with α2,3-linked sialic acid have smaller conformational freedom whereas the glycans that

terminate with α2,6-linked sialic acid have larger flexibility.[49] Perhaps, the hook-like shape of 6'SLN compensates for the larger flexibility of the glycan (figure 3.7 b).

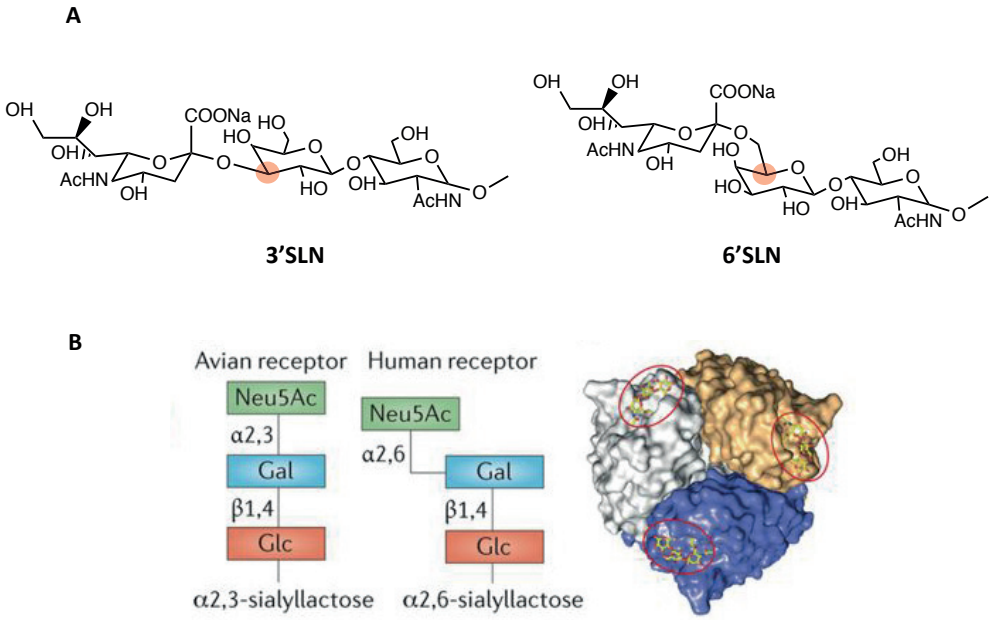

Figure 3.6: Chemical structures of 3'SLN and 6'SLN trisaccharides (A). 3'SLN binds to avian strains with high affinity whereas 6'SLN binds to human strains with high affinity. Illustrations of 3'SLN and 6'SLN trisaccharides together with crystal structure of HA head domain where sialic acid binding points are highlighted (B). Graphic B reproduced from Stencel-Baerenwald et al.[49]

3.7. Designing virucidal nanomaterials against influenza

Cagno et al. demonstrated that gold nanoparticles coated with MUS ligand inhibit a broad range of HSPG-dependent viruses with virucidal mechanism.[18] There are two key points in the virucidal mechanism of inhibition described in this study: 1. Multivalent nanoparticles with sulfonate end groups bind to viral ligands with high affinity 2. Sufficiently long, rigid linker exerts local forces that eventually lead to deformations in the viral proteins.

Initially, a similar approach was followed in this project. Gold NPs were coated with sialic acid and their antiviral activity was tested against different sialic acid dependent viruses such as influenza, adenovirus 37 and enterovirus 68. However, NPs did not show any antiviral activity against these viruses. The results were attributed to the weak interaction between the viruses and the sialic acid molecule that is in the millimolar (mM) range.[49] As previously described in this chapter, every sialic acid targeting virus binds to a different glycan sequence with high affinity. Therefore, the antiviral materials should be designed specific to the virus.

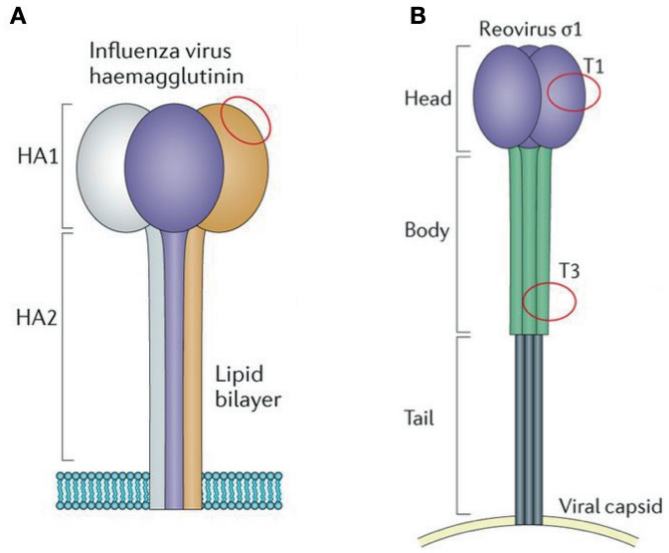

Figure 3.7: Sialic acid binding points of hemagglutinin is at the top of the head domain (A) whereas it is at the side of the head domain and in the lower part of the body domain the case of reovirus. Graphic reproduced from Stencel-Baerenwald et al.[49]

Hemagglutinin has a spike-like structure with exposed sialic acid binding points on the head domain. Therefore, to target HA with multivalent nanomaterials is relatively straightforward. To target some other sialic acid binding viruses can be difficult due to the structure of the viral ligands. For example, in the case of reovirus, the sialic acid binding points are hidden at the bottom part of the head domain.[49] Therefore, to form multivalent interactions between the nanomaterial and the reovirus can be difficult to achieve. Enterovirus 68, on the other hand, has canyon-like viral

ligands.[76,77] To reach the sialic acid binding points with nanomaterials should be more complicated in comparison to spike-like viral ligands. Therefore, in-depth studies are required to inhibit these viruses with nanomaterials.

Crystal structure of HA and its distribution on the viral surface should be considered when the antiviral nanomaterial is designed (figure 3.8). The distance between sialic acid binding points on HA is 4-5 nm. Therefore very high density of 6'SLN molecules on the nanomaterial surface is not necessary for efficient binding. On the contrary, binding affinity may decrease if the density of 6'SLN molecules is very high.[45] Moreover, sufficiently long, rigid spacer is important for strong inhibitory effect. The importance of the spacer in a multivalent material was deeply discussed in a review by Sumati et al.[78] Free energy of interaction between a multivalent material and the viral ligand has enthalpic (ΔH) and entropic ($-T\Delta S$) contributions (Equation 1). In a multivalent binding event, enthalpic change due to simultaneous binding adds to the strength of interaction. In return, entropic penalty should be paid since spacer ligands loose the degree of freedom. To reduce the entropic penalty paid, the spacer size and rigidity should be optimum.

Very long, hydrophilic spacers lead to large entropic penalties in the aqueous medium, whereas smaller, hydrophobic spacers are more favorable for a strong interaction. As discussed earlier, rigidity of hydrophobic ligands is also important for virucidal inhibition mechanism.[18]

Another important consideration is the core size of the nanomaterial. Influenza virus has around 300-500 HA trimmers with a spacing of 10-14 nm.[79] Therefore, nanomaterials that have a size below 10 nm, can only reach one HA trimer. To reach more than one HA with a single nanomaterial might offer advantages and disadvantages. Higher number of binding points between the nanomaterial and the viral surface is the advantage of bigger nanomaterials. On the other hand, the size mismatch between the bigger nanomaterials and the hemagglutinin may limit the local deformations induced.

On the basis of concepts discussed above, nanomaterials that are coated with rigid spacer bearing 6'SLN trisaccharide should be ideal to inhibit human influenza viruses with virucidal inhibition mechanism. As mentioned above, it is difficult to speculate on the ideal core size of the nanomaterials to target influenza. However, in this project, the total size of the nanomaterial was envisioned to be relatively small (<10 nm). Two different nanomaterials bearing gold or cyclodextrin core were designed in order to inhibit human influenza virus with virucidal inhibition mechanism. The next two chapters discuss in detail the synthesis protocols as well as antiviral activity of the nanomaterials designed.

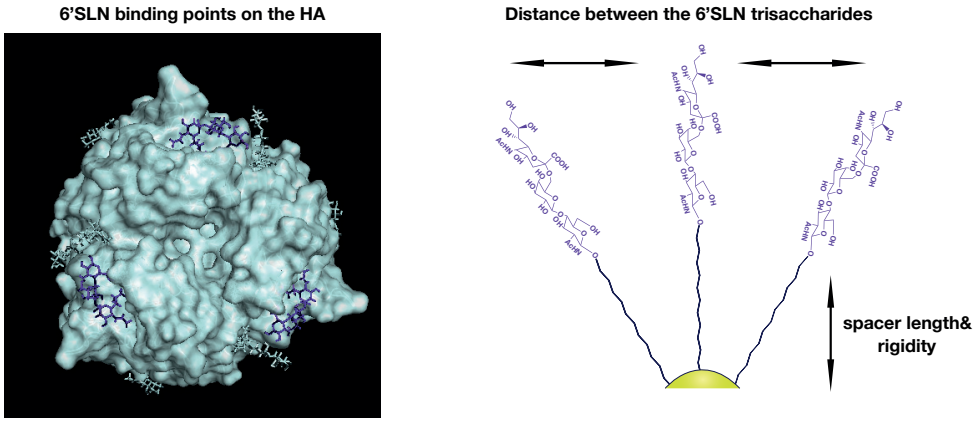

Figure 3.8: Crystal structure of the HA should be considered to design nanomaterials to target human influenza strains. Optimum density of the 6'SLN moieties as well as relatively long, rigid linker is important to inhibit influenza with virucidal mechanism.

CHAPTER 4

Gold Nanoparticles Against Influenza

Gold NPs are widely studied in the field of nanomedicine due to the stability of gold in the aqueous medium as well as straightforward synthesis and modification methods.[20,80–83] In this project, multivalent gold nanoparticles bearing 6'SLN end-groups were synthesized in order to target the human influenza virus. The NPs were designed according to the parameters highlighted in the previous two chapters. The easiness of gold NP modification enabled us to conduct a deep structure-activity relationship.

The first topic of this chapter is the synthesis protocols of gold NPs against influenza. Second topic is comparative dose-response assays, which demonstrates the antiviral activity of NPs having different ligand compositions. Dose-response assays are also a good indication of binding affinity between the viruses and NPs. Following the dose-response assays, the virucidal activity of NPs, which is the crucial part of this project, is demonstrated. The chapter also involves data on the toxicity as well as virus specificity of the NPs.

4.1. Materials and Methods

4.1.1. Synthesis of gold nanoparticles targeting Influenza virus

Materials: All the solvents were purchased from sigma Aldrich. Tetrachloroauric acid ($HAuCl_4$) was purchased from Acros chemicals. HS-PEG(5) and HS-PEG(4)-COOH was purchased from PurePEG. Sodium borohydride ($NaBH_4$), 16-mercaptohexacanoic acid, N-hydroxysuccinimide ester (NHS), ethylcarbodiimide hydrochloride (EDC-HCl) and 4-(dimethylamino)-pyridin (DMAP) were purchased

from Sigma-Aldrich. HS-PEG(8)-COOH was purchased from Iris Biotech. Neu5Acα(2,6)-Galβ(1-4)-GlcNAc-β-ethylamine was purchased from TCI chemicals.

Methods: The nanoparticles were synthesized in four steps (figure 4.1). Firstly, PEG5 NPs were synthesized. Then the ligand exchange reactions were conducted with the spacer ligand having a carboxylic acid end group. Thirdly, carboxylic acid end group of the spacer ligand was NHS activated in order to graft the trisaccharide, 6'SLN.

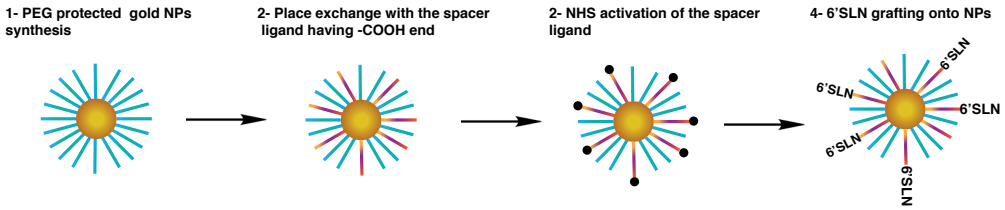

Figure 4.1: Illustration showing the steps to synthesize 6'SLN grafted gold NPs.

Synthesis of PEG(5) NPs: 88.6 mg of $HAuCl_4$ in 15 mL of EtOH was stirred with 56 mg of HS-PEG(5) in 5 mL of EtOH for 10 minutes. To the mixture 94.6 mg $NaBH_4$ in 37.5 mL of ethanol (EtOH) was added dropwise within 5 minutes. For complete NP formation, the reaction was allowed to run overnight. Resulting NPs were diluted in H_2O and concentrated using amicon filters (cut-off MW: 30kDa). Once concentrated, NPs were further washed with H_2O.

PEG(5)_C15-COOH mixed ligand NPs: A ligand exchange reaction was performed with 1.5 mg of 16-mercaptohexacanoic acid and 20 mg of PEG(5) NPs, in DMF, overnight. The NPs were precipitated from DMF-diethyl ether mixture and further washed three times with the same solvent mixture. A last wash with only diethyl ether was done and NPs dried under vacuum.

PEG(5)_PEG(4)-COOH mixed ligand NPs: A ligand exchange reaction was performed with 3 mg of HS-PEG(4)-COOH and 20 mg of PEG(5) NPs, in DMF, overnight. The NPs were precipitated from DMF-diethyl ether mixture and further

washed three times with the same solvent mixture. A last wash with only diethyl ether was done and NPs dried under vacuum.

PEG(5)_PEG(8)-COOH mixed ligand NPs: A ligand exchange reaction was performed with 20 mg of HS-PEG(8)-COOH and 20 mg of PEG(5) NPs, in DMF, overnight. The NPs were precipitated from DMF-diethyl ether mixture and further washed three times with the same solvent mixture. A last wash with only diethyl ether was done and NPs dried under vacuum.

NHS Activation of of NPs: NHS activation of all the mixed ligand NPs described above was conducted following the same method. 15 mg of NPs were activated using 10 mg N-hydroxysuccinimide ester (NHS), 2 mg of ethylcarbodiimide hydrochloride (EDC-hcl) and 0.1 mg of 4-(dimethylamino)-pyridin (DMAP) in DMF, overnight. The NPs were precipitated from DMF-diethyl ether mixture and further washed three times with the same solvent mixture. A last wash with only diethyl ether was done and NPs dried under vacuum.

NPs with low grafting density of 6'SLN (L): 5 mg of NHS-activated NPs in 1 mL of dmso was mixed with 1.7 mg of Neu5Acα(2,6)-Galβ(1-4)-GlcNAc-β-ethylamine in 3 mL of 0.1 M phosphate buffer (pH: 7.5). After 5 hours reaction, 6'SLN grafted NPs were diluted in H_2O and cleaned with amicon filters.

NPs with high grafting density of 6'SLN (H): 5 mg of NHS-activated NPs were mixed with 1.7 mg of Neu5Acα(2,6)-Galβ(1-4)-GlcNAc-β-ethylamine in 2 mL of DMSO and the reaction was stirred overnight. 6'SLN grafted NPs were diluted in H_2O and cleaned with amicon filters.

Synthesis of the initial NPs (group A) can be found in the appendix A.

4.1.2. Characterization of gold nanoparticles targeting Influenza virus

Determining the core size of the NPs:

The core size of the NPs was determined using transmission electron microscopy (TEM). Aqueous solution of PEG(5) NPs was further diluted with EtOH and dripped onto the carbon grid with drop casting method. The measurement was conducted using Talos transmission electron microscope, at 200kV accelerating voltage. TEM micrographs were analyzed with Fiji software using a custom-made macro (developed by Dr. Marie Mueller) (figure 4.2).

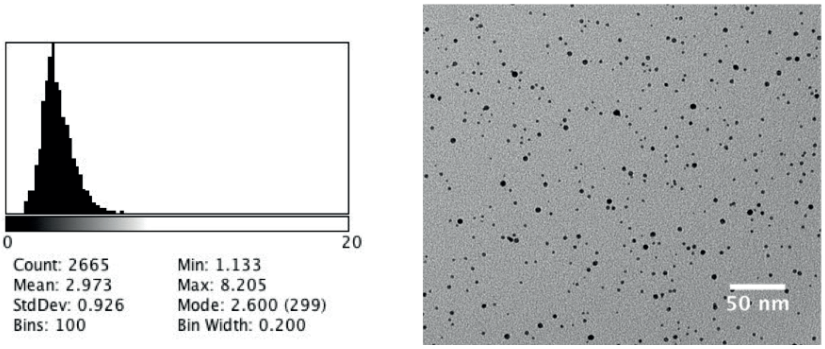

Figure 4.2: TEM measurements were conducted in order to determine the core size of the NPs. The average size of the NPs was determined using Fiji software.

Ligand Packing Density:

The ligand packing density can be estimated from TGA and TEM results, by doing certain assumptions. Mass based ratio between the organic and the inorganic part can be determined doing TGA analysis. TGA analysis was conducted after ligand exchange reactions, before grafting the trisaccharide. It was assumed that the ligand ratio does not change during 6'SLN grating, since no thiolated molecule is involved in the reaction. 5 mg of NPs were put in the alumina crucibles and heated up to 900°C with a rate of 10°C/minute. The organic content melts and evaporates before 900°C. The resulting curve represents the change in the total mass due to the loss of the organic part. From this curve, the ratio between the organic and inorganic content of

NPs can be calculated. NPs loose 20-25% of their weight in a typical TGA measurement (figure 4.3). This corresponds to an average ligand density of ~5.2 ligands/nm^2. As an example, TGA curve of HS-PEG(5) & HS-PEG4-COOH mixed ligand NPs was demonstrated. TGA measurement alone is not sufficient to determine the ligand ratio of NPs. NMR studies are required to determine the ligand r ratio.

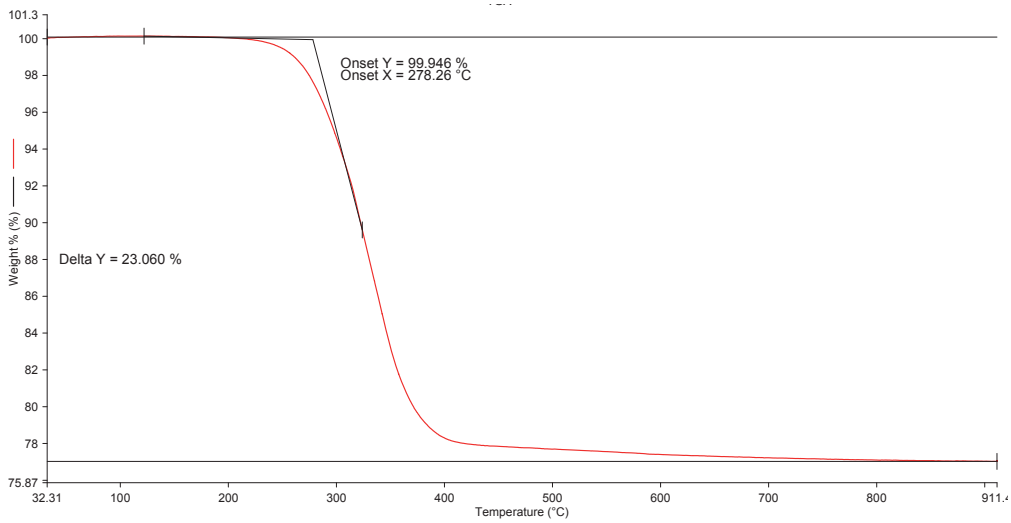

Figure 4.3: TGA curve of HS-PEG(5) & HS-PEG(4)-COOH NPs shown as an example

NMR Characterization of Nanoparticles:

Ligand ratio of NPs as well as the density of 6'SLN molecules on the NP surface was determined with ^{1}H NMR. All the experiments were conducted with Bruker AV-400 Mhz and the data analyzed with MestreNova. First of all, gold NPs have to be etched before doing NMR measurements. Etching can be done with iodine or potassium cyanide (KCN) in methanol-d_4. Since both chemicals are very reactive, it is possible to observe some changes in the NMR spectrum of organic molecules due to etching. However, peak integrals are not significantly affected. In this project iodine etching was done in order to determine the ligand ratio between HS-PEG5 and the spacer ligand. A specific peak from HS-PEG5 ligand, near hydroxyl end group, clearly appears after etching with iodine whereas it is hidden after etching with KCN. This peak appears between 3.5-3.7 ppm and corresponds to two hydrogens near hydroxyl end group. The specific peak from the spacer ligand that have a carboxylic acid end

appears between 2.0-2.6 ppm and corresponds to two hydrogens near carboxylic acid end. By comparing the integral of these triplets, the ligand ratio of the NPs can be calculated. Figure 4.4 shows ^{1}H NMR spectra of binary ligand NPs where the spacer ligand is HS-C15-COOH (left) and HS-PEG4-COOH (right). The other NPs with PEG spacer ligands have NMR spectrums similar to the one on the right. It should be noted that iodine alters the peak positions as it reacts with functional groups or coordinates to the polar parts of the molecule. The specific peak that belongs to HS-C15-COOH molecule is divided into two because the majority of –COOH groups reacted with iodine. The small peak belongs to the remaining molecules, which did not react with iodine.

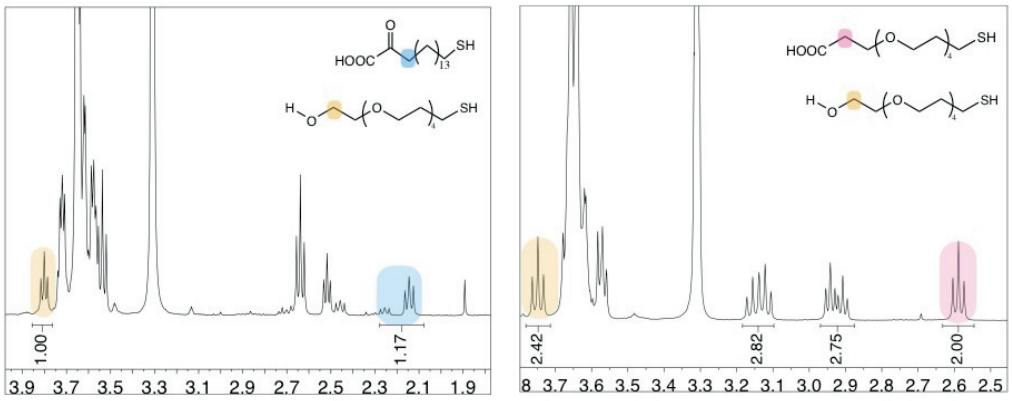

Figure 4.4: Ligand composition characterization of NPs after the ligand exchange reaction. The specific peak from HS-PEG(5) is compared to the specific peak from HS-C15-COOH (left) and HS-PEG(4)-COOH (right).

Iodine solution to etch gold NPs may lead to peak broadening if the quantity of organic molecules on the NPs is small. 6'SLN coated NPs were etched with KCN in order to obtain sharper peaks. The only problem is that KCN reacts with certain end-groups from the 6'SLN trisaccharide.

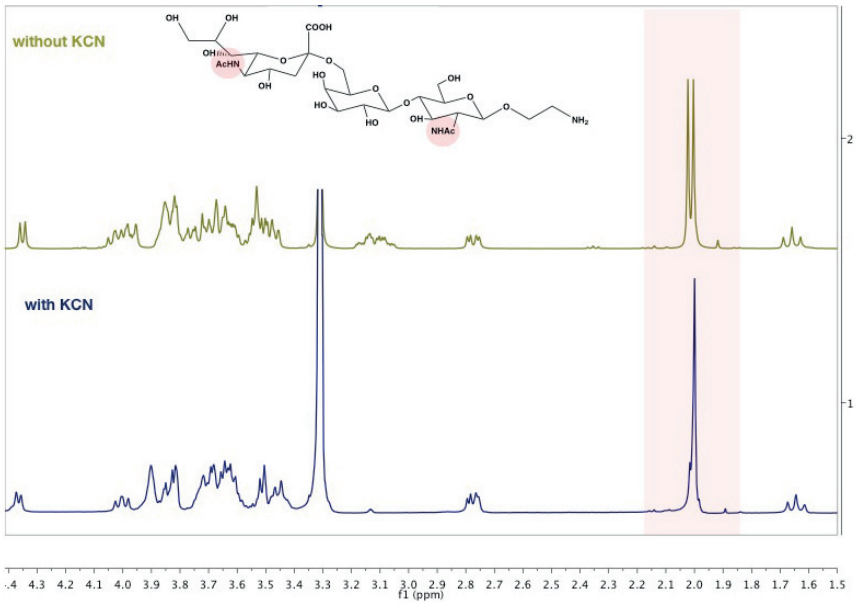

Figure 4.5: The NMR spectrum of 6'SLN trisaccharide with and without KCN.

To determine a specific peak from the 6'SLN trisaccharide, which is not affected by KCN etching, is important. Figure 4.5 shows the NMR of 6'SLN with and without KCN. Two singlets of acetylamine end-groups merge with the addition of KCN. Therefore these singlets may not be reliable for the analysis. The doublet at 4.3-4.4 ppm is not hidden under the other peaks and is not much affected by KCN. Therefore, it is a reliable peak to calculate the density of 6'SLNs on the NPs.

For the NMR characterization of 6'SLN coated NPs, it was assumed that the ligand ratio between the PEG5 and the spacer ligand does not change during 6'SLN grafting since no thiol is involved in the reaction. Then the specific peak (2H, triplet at 2.0-2.6 ppm) from the spacer ligand was compared to the specific peak from the 6'SLN (1H, dublet at 4.3-4.4 ppm). The triplet from the spacer ligand is usually divided into two due to amide bond formation. Number of spacer ligands with 6'SLN can also be calculated through these triplets, as long as they do not overlap. In the case of PEG spacers, two triplets are quite separate. Therefore, it is possible to calculate the 6'SLN density through these triplets, as well (figure 4.6). On the other hand, there is an overlap between the two triplets in the case of C15 spacer (figure 4.7). Therefore, it is

not possible to calculate the number of spacers with 6'SLN groups through the divided triplets.

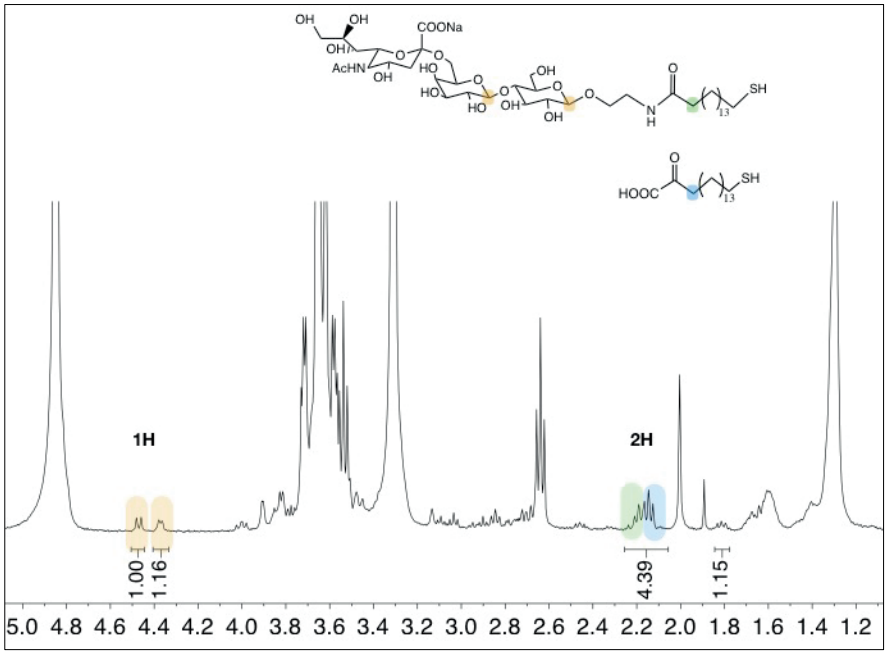

Figure 4.6: NMR spectrum of 6'SLN grafted gold NPs where the spacer ligand is C15.

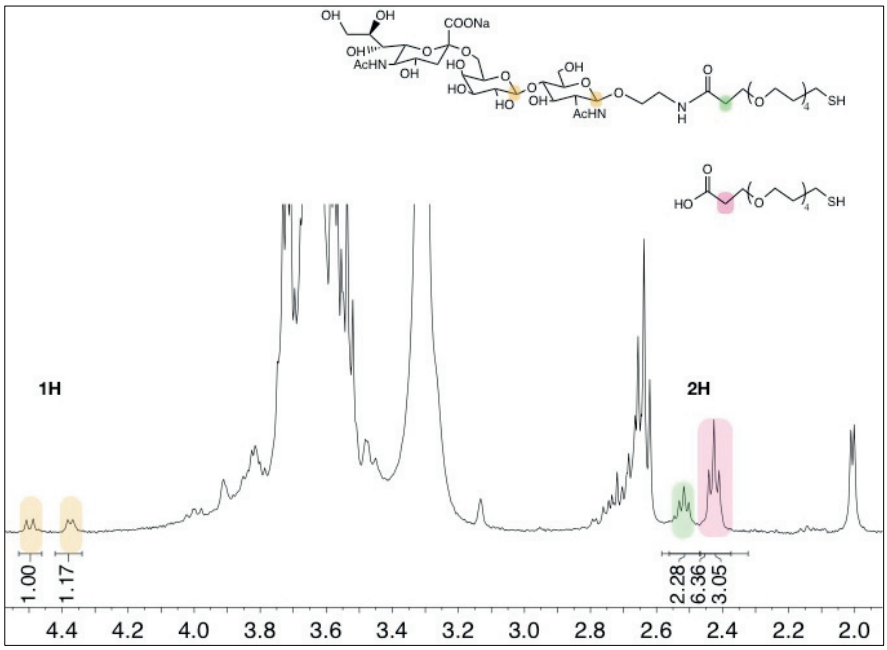

Figure 4.7: NMR spectrum of 6'SLN grafted gold NPs where the spacer ligand is PEG4.

4.1.3. Antiviral assays against influenza

Materials: DMEM– Glutamax medium was purchased from thermofischer scientific. Wash buffer (Tween®), 3,3'-diaminobenzidine (DAB) tablets were purchased from Sigma Aldrich. Primary antibody (Influenza A monoclonal antibody) was purchased from Light Diagnostics. Secondary antibody (Anti-mouse IgG, HRP-linked antibody) was purchased from Cell Signaling Technology®**.** The CellTiter 96® AQ_{ueous} One Solution Cell Proliferation Assay that contains a tetrazolium compound [3-(4,5-dimethylthiazol-2-yl)-5-(3-carboxymethoxyphenyl)-2-(4-sulfophenyl)-2Htetrazolium, inner salt; MTS] and an electron coupling reagent (phenazine ethosulfate; PES) was purchased from Promega.

Dose-response Assays

All the experiments were conducted using MDCK cell line. The cells were passaged and plated using DMEM-Glutamax medium with fetal bovine serum (fbs). Dose-response experiments were conducted at the MOI value of ~ 0.1. In a 96-well plate, 10,000 cells/well plated the day before the experiment. A fix virus concentration (~10^3 virus particles) was incubated with varying dose of materials, for 1 hour at 37°C. The mixture then transferred onto cells. After one 1 hour, the mixture was removed, the cells were washed and fresh medium was added.

In 24 hours, the infection was analyzed with immunocytochemical (ICC) assay. Primarily, the cells were permeabilized with methanol. Then the primary antibody wash added and incubated for 1 hour. The cells were washed with wash-buffer three times; then secondary antibody was added. After 1 hour the cells were washed again with wash buffer and the DAB solution was added. After the addition of the DAB buffer, the infected cells turned into brownish color. The infected cells were counted using the light microscope. EC_{50}, EC_{90} and EC_{99} concentrations of NPs were calculated using the software GraphPad Prism.

Virucidal Assays

The virus (ffu:10^5/mL) and the NPs (at their IC_{99} concentration) were incubated for 1 hour at 37°C. Serial dilutions of the virus-material complex together with the non-treated control was conducted, and transferred onto the cells. After 1 hour, the mixture was removed and the fresh medium was added. Next day, viral titers were evaluated with ICC assay. For the ICC assay, the same procedure described above was followed.

MTS Assays

In a 96-well plate, 10,000 MDCK cells/well plated the day before the experiment. MDCK cells were incubated with a varying dose of NPs (same concentration range in the dose-response assays) overnight. The NPs were removed and the cells were washed. 100 μL of medium and 20 μL of MTS solution were added onto the cells. After an incubation time of 4 hours, absorbance measurements (at 490 nm) were conducted using a plate-reader.

4.2. Designing gold NPs to target the influenza virus

As discussed in the previous two chapters, multivalency enhances the binding affinity between the virus and the NPs by reducing the dissociation constant. At the start of the project, 6'SLN trisachharide (molecule only) was tested against influenza H1N1 Netherlands/09 strain. However, a proper dose-response assay could not be conducted since the toxicity limit was reached before 90% inhibition of the virus. Still, EC_{50} concentration was higher than 500 μg/mL. To conjugate 6'SLNs onto NPs considerably improved the antiviral activity and eliminated the toxicity problem, as it will be shown in this chapter.

In order to find out the ideal spacer to target the HA trimer, two different NPs with a similar 6'SLN density but different type of spacer ligand, HS-PEG8-COOH and HS-C11-COOH (MUA), were synthesized at the start of the project (figure 4.8). PEG8 spacer is hydrophilic and longer whereas C11 is hydrophobic and shorter. Antiviral

activity of NPs against two different human Influenza strains, Neth/09 and H1N1 Clinical, were tested. Clinical strains are particularly important since they are the circulating influenza strains. H1N1 subtype was selected since the H1N1 strains bind to 6'SLN with high affinity, almost with no exception, according to glycan array studies. On the other hand, not all the H3N2 strains bind to 6'SLN with high affinity. Both NPs inhibited the tested strains (table 4-1). However, in the case of C11 the variation between the half inhibitory concentrations was larger. We therefore we concluded that C11 might be too short to inhibit certain influenza strains.

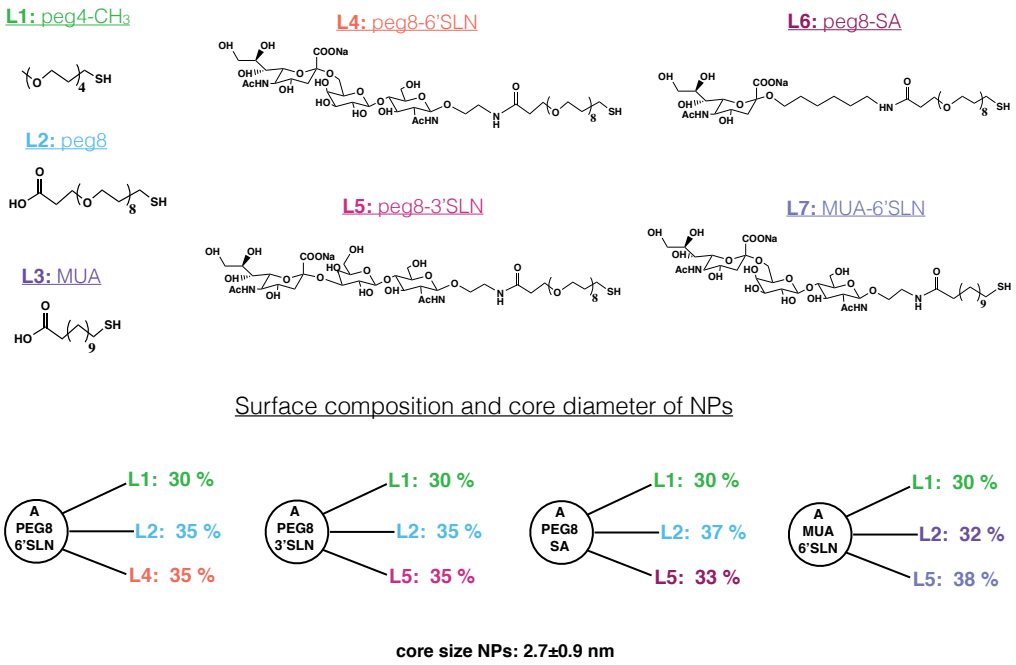

Figure 4.8: The NPs with different linkers as well as end-groups synthesized for the preliminary antiviral assays.

Moreover, to demonstrate 6'SLN is the glycan sequence that binds human influenza viruses with high affinity, NPs coated with 6'SLN, 3'SLN and sialic acid (SA) were synthesized. The resulting NPs have similar ligand compositions but different saccharide end-groups. A big difference was observed between the EC_{50} concentrations of 6'SLN coated NPs versus 3'SLN and SA coated NPs. A-PEG8-3'SLN and A-PEG8-SA poorly inhibited Neth/09 strain and did not inhibit the clinical strain.

Table 4-1: Preliminary studies in which the antiviral activity of NPs with different linkers as well as end-groups were compared

	EC_{50} H1N1 Neth/09 (µg/mL)	**EC_{50} H1N1 Clinical (µg/mL)**
A-MUA-6'SLN	0.5	12
A-PEG8-6'SLN	0.2	0.1
A-PEG8-3'SLN	117.8	N/A
A-PEG8-SA	92	N/A

Apart from the binding affinity, virucidal activity of NPs is the other important focus of this project. NPs with PEG(8) spacer efficiently inhibited influenza. However, for a strong virucidal activity hydrophobic spacer is needed. As concluded from the first experiments, C11 was hydrophobic but probably too short to target HA of certain influenza strains. Therefore, the crystal structure of hemagglutinin was reconsidered to design gold NPs to target HA. Three sialic acid binding pockets that are ~3 nm apart from each other, are located on the globular head of HA. The surface structure of NPs is important in order to target shallow sialic acid binding pockets (figure 4.9). In this respect, chemical properties of spacer ligand as well as the density of 6'SLN groups influence the binding between the NPs and HA.

Regarding the preliminary results as well as the structural considerations described above, HS-C15-COOH was envisioned to be the ideal linker based on two reasons: 1) C15 is sufficiently long to target three sialic acid binding points, that are ~4 nm apart, on the HA trimer 2) Carbon based rigid linker enhances the virucidal activity. Comparative dose-response studies were conducted with multivalent gold NPs having different ligand compositions to support this hypothesis.

4.3. The influence of density of 6'SLN groups on the NP-HA interaction

In order to investigate the importance of 6'SLN density, HS-PEG(5)& 16-mercaptohexadeconic acid (C15) mixed ligand gold nanoparticles with varying density of 6'SLN were synthesized (figure 4.10). PEG(5) enhances water solubility of NPs whereas C15 is the spacer ligand to graft the triscahharide.

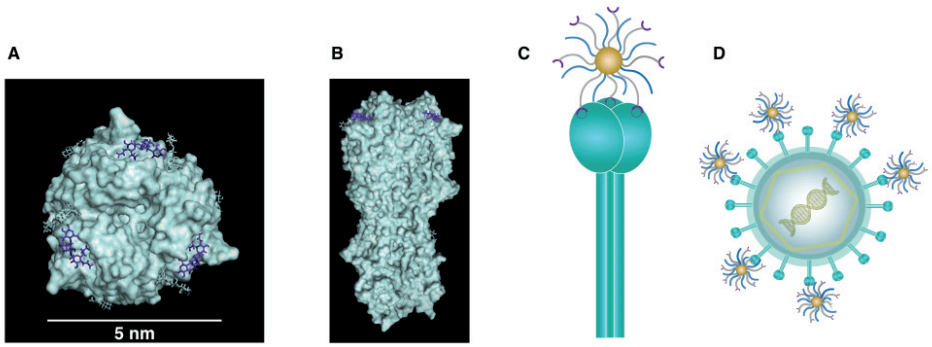

Figure 4.9: Gold NPs target HA located on the viral envelope. Therefore, crystal structure of the HA trimer was taken into consideration to design NPs.

An optimum trisachharide density is important for high affinity binding between the HA trimer and NPs since any extra trisaccharide will hinder the interaction. In order to find out the optimum trisaccharide density, NPs having the same core and ligand composition but different 6'SLN density were synthesized. 3'SLN grafted NPs and PEG(5) NPs served as control NPs.

Dose-response assays against two human influenza A subtypes H1N1 (Netherlands/09), H3N2 (Singapore/04) and one B type were conducted in order to compare the antiviral activity of NPs. NPs were compared based on their half-inhibitory concentrations (EC_{50}). Lower EC_{50} concentrations indicate a stronger antiviral activity.

The strain, which was inhibited with the smallest NP concentration, was H1N1 Netherlands/09 (table 4-2). NPs also inhibited H3N2 strain Singapore/04 with high efficiency (table 4-3). On the other hand, higher NPs concentrations were needed to inhibit influenza B virus, relative to influenza A subtypes (table 4-4).

C15-6'SLN-L NPs (22 trisaccharides/NP) had the lowest EC_{50} concentration against three different influenza viruses tested. This result indicates that optimum trisaccharide concentration is independent from the hemagglutinin mutations. C15-6'SLN-H NPs (38 trisaccharide/NP) showed a stronger inhibition activity than the C15-6'SLN-LL NPs (8 trisaccharide/NP). It is possible that C15-6'SLN-H NPs have

slightly excess trisaccharide, whereas C15-6'SLN-LL NPs are probably unable to target three sialic acid binding points on the HA.

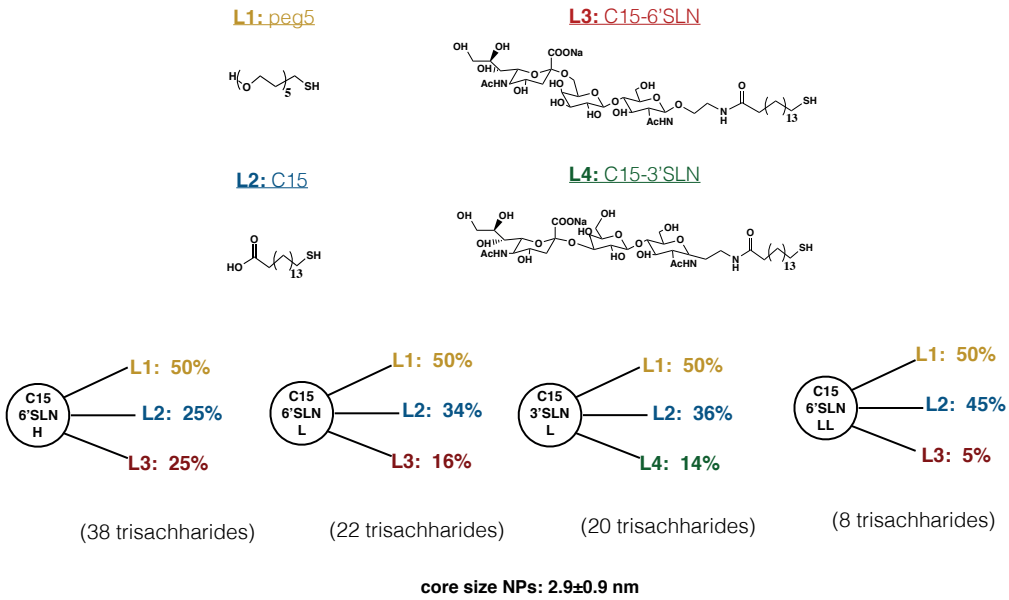

Figure 4.10: Gold NPs having different 6'SLN density. 3'SLN coated NPs were synthesized as well for an additional comparison.

Control experiments were conducted with C15-3'SLN-L NPs and PEG(5) NPs. 3'SLN grafted NPs inhibited the tested viruses at much higher NPs concentrations, relative to the NPs with a similar density of 6'SLN trisachharides: almost 50 times higher EC_{50} concentration to inhibit H1N1/Neth09 strain (table 2) was required. PEG(5) NPs on the other hand showed no inhibition activity against any virus tested.

Table 4-2: Comparative dose-response assays against **Influenza A H3N2 Singapore/2004**

NPs	**EC_{50} (µg/mL)**	**EC_{50} NPs(nM)**	**EC_{50} 6'SLN (nM)**
C15-6'SLN-L	0.13	0.64	14.08
C15-6'SLN-H	0.45	2.2	83.6
C15-6'SLN-LL	1.1	5.4	43.2
C15-3'SLN-L NPs	5.3	27.2	544
PEG5 NPs	N/A	N/A	N/A

Table 4-3: Comparative dose-response assays against **Influenza A H3N2 Singapore/2004**

NPs	EC_{50} (µg/mL)	EC_{50} NPs(nM)	EC_{50} (nM) 6'SLN
C15-6'SLN-L	0.58	2.8	61.6
C15-6'SLN-H	1.12	5.9	224.4
C15-6'SLN-LL	1.9	9.4	75.2
C15-3'SLN-L NPs	4.5	22	440
PEG5 NPs	N/A	N/A	N/A

Table 4-4: Comparative dose-response assays against **Influenza B Yamagata**

NPs	EC_{50} (µg/mL)	EC_{50} NPs(nM)	EC_{50} (nM) 6'SLN
C15-6'SLN-L	13.7	67	1474
C15-6'SLN-H	17.25	85	3230
C15-6'SLN-LL	53.3	260	2080
C15-3'SLN-L NPs	>100	>100	>1000
PEG5 NPs	N/A	N/A	N/A

4.4. The influence of the spacer ligand

In order to further demonstrate C15 enhances the antiviral activity of NPs, three different NPs with a similar 6'SLN density but different type of spacer were synthesized (figure 4.11). PEG(5) NPs were initially synthesized followed by ligand exchange reactions with C15, PEG4 and PEG8 spacer ligands (figure 4.12). C15 and PEG4 spacer have a similar length but different chemical structure. C15 is hydrophobic whereas PEG4 is hydrophilic. PEG8 spacer is also hydrophilic but its molecular weight is higher than PEG4 hence it is a longer spacer. The NPs synthesized are similar in chemical composition with a variation limited to 10%. Low 6'SLN density (22±2 triscahharides/NPs) and high 6'SLN density (36±3 triscahharides/NPs) NPs were synthesized in order to make a better comparison.

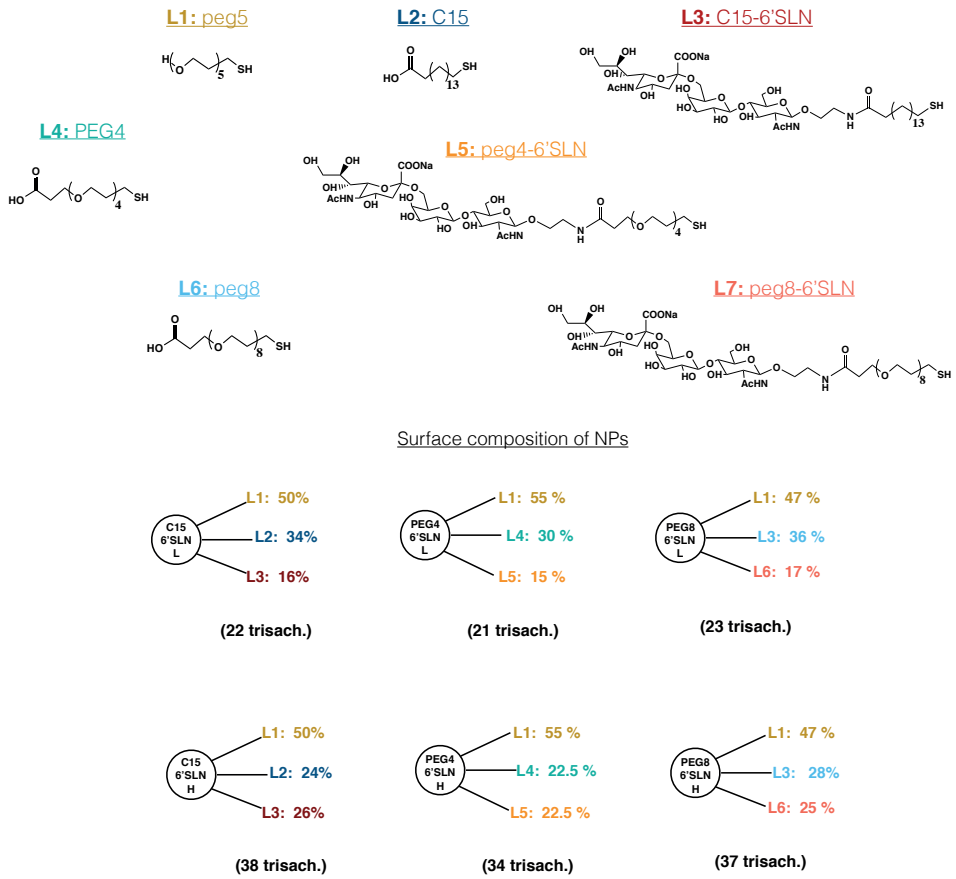

Figure 4.11: 6'SLN coated gold NPs with PEG4, PEG8 or C15 spacer ligands

Comparative dose-response assays were conducted against H1N1 Neth/09 (table 4-5). EC_{50} concentration of NPs with C15 spacer was considerably lower than the NPs with PEG spacers. In the case of NPs with C15 spacer, lower 6'SLN density provided a stronger antiviral activity. Conversely, lower 6'SLN density provided a weaker antiviral activity when the spacer ligand is PEG4 or PEG8. Even though the NPs have similar density of 6'SLNs, their distribution on the NPs surface can be different. This, in turn, may affect the inhibitory concentrations. Also, not necessarily every NP inserts exactly three 6'SLN molecules onto the sialic binding pockets of the HA trimer. It can be only two or even one, in some NP-HA interactions. In the case of C15 spacer, two 6'SLN molecules can be sufficient for high affinity binding, whereas it may not be sufficient for PEG spacers.

Comparative dose-response studies showed that the chemical structure of the spacer ligand significantly affects the NP concentration required to inhibit the influenza virus. The shift in dose-response curves clearly demonstrates the influence of spacer on the EC_{50} values (figure 4.13).

Table 4-5: Comparative dose-response studies against Neth/09 strain with NPs having different spacer ligands.

Spacer	**EC_{50} (µg/mL) Low 6'SLN density**	**EC_{50} (µg/mL) High 6'SLN density**
C15	0.17	0.5
PEG4	33.56	6.53
PEG8	22.81	13.83

This result indicates that chemical structure of the linker is an important factor determining the binding affinity. Hydrophilic ligands have a higher degree of freedom in aqueous media and therefore higher entropic penalty must be paid for binding. This in turn leads to a higher dissociation constant and reduces the binding affinity between the NPs and the virus.

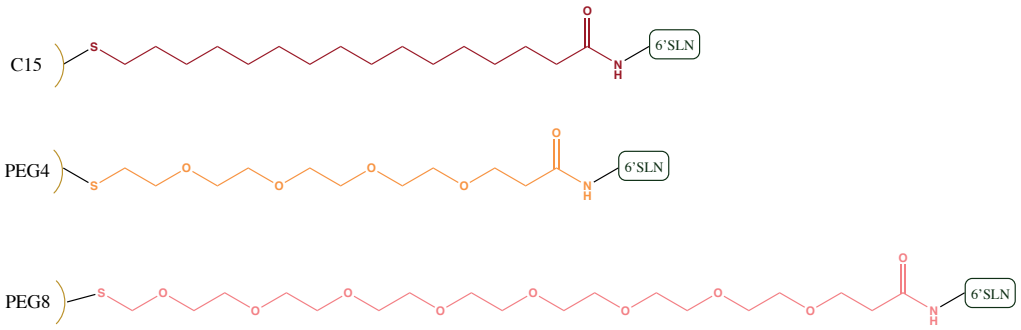

Figure 4.12: Chemical structure of C15, PEG4 and PEG8 spacer ligands.

Additionally, C15 ligand is capable of making hydrophobic interactions with the viral proteins whereas PEG4 and PEG8 ligands are not. It is possible that, once NPs

interacts with 6'SLN binding pockets on the HA, hydrophobic interactions between the HA and the linker may contribute to binding.

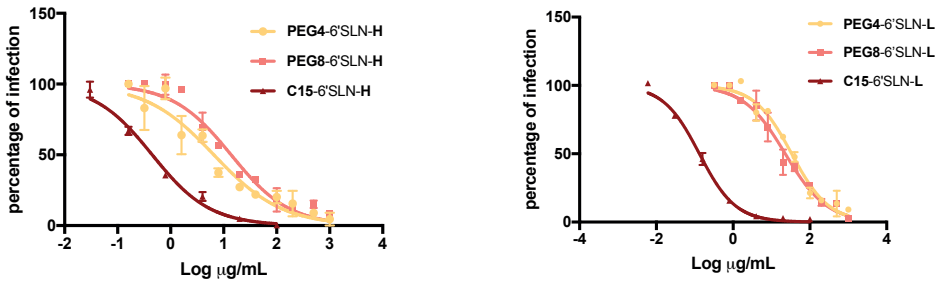

Figure 4.13: Dose-response curves showing the antiviral activity of NPs with different spacers having high density of 6'SLN (left) and low density of 6'SLN (right).

In comparison to other NPs, C15-6'SLN-L NPs showed a strong antiviral activity against all the viruses tested. EC_{50} and EC_{90} values were considerably lower, perhaps due to the sufficient amount of 6'SLN moieties as well as the length and the hydrophobicity of the spacer. Therefore, the following experiments were mainly conducted with C15-6'SLN-L NPs.

4.5. Antiviral Activity of gold NPs against different influenza strains

Influenza A is a rapidly mutating virus. Therefore, many influenza A subtypes and several strains of each subtype exist. For example H3N2 has strains such as H3N2 Hong Kong/1968, H3N2 Singapore/2004 and H3N2 Victoria/2011. It is important to demonstrate the antiviral activity of NPs against different influenza strains since the project is about targeting conserved sialic acid binding pockets on the HA trimer. Therefore, C15-6'SLN-L NPs were tested against different influenza strains (table 4-6). Most of the strains tested are influenza A virus H1N1 or H3N2 subtypes. Additionally NPs were tested against one strain of influenza B, Yamagata. NPs inhibited majority of strains tested, at sub-nanomolar NP and nanomolar 6'SLN concentrations. Exceptionally, NPs had no inhibitory activity against some H3N2 strains such as Bej/92. Indeed, many studies demonstrated that recently the crystal

structure of H3 protein was significantly altered. Therefore, some H3N2 strains gave unexpected results on the glycan array studies.[84–86] It is possible that, 6'SLN binding pockets of these H3N2 strains were modified or lost upon years.

Table 4-6: Antiviral activity of C15-6'SLN-L NPs against different influenza strains.

Strain	EC_{50} (μg/ml)	EC_{50} NPs(nM)	EC_{50} 6'SLN (nM)
H1N1 Neth/09	0.17	0.84	18.4
H1N1 Wsn	8.5	42	924
H3N2 Vic/11	0.1	0.49	10.7
H3N2 Sing/04	0.54	2.6	57.2
H3N2 Bej/92	N/A	N/A	N/A
B Yamagata	0.63	3.08	67.7
H1N1 Clinical/18	0.11	0.53	11.6
B Clinical/18	0.76	3.7	81.4
H3N2 Clinical/18	N/A	N/A	N/A

It is also very important to show the inhibitory activity of NPs against the recent clinical strains. Clinical influenza strains are isolated from patients in the hospitals. They are usually from the current year or the previous year. To conduct antiviral assays against clinical strains is important for two reasons. Firstly, they are the recent strains in circulation. Therefore, if a drug is successful on the clinical strains, it has a bigger potential of reaching the market. Secondly, clinical strains do not have a long passage history. Viral reproduction using several different cell-lines affects the attachment ligands of the virus. Particularly viral reproduction on the egg cells completely changes the receptor preference of the viruses originated from humans. Clinical strains have the minimum number of passages so they best represent the original human viruses. C15-6'SLN-L NPs inhibited clinical strains, influenza A H1N1 and influenza B, from 2018. EC_{50} concentration to inhibit the clinical strains was comparable to other strains tested. However, NPs could not inhibit clinical H3N2 strain.

In order to determine if NPs are specific to influenza, dose-response assays against HSV-2 and enterovirus 68 were conducted. HSV-2 is known to be HSPG dependent virus and enterovirus 68 is known to be sialic acid dependent virus. C15-6'SLN-L NPs showed no inhibitory activity against these viruses.

4.6. Virucidal assays against human influenza viruses

The ultimate goal of this project is to inhibit influenza virus with virucidal mechanism. In the previous sections of this chapter, antiviral activity of NPs was demonstrated with dose-response assays. Virucidal assays were then performed in order to find out if the inhibition is irreversible (figure 4.14). In a typical virucidal assay, NPs are incubated with the virus at their corresponding IC_{99} concentration for a certain amount of time. The inoculum then undergoes into serial dilutions and the residual infectivity of the virus relative to the control is measured.[9] A significant reduction in the viral titer (at least 1 log unit) relative to the control is an indication of virucidal inhibition mechanism. One challenge of virucidal assays is adjusting concentration of the virus and NPs at which the assay is conducted. To have reliable results in a virucidal assay, the virus titer should be high enough ($>10^5$ virus particles/mL). However, dose-response assays are conducted with a smaller virus concentration (10^3-10^4 virus particles/mL). Therefore, the concentration of NPs should be adjusted if the viral concentration is very high.

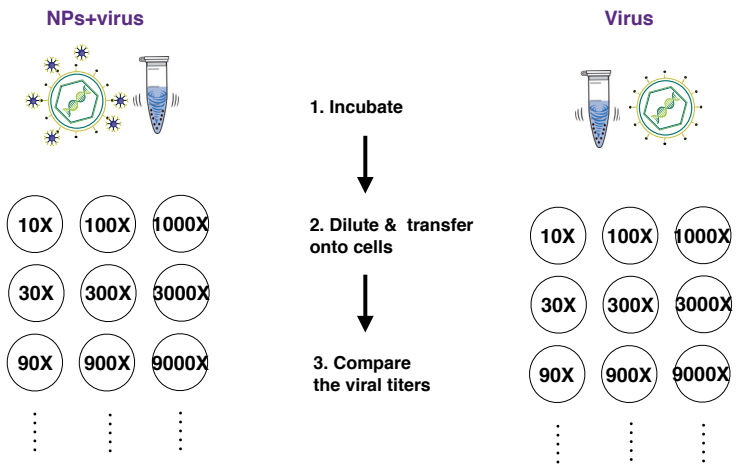

Figure 4.14: Illustration showing the steps of a typical virucidal assay

At the beginning of this chapter, it was demonstrated that one of the initial NPs, A-PEG8-6'SLN, showed a strong antiviral activity against influenza. However, NPs were redesigned to have the C15 spacer instead of PEG8 since hydrophobic content is important for the virucidal activity.

A-PEG8-6'SLN and C15-6'SLN-L NPs have different ligand compositions but similar inhibitory concentrations against Neth/09 strain (table 4-7). Despite the fact that the inhibitory concentrations are comparable, there is a difference in the virucidal activity (figure 4.15). A-PEG8-6'SLN NPs shows some virucidal activity due to the rigidity of the gold core. Also A-PEG8-6'SLN NPs contains PEG(4)-CH_3 ligands. The hydrophobic end of the PEG ligand may also contribute to the virucidal activity. In the case of C15-6'SLN-L NPs, the virucidal activity was enhanced by the rigid spacer (almost 1 log unit more reduction in the viral titer).

Table 4-7: The inhibitory concentrations of A-PEG8-6'SLN and C15-6'SLN-L NPs against H1N1 Neth/09 strain.

	EC_{50} (μg/mL)	**EC_{90}** (μg/mL)	**EC_{99}** (μg/mL)
A-PEG8-6'SLN	0.2	2.4	34
C15-6'SLN-L	0.13	3.5	57

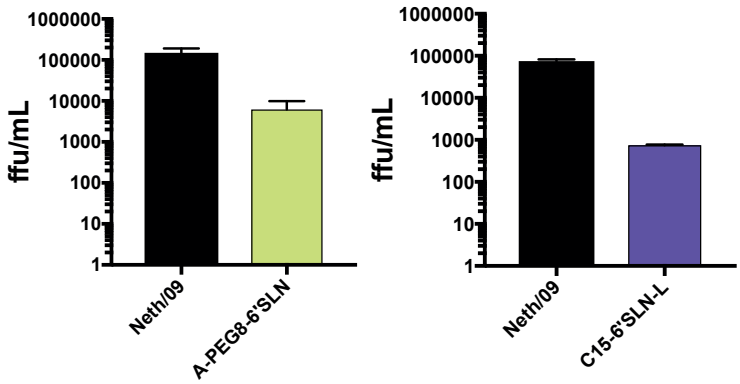

Figure 4.15: Comparison of virucidal activities of A-PEG8-6'SLN and C15-6'SLN-L NPs against H1N1 Neth/09.

The virucidal activity of the C15-6'SLN-L NPs against other influenza strains was tested, as well. Virucidal assays have to be conducted with a high concentration of virus, however reaching high titers with certain influenza strains is difficult. Therefore, in this project virucidal assays against Netherlands, B and Singapore, and Vic/11 were conducted (figure 4.16). Virucidal activity of the C15-6'SLN-L NPs against Neth/09 and Sing/04 strains was tested by increasing the virus concentration ten times relative to the dose-response experiments.

Table 4-8: Inhibitory concentrations of C15-6'SLN-L NPs against different influenza strains. The virucidal assays were conducted at EC99 concentrations.

	EC_{50} (µg/mL)	**EC_{90}** (µg/mL)	**EC_{99}** (µg/mL)
H1N1 Neth/09	0.13	3.5	57
H3N2 Sing/04	0. 45	4.3	37
H3N2 Vic/11	< 0.16	< 0.16	100
B/Yam	13.7	339	-

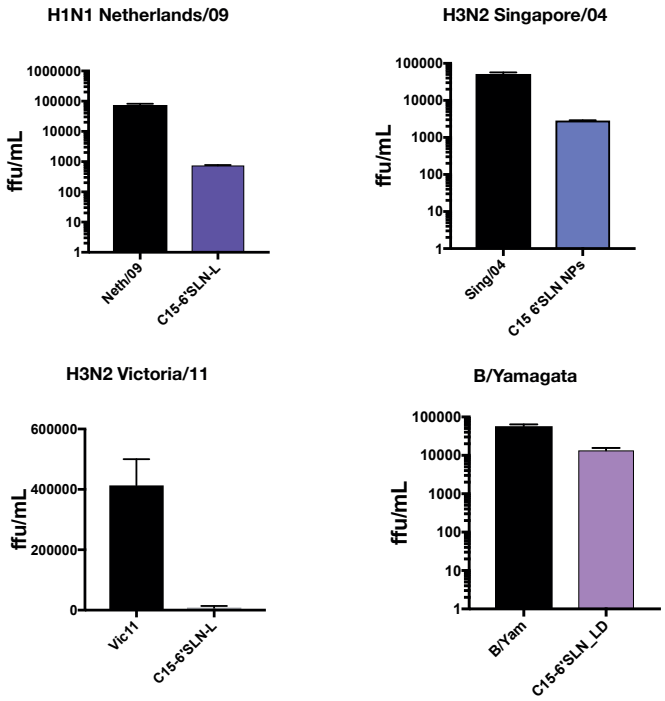

Figure 4.16: Virucidal activity of C15-6'SLN-L NPs against different influenza strains

The titer of the Neth/09 strain was reduced by 2 log units whereas Sing/04 was reduced by 1.5 log units. 1-2 log units reduction in the viral titer indicates that the inhibition is irreversible. One problem with influenza B/Yamagata was the big variation between different results. Also the inhibitory concentrations were higher in comparison to influenza A strains. Therefore, the virucidal assay was conducted at EC_{90} concentration of NPs. As a result, the virucidal activity was weaker.

To conduct the virucidal assays, NP concentrations were not increased linearly with the virus concentration, to be on the safe side. However, it is possible to increase the NP concentration further for a stronger virucidal activity. Indeed, the virucidal assay for Vic/11 strain was conducted at higher virus as well as NPs concentrations. The main purpose of working with this strain was the TEM studies, which requires higher concentrations of the inoculum.

In order to study the effect of the 6'SLN density on the virucidal activity, comparative studies with C15-6'SLN-L and C15-6'SLN-H NPs were conducted. The latter has a higher EC_{99} concentration; therefore the NP concentrations in the virucidal assays were different. There was a slight difference in the virucidal activity, but nothing noteworthy (figure 4.17). If the EC_{99} concentration of the material is very high (above 500 µg/mL), to results of the virucidal assay may give false positive results. Therefore, virucidal assays were not conducted with the other NPs.

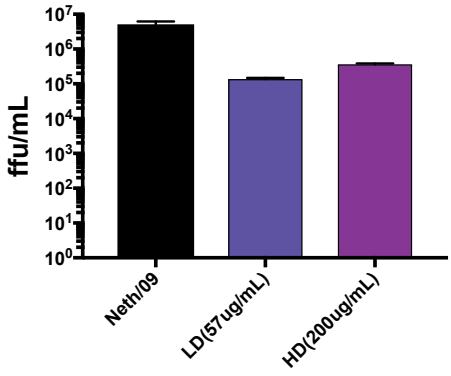

Figure 4.17: The effect of 6'SLN density on the virucidal activity was evaluated by comparing C15-6'SLN-L and C15-6'SLN-H NPs.

4.7. TEM studies demonstrating the interaction between the influenza virus and the NPs

In order to visually demonstrate the interaction between the NPs and the influenza virus, dry TEM studies were conducted. C15-6'SLN-L NPs were incubated with the purified influenza H3N2 Vic/11 virus for 1 hour. TEM grids were prepared, without further dilution because high inoculum concentration is important for the TEM studies. Methyl tungsten staining was then applied onto the grids. The control experiment was conducted with PEG(5) NPs which showed no inhibitory activity against influenza virus in the dose-response assays.

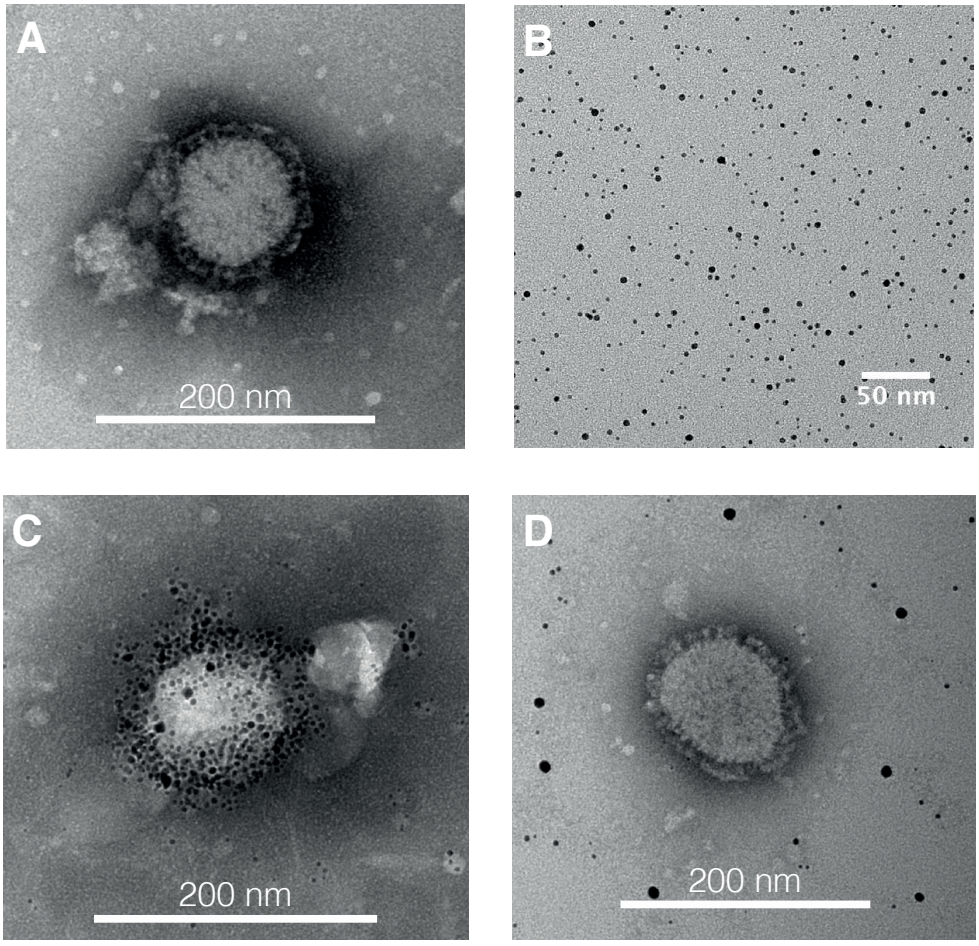

Figure 4.18: TEM image of the H3N2 Vic/11 influenza virus (A). TEM image of gold NPs (B). TEM image of C15-6'SLN-L NPs-H3N2 Vic/11 influenza virus complex (C) TEM

image of PEG(5) NPs-H3N2 Vic/11 influenza virus complex. TEM images with viruses are produced by Valeria Cagno in the Universtiy of Stanford.

Figure 4.18 A shows the virus before incubation with NPs. The viral envelop covered with the HA and NA proteins is clearly seen in the image. Figure 4.18 C shows the virus incubated with C15-6'SLN-L NPs for 1 hour. As the image demonstrates, NPs are densely located on the viral envelope. Figure 4.18 D shows the virus incubated with PEG(5) NPs. Similar to dose-response assays, no interaction between the virus and the NPs was observed.

4.8. Cell Viability Assays

The aim of this project was to design NPs that are virucidal against influenza while being non-toxic to cells. Therefore, toxicity tests were an important part of the project. During the initial stage of the project, we only focused on the viability of the cells. It is possible to conduct very detailed toxicity studies at later stages of the research. Particularly in the in-vivo stage, it is very important to characterize the toxicity of NPs on the tissues.

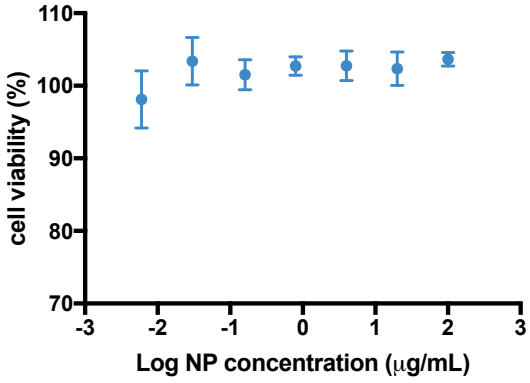

Figure 4.19: The plot shows the viability of the cells treated with a varying concentration of C15-6'SLN-L NPs.

MTS assay is a colorimetric assay demonstrating metabolic activity of the cells. Number of viable cells correlates with NAD(P)H-dependent cellular oxidoreductase

enzymes that reduce MTS tetrazolium. The reduction reaction results in a color change and can be observed through absorbance measurements.

NPs were incubated with the cells overnight, and then MTS treatment was conducted. The MTS assay was evaluated with the plate reader. Similar to dose-response assays, the median lethal dose (LD_{50}) can be calculated from the MTS assay.

Table 4-9: Table showing the toxicity of other gold NPs synthesized. The assays were conducted at the same concentration range dose-response assays were conducted.

NPs	LD_{50} (μg/mL)	NPs	LD_{50} (μg/mL)
C15-6'SLN-L	>100	PEG4-6'SLN-L	>100
C15-6'SLN-H	>100	PEG8-6'SLN-L	>100
C15-6'SLN-LL	>100	PEG4-6'SLN-H	>100
C15-3'SLN-L	>100	PEG4-6'SLN-H	>100

Toxicity tests were conducted at the same NP concentration range as the dose-response assays. NP treated cells were compared to non-treated cells. There was no significant difference between the NP treated cells and non-treated cells at the NP concentration range of 0.03-100 μg/mL. Almost, 100% of the cells were viable. Indeed, any gold NPs synthesized in this project, were non-toxic in this concentration range (table 4-9). Figure 4.19, shows the toxicity test results of C15-6'SLN-L NPs.

4.9. Conclusion

In this chapter it was shown that gold NPs successfully inhibited human influenza viruses with virucidal inhibition mechanism. The chemical structure of the spacer ligand as well as 6'SLN density plays a big role in the inhibitory activity. Any hydrophobic content, even if it is a small quantity, enhance binding as well as virucidal activity. For example, A-PEG_8-6'SLN NPs that contain PEG ligand with a hydrophobic end (HS-PEG4-CH_3) inhibited influenza virus at very small NP concentrations and showed some virucidal activity. C15-6'SLN-L NPs inhibited

several human influenza viruses at very low NP concentrations, including recent clinical strains. Virucidal assays against H1N1 Netherlands/09, H3N2 Vic/11 and Sing/04 resulted in more than 1 log unit reduction in the viral titer, indicating virucidal inhibition mechanism. Certain H3N2 strains could not be inhibited, probably due to changes in the glycan binding affinity of the viral ligands.

Gold is a biocompatible however, not biodegradable material. Therefore, it is unlikely that gold nanoparticles will be used to treat influenza. For this reason, further biological assays such as ex-vivo and in-vivo were not conducted with gold NPs.

CHAPTER 5

Modified Cyclodextrins Against Influenza

Cyclodextrins are cyclic oligosaccharides that can be formed by 6 (α-cyclodextrin), 7 (β-cyclodextrin) or 8 (γ-cyclodextrin) glucose molecules (figure 5.1). Among the three, β-cyclodextrin has the most stable chemical structure. Cyclodextrins are widely used in the drug delivery systems for different purposes such as enhancing the solubility and stability of the drug; increasing the circulation time; reducing irritations.[87–89] Furthermore, cyclodextrins can serve as multivalent scaffolds as they can be modified selectively with functional groups such as azide, thiol and carboxylic acid.[90,91] In this project cyclodextrins were used as multivalent scaffolds to target hemagglutinin trimer as an alternative to gold NPs.

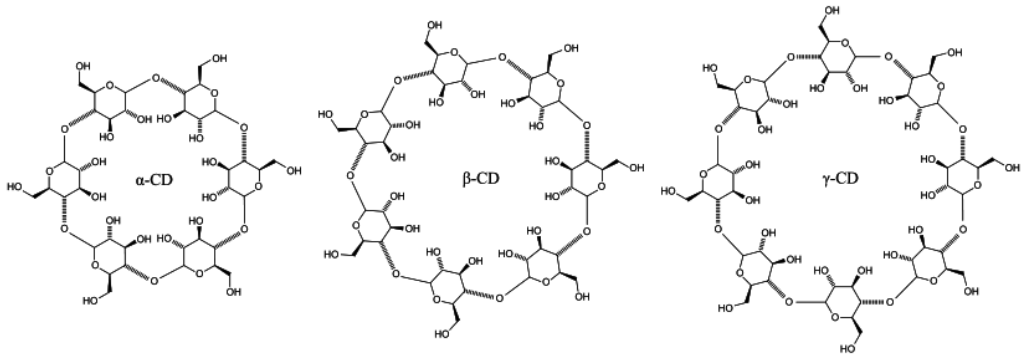

Figure 5.1: Chemical structure of alpha, beta and gamma cyclodextrin

β-Cyclodextrin (β-CD) was envisioned to be the ideal organic scaffold to replace gold NPs in comparison to other organic scaffolds such as dendrimers, dendrons and polymer nanoparticles (figure 5.2). First of all, the core diameter of β-CD (d~1.5 nm) is comparable to the gold NPs (~3 nm) and matches well with the HA globular head

(~5 nm). Different from many other organic materials, cyclodextrin has a rigid structure, which contributes to the virucidal activity together with the spacer ligand. Also, cyclodextrins can be modified to have maximum 7 trisaccharides, and more realistically 2-4, that corresponds to the number of sialic acid binding points on the HA globular head. Therefore, β-CD was modified with rigid spacer ligands and 6'SLN was grafted in a similar way to gold nanoparticles.

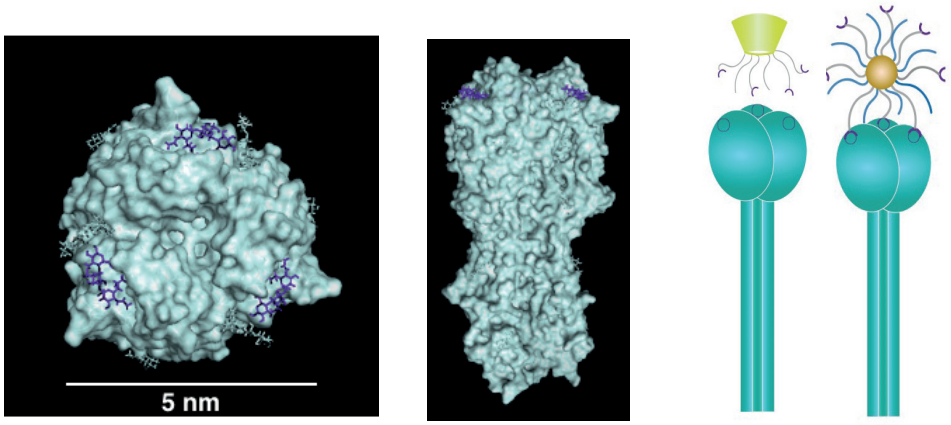

Figure 5.2: To target HA trimers, gold core was modified into cyclodextrin core, to make a completely organic nanomaterial.

5.1. Materials and Methods

5.1.1. Synthesis of the modified cyclodextrins

Materials: All the solvents were purchased from sigma Aldrich. N-hydroxysuccinimide ester (NHS), ethylcarbodiimide hydrochloride (EDC-HCl) and 4-(dimethylamino)-pyridin (DMAP), 6-heptenoic acid was purchased from Sigma-Aldrich. Neu5Acα(2,6)-Galβ(1-4)-GlcNAc-β-ethylamine was purchased from TCI chemicals. Heptakis-(6-deoxy-6-mercapto)-beta-Cyclodextrin and Carboxymethyl-beta-Cyclodextrin sodium salt was purchased from cyclodextrin shop. 11-dodecenoic acid was purchased from abcr GmbH. 14-pentadecenoic acid was purchased from Larodan AB.

Methods: Cyclodextrin derivatives to target influenza virus were synthesized in three steps (figure 5.3). The first step is the conjugation of the spacer ligands onto the β-cyclodextrin through thiol-ene reaction, which is an organic reaction between a thiol and alkene to form an alkyl sulfide under UV light. The second step is NHS activation of the –COOH end group of the spacer ligand. The last step is 6'SLN grafting onto the spacer ligands. To conduct the control experiments, 6'SLN modified β-cyclodextrin without additional spacer ligands, which lacks the first step, was synthesized.

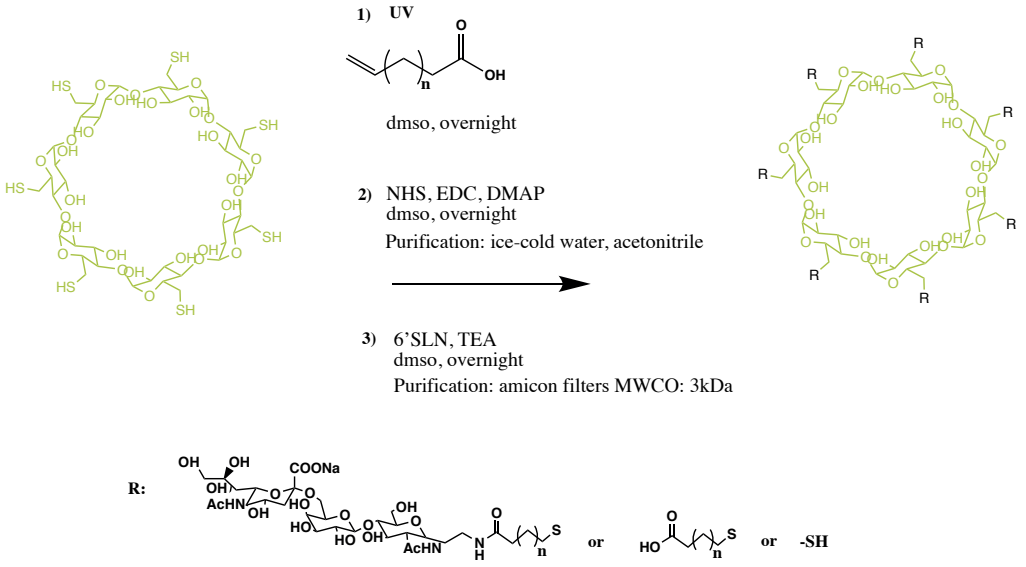

Figure 5.3: Reaction procedure to synthesize 6'SLN modified β-cyclodextrin.

Step1: Modification of cyclodextrins with spacer ligands

0.04 mmol Heptakis-(6-deoxy-6-mercapto)-beta-Cyclodextrin was mixed with 0.28 mmol of bi-functional molecules bearing an allyl and a carboxylic acid groups. (6-heptenoic acid, 11- dodecenoic acid or 14-pentadecenoic acid) in 5 mL of dmso. An overnight reaction was conducted under the UV light.

Step2: NHS activation

To the reaction mixture described above 1.12 mmol NHS 0.56 mmol EDC-HCl and 0.02 mmol DMAP was added. The activation reaction was conducted overnight. Next day, the resulting cyclodextrin was first precipitated from ice-cold water. Then from acetonitrile and lastly from diethyl ether. The product was dried under vacuum.

Step3: 6'SLN grafting

5.6 μmol Neu5Acα(2,6)-Galβ(1-4)-GlcNAc-β-ethylamine was mixed with 1.6 μmol of the CD derivative obtained in the step 2. 15 μmol TEA was added and the reaction was conducted overnight in 1 mL dmso. Next day, the material was diluted with 0.01 M phosphate buffer (pH:7.5) and concentrated using amicon filters (MWCO:3k). The resulting material was further washed ten times with distilled water.

6'SLN grafted β-cyclodextrins without spacer ligands

Carboxymethyl-beta-Cyclodextrin sodium salt (0.04 mmol) was activated with 1.12 mmol NHS 0.56 mmol EDC-HCl and 0.02 mmol DMAP was added. The activation reaction was conducted overnight. Next day, the resulting cyclodextrin was first precipitated DCM-diethyl ether mixture and further washed three times. The product was dried under vacuum. 6'SLN grafting was conducted in the same way as step 3.

Sialic acid (aminohexyl Neu5Ac) grafted β-cyclodextrins

Aminohexyl Neu5Ac was synthesized following a previously reported protocol.[92] The details of the synthesis as well as the characterization results can be found in the appendix B. Step 1 and 2 were conducted with 6-hexadecenoic acid modified β-cyclodextrin. 5.6 μmol aminohexyl Neu5Ac was mixed with 1.6 μmol of the CD derivative obtained in the step 2. 15 μmol TEA was added and the reaction was conducted overnight in 1 mL dmso. Next day, the material was diluted with 0.01 M phosphate buffer (pH:7.5) and concentrated using amicon filter (MWCO:3k). The resulting material was further washed ten times with the distilled water.

5.1.2. Antiviral Assays Against Influenza

In-vitro dose-response and virucidal assays were conducted in the same way with the gold NPs described in chapter 4.1.2.

Ex-vivo experiments

Ex-vivo experiments were conducted by Dr. Valeria Cagno, in the University of Geneva. Human airway epithelia reconstituted *in vitro, MucilAir* tissues, (Epithelix Sàrl, Geneva, Switzerland) were cultured at the air-liquid interface from a mixture of nasal polyp epithelial cells originating from 14 healthy donors. Influenza H1N1 Neth/09 ($5X10^5$ virus particles/mL) and CD-C11-6'SLN (25 μg) were transferred onto tissues without pre-incubation, together with non-treated control. After 4 hours of incubation time, the tissues were washed twice. On a daily basis, the basal medium was changed. To conduct daily qPCR measurements, 200 uL of medium was added onto tissues and then collected in 20 minutes. RNA extracted with NucliSens easyMAG (bioMérieux, Marcy L'Etoile, France) was quantified by using qPCR with the QuantiTect kit (#204443; Qiagen, Hilden, Germany) in a StepOne ABI Thermocycler.

In-vivo experiments

In-vivo experiments were conducted by Dr. Ronan Le Goffic and Dr. Valeria Cagno in French National Institute for Agricultural Research,Paris. Four groups of five BALB/c mice were intranasally treated at day 0 with 50 μl of PBS or CD-C11-6'SLN (25 μg) and immediately inoculated with H1N1 Neth/09 (10^2 pfu). On a daily basis, body temperature and the weight of the mice were measured. Two days post-infection, 2 groups of mice were killed. Lung homogenate and nose mucosa were collected to quantify the viral titer through qPCR mesurements. The other treated group was retreated with the same amount of CD-C11-6'SLN. Two days after, all the remaining mice were killed, lung homogenate and nose mucosa were collected. After the tissue disruption, the RNA was extracted with Trizol and quantified by using qPCR.

5.1.3. Characterization of the modified cyclodextrins

^{1}H NMR studies were conducted in order to characterize the cyclodextrin derivatives. First of all, peak broadening occurs once the spacer ligands are grafted onto the cyclodextrin since the freedom of the molecules is restricted (figure 5.4).

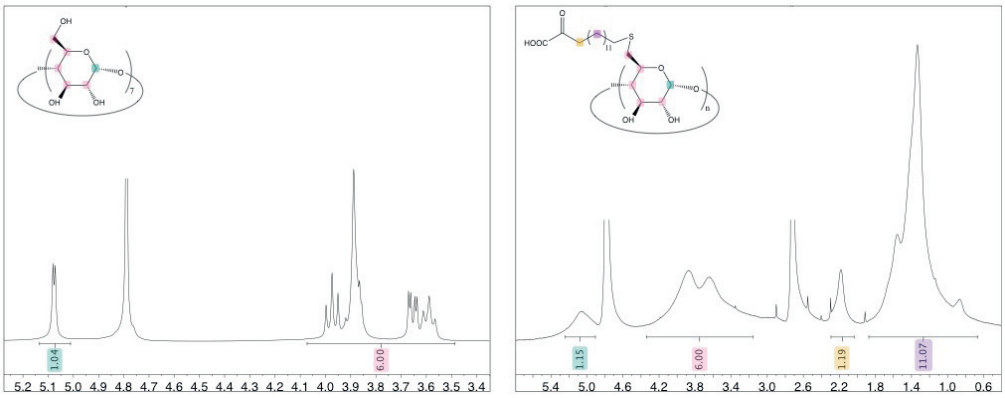

Figure 5.4: Peak broadening effect upon grafting of spacer ligands onto β-CD (solvent: D_2O).

Even though, broadening may increase the error percentage of the integrals, it is possible to calculate the average number of 6'SLN trisaccharide and spacer ligand per CD (figure 5.5).

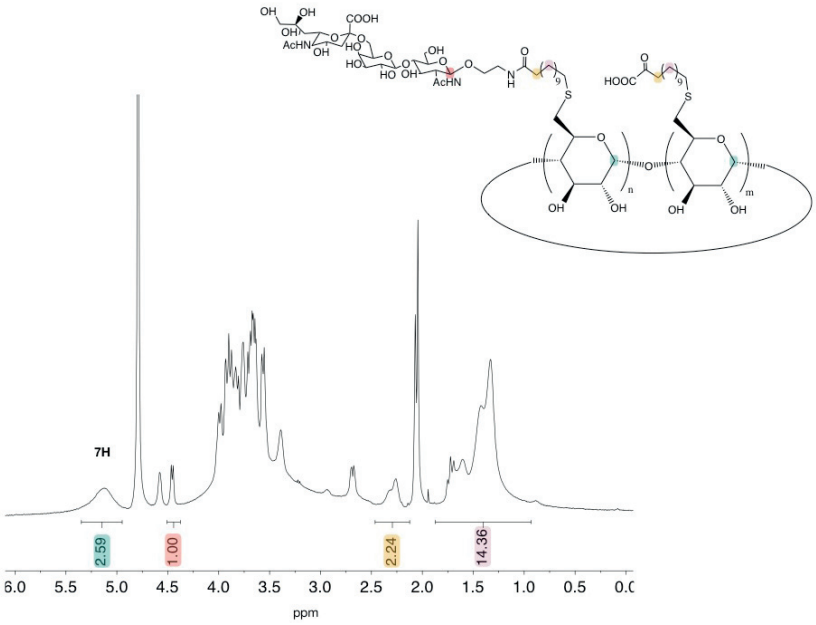

Figure 5.5: NMR spectrum of the CD-C11-6'SLN. Average number of 6'SLN per β-CD is calculated by comparing the specific peaks from each molecule (NMR solvent: D_2O).

The specific peak from the 6'SLN molecule (the doublet at 4.4 ppm which corresponds to 1H) was compared to the specific peak from cyclodextrin (the peak at 5-5.5 ppm, corresponds to 1H/glucose forming the cyclodextrin). The specific peak for the spacer ligand (the peak at 2.2-2.5, corresponds to 2H near carboxylic acid end-group) involves both free and 6'SLN grafted spacer ligands.

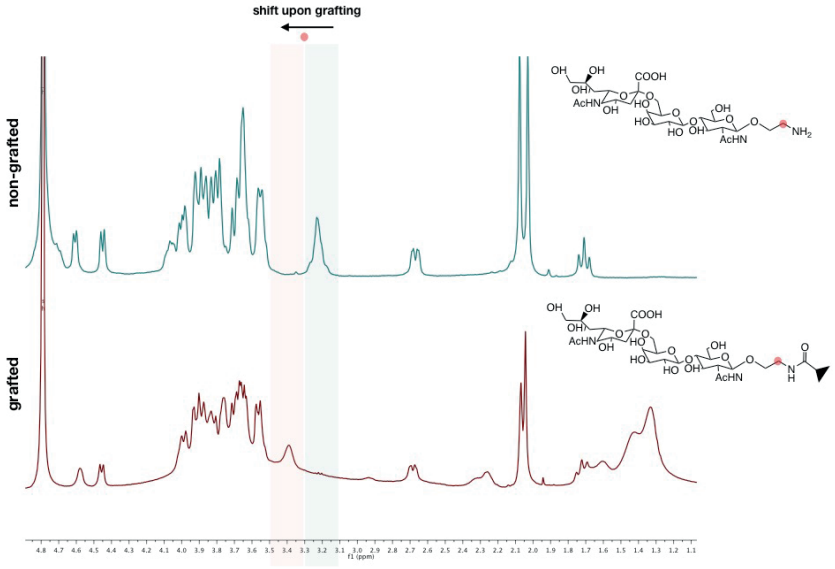

Figure 5.6: The grafting of 6'SLN onto spacer ligand is monitored through the shift of a peak from the amine terminated 6'SLN.

It is also possible to observe amide bond formation in the NMR spectrum. When amine terminated 6'SLN trisaccharide is grafted onto the spacer ligand, the hydrogens near the amine end-group shifts from 3.1-3.3 ppm to 3.3-3.5 ppm (figure 5.6). This small shift is typically observed upon amide bond formation.

Table 5-1: Average number of 6'SLN/CD core calculated by NMR. To calculate the estimated molecular weight the average number of spacer ligands was assumed to be 4.

	6'SLN/CD	Estimated MW
CD-C1-6'SLN	~ 2.8	~ 3.7 kDa
CD-C6-6'SLN	~ 2.8	~ 3.9 kDa
CD-C11-6'SLN	~ 2.7	~ 4 kDa
CD-C14-6'SLN	~ 3.1	~ 4.4 kDa

6'SLN grafted cyclodextrins bearing a spacer of different length were characterized in the same way (table 5-1). The increase of the spacer ligand length can be observed in the stacked spectrum (figure 5.7). As the spacer length increases (from top to bottom), the peak between 1-1.8 ppm enhances.

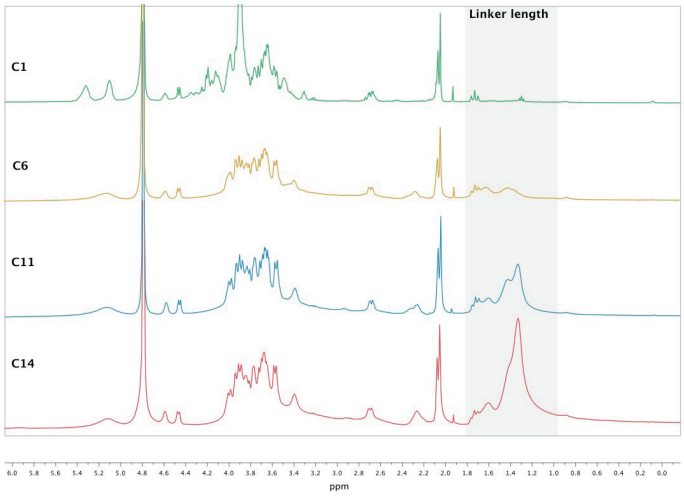

Figure 5.7: The stacked NMR spectrum of 6'SLN grafted β-CDs with different spacer size.

5.2. The influence of the spacer on the inhibitory activity

6'SLN coated Gold NPs bearing C15 spacer successfully inhibited influenza with virucidal inhibition mechanism. To repeat these results with the cyclodextrin core, certain structural considerations have to be done.

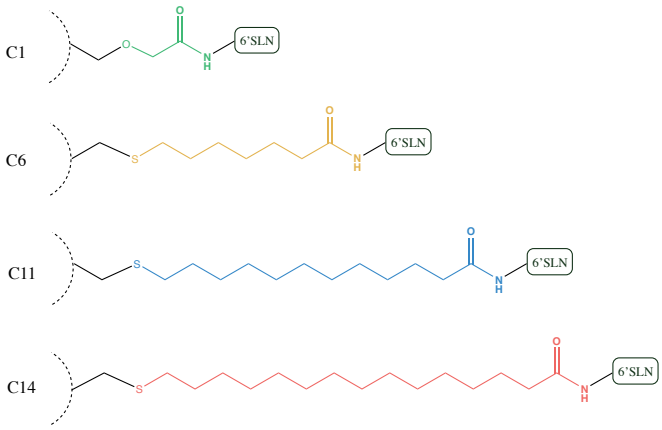

Figure 5.8: 6'SLN grafted β-CDs with different spacer size

The size of the gold core (~ 3 nm) and β-CD (~ 1.5 nm) are comparable. However, gold NPs contain much higher number of ligands. Therefore, the ideal spacer may not be the same. For this reason, 6'SLN trisaccharides were grafted onto β-CD bearing C6, C11or C15 spacers as well as onto β-CD without any additional spacer (C1).

Table 5-2: Comparative dose-response assays against **Influenza H1N1 Neth/09**

CD	**EC_{50}** (μg/mL)	**EC_{50} 6'SLN** (nM)	**EC_{50} CD** (nM)	**EC_{90}** (μg/mL)
C6-6'SLN	0.29	213	74	2.7
C11-6'SLN	0.17	114	42.5	3.4
C14-6'SLN	0.79	570	179	36
C1-6'SLN	171	121,000	46,000	-

Table 5-3: Comparative dose-response assays against **Influenza H3N2 Sing/04**

CD	**EC_{50}** (nM)	**EC_{50} 6'SLN**(nM)	**EC_{50} CD**(nM)	**EC_{90}** (μg/mL)
C6-6'SLN	0.27	185	69	1.7
C11-6'SLN	0.17	121	42.5	0.7
C14-6'SLN	0.22	156	50	2.7
C1-6'SLN	191	121,000	51,600	-

Table 5-4: Comparative dose-response assays against **Influenza B Yamagata**

CD (B/Yam)	**EC_{50}** (μg/mL)	**EC_{50} 6'SLN** (μM)	**EC_{50} CD**(μM)	**EC_{90}**(μg/mL)
C6-6'SLN	4.5	3	1	-
C11-6'SLN	2.2	1.5	0.5	48
C14-6'SLN	20.38	14	4.5	92
C1-6'SLN	127	89	34	-

In a similar way to the previous chapter, the resulting cyclodextrins were tested against H1N1 Neth/09, H3N2 Sing/04 and B/Yamagata. Except the cyclodextrin without additional spacers (C1), all the other cyclodextrin derivatives had a good inhibitory activity against the influenza strains tested. Introducing a sufficiently long

spacer ligand clearly enhanced the end-group flexibility. Therefore, the binding affinity between the CD-C1-6'SLN and the HA trimer is much weaker in comparison to other CD derivatives. As a result, the inhibitory concentrations were much higher. As it was the case for gold NPs, influenza B/Yamagata was inhibited (table 5-3) at higher material concentrations in comparison to Neth/09 and Sing/04 strains (table 5-1 and 2). In comparison to CD-C11-6'SLN and CD-C6-6'SLN, the inhibitory concentrations of the CD-C15-6'SLN was higher. However, this can also be because of aggregation of the macromolecule, since it has more hydrophobic content. In terms of toxicity, there was no big difference between the three CD derivatives (figure 5.9). At all the concentrations tested, the cell viability was above 90%.

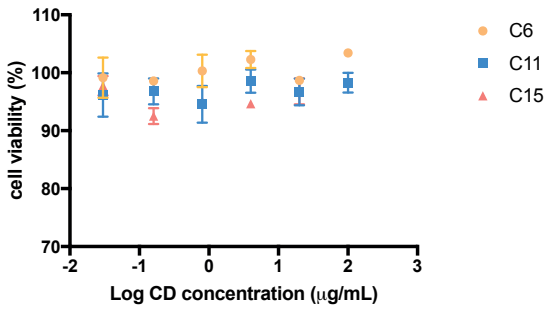

Figure 5.9: Cell Viability assays. MDCK cells were treated with varying concentration of CDs and MTS assays were conducted.

At this point, it was important to select the most promising cyclodextrin derivative to conduct the further biological assays such as ex-vivo and in-vivo. Therefore, a comparative virucidal assay was also conducted (figure 5.10). CD-C11-6'SLN and CD-C6-6'SLN had comparable inhibitory and virucidal activity. At a concentration of 100 mg/mL, both reduced the viral titer by three logs. To conduct these experiments, several batches of 6'SLN grafted CDs were synthesized. All the batches of CD-C11-6'SLN had a good inhibitory activity, however one batch of CD-C6-6'SLN had a weaker inhibitory activity. We thought that CD-C6-6'SLN might be more sensitive to synthesis related variations. Therefore, CD-C11-6'SLN was selected to conduct ex-vivo and in-vivo experiments.

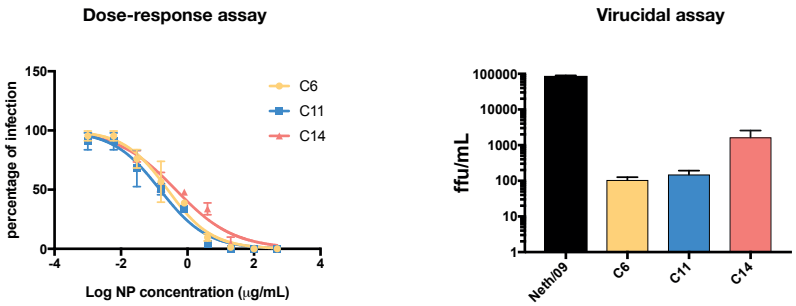

Figure 5.10: Comparative dose-response curves (left) and virucidal assays against H1N1 Neth/09

5.3. Mono sialic acid grafted β-CD

In the previous chapter, it was demonstrated that mono sialic acid grafted gold NPs poorly inhibited H1N1 Neth/09 and Clinical strains. Mono sialic acid was also grafted onto β-CD and was tested against H1N1 Neth/09, H3N2 Sing/04 and B/Yam. Surprisingly the inhibitory activity was strong this time (table 5-5).

Table 5-5: Inhibitory activity of SA grafted β-CD against influenza

CD	EC_{50} Neth/09	EC_{50} Sing/04	EC_{50} B/Yam
C12-SA	0.9 µg/mL	1.2 µg/mL	2.2 µg/mL

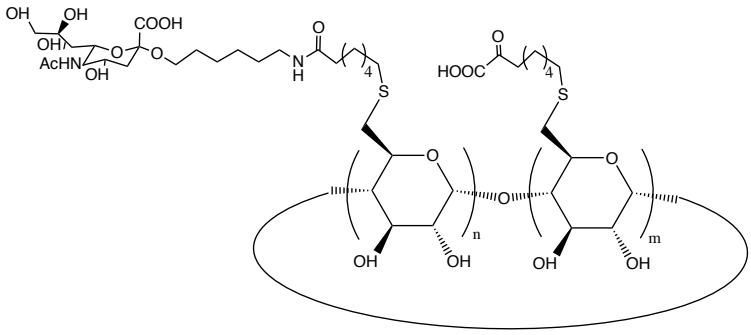

Figure 5.11: Chemical structure of sialic acid (Neu5Ac) grafted β-CD

This is probably because the structure of the scaffold as well as the spacer positively contributes to binding. Therefore, three sugars may not be necessary for a strong binding to the HA trimer. This result indicates that the spacer ligand and the core material have a strong influence on the binding affinity. Sialic acid grafted β-CD also showed some virucidal activity (figure 5.12). However, the assay needs to be repeated since the virus concentration was very low.

For the time being, sialic acid grafted β-CDs were not further investigated since the scope of this thesis is specific irreversible inhibition. However, sialic acid grafted β-CDs have the potential of becoming broad-spectrum antivirals against sialic acid targeting viruses. Therefore, the broad-spectrum virucidal activity of sialic acid grafted β-CDs will be studied in the near future.

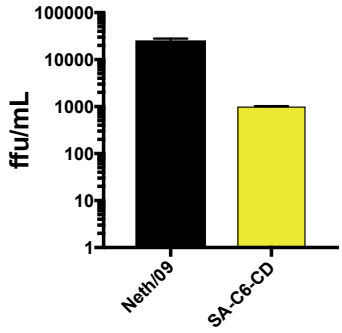

Figure 5.12: Virucidal activity of SA-CD against H1N1 Neth/09

5.4. In-vitro Virucidal activity of CD-C11-6'SLN

In-vitro virucidal activity of CD-C11-6'SLN against influenza H1N1 Neth/09, H3N2 Sing/04, H3N2 Vic/11 and B/Yam was firstly evaluated with in-vitro assays. Virucidal assays were conducted with 100 mg/mL CD-C11-6'SLN, even though EC_{99} concentration was lower. Therefore, it is possible that some degree of virustatic inhibition was also involved. However, most of the effect is virucidal. As it was mentioned in the previous chapter, to enhance the virucidal effect, it is possible to increase the material concentration. The limit is, to increase the material concentration linearly with the virus concentration. The reason why the concentrations were

increased is to make a good estimation for ex-vivo and in-vivo concentrations. For ex-vivo and in-vivo, to inactivate the virus (almost completely) at the first instance is important. Virustatic effect will not be a problem, since the virus continuously replicate.

Figure 5.13 shows that CD-C11-6'SLN reduced the viral titers of H1N1 Neth/09, H3N2 Sing/04, H3N2 Vic/11 by 2-3 log units. As it was the case for gold NPs, the virucidal activity against influenza/B was weaker.

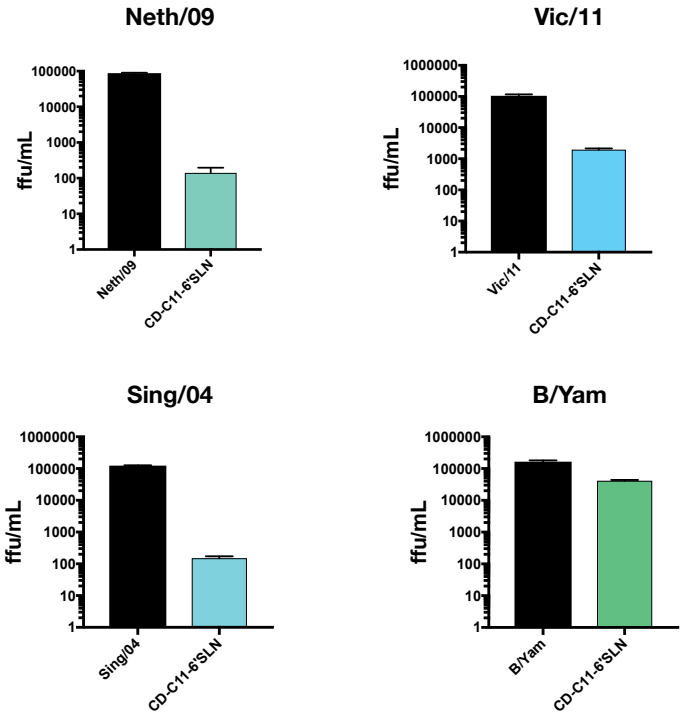

Figure 5.13: Virucidal activity of CD-C11-6'SLN against different influenza strains

To show the time dependence of the virucidal activity, H1N1 Neth/09 was incubated with CD-C11-6'SLN for 15 minutes, 1 hour and 2 hours (figure 5.14). Following the incubation period, the dilutions were conducted. We observed that the virucidal inhibition starts within 15 minutes, then further increases next 45 minutes. After 1 hour, the viral titer does not further decrease.

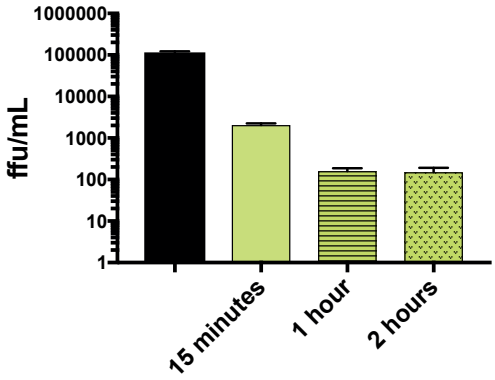

Figure 5.14: Time dependence of virucidal activity. Influenza strain:H1N1 Neth/09

5.5. CD-C11-6'SLN against Clinical Strains

As it was mentioned in the previous chapter, the clinical strains are very important because of two reasons: 1) they are recently circulating strains 2) the viral ligands are not adapted to cell-lines. Therefore, CD-C11-6'SLN was tested against H1N1, H3N2 and B Clinical influenza strains. In line with the other results, the strongest inhibitory activity was against influenza A H1N1. The inhibitory activity was weaker against influenza B and there was no inhibitory activity against H3N2 (table 5-6).

Table 5-6: Antiviral activity of C11-6'SLN against Clinical strains

CD	EC_{50} H1N1	EC_{50} B	EC_{50} H3N2
C11-6'SLN	0.5 µg/mL	17 µg/mL	N/A

5.6. Ex-vivo inhibitory activity of CD-C11-6'SLN

Ex-vivo experiments, where the dilutions naturally occur, are crucial to demonstrate the virucidal activity. MucilAir® is a human airway epithelia reconstituted *in vitro* (figure 5.15). *To create the tissues,* a mixture of nasal polyp epithelial cells originating from 14 healthy donors was cultured at the air-liquid interface. These tissues mimic very well the human upper respiratory track, where the influenza

infection begins and progresses. Therefore the results of ex-vivo experiment are very valuable.

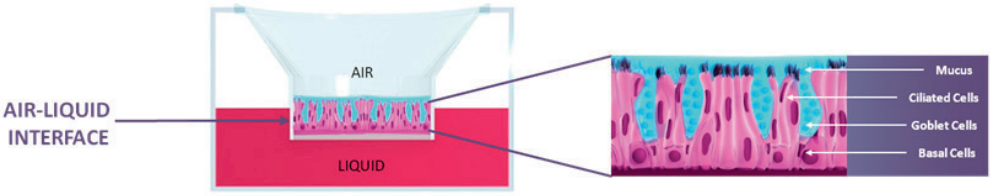

Figure 5.15: Illustration showing the structure of the MucilAir

To conduct the ex-vivo experiments, CD-C11-6'SLN and the virus are (H1N1 Neth/09) simultaneously transferred onto tissues, without prior incubation. After a certain amount of time, the tissues are washed and the progress of the infection was monitored on a daily basis. It is very important to inactivate the virus as much as possible at the initial step of the experiment. Therefore, the material concentrations should be sufficiently high. There is no more concern of virustatic effect as it was the case for in-vitro experiments since the inoculum will be removed but the experiment will continue for several days.

As figure 5.16 shows, 24 hours after the first treatment, the viral concentration in the non-treated tissues increases by two log units, whereas it decreases by two log units in the treated tissues. The infection further progresses after 48 hours, reaching 10^9/mL virus particles. After 72 hours, the viral titer starts to decrease probably because the tissues are not healthy enough for the virus to continue replicating. In the case of the treated tissues, the viral titer increases by 1 log unit after 24 hours and the virus concentration remain constant the next days. It is interesting that the virus concentration does not increase or decrease further after 48 hours. If a considerable amount of active virus would remain, the infection would progress during the days following the treatment, reaching higher viral titers.

qPCR counts both active and inactive viruses. It is possible that the inactive viruses are trapped in the cavities of the tissues in the beginning of the assay. As time passes, the virus particles might be degraded and slowly washed away during the daily

treatments. More studies needs to be conducted in order to understand the constant viral titer observed in the treated tissues.

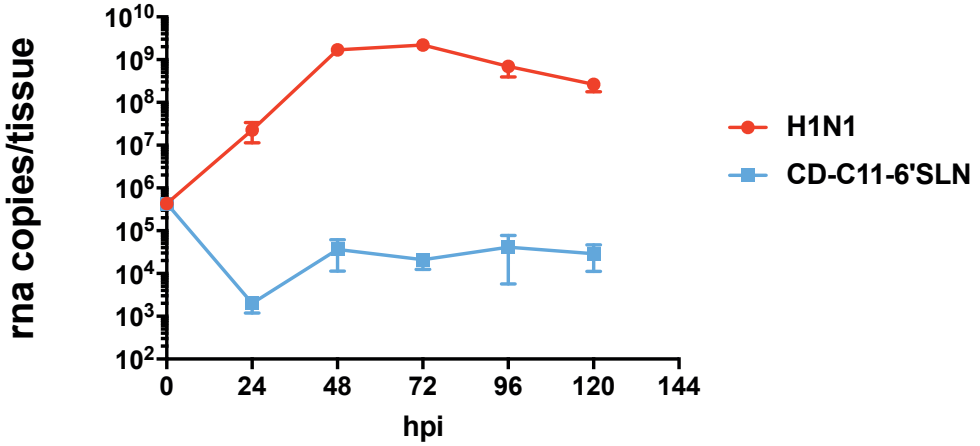

Figure 5.16: The virus concentration in the tissues was measured on a daily basis. The viral titer was evaluated with qPCR measurements

All aside, there is a difference of 5 log units between the CD-C11-6'SLN treated and non-treated tissues at the peak of the infection (72 hours after the treatment), that clearly shows the virucidal activity. Moreover, CD-C11-6'SLN treated tissues were in a very good condition, very comparable to their initial state. Successful ex-vivo results points out that CD-C11-6'SLN can also show a strong in-vivo antiviral activity. Therefore, in-vivo experiments were performed.

5.7. In-vivo inhibitory activity of CD-C11-6'SLN

After successful ex-vivo results, in-vivo mouse model experiments were conducted. The mice were simultaneously treated with H1N1/Neth 09 and CD-C11-C6 together with pbs treated controls at day 0. The temperature and the weight of the mice were measured on a daily basis.

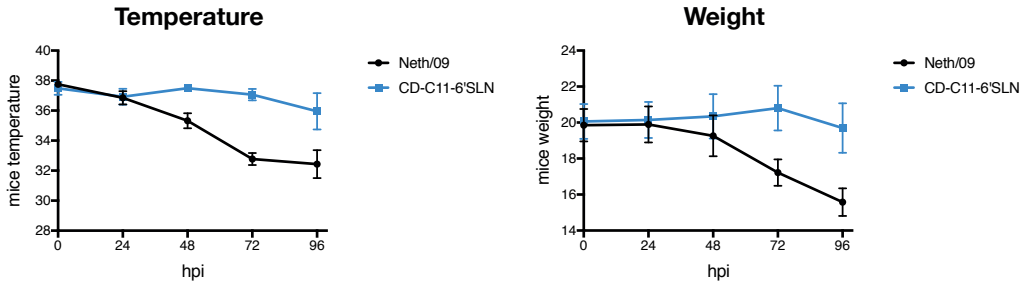

Figure 5.17: The curves showing the temperature and weight of the CD-C11-6'SLN treated mice and non-treated mice

48 hours after the treatment, CD-C11-C6 treated mice kept the initial body weight and temperature whereas pbs treated mice significantly lost weight and their body temperature decreased. At day 2, half of the mice were killed and the rest of the mice retreated with CD-C11-6'SLN. At day 3, the retreated mice were still healthy in terms of body weight and temperature. However, at day 4, the retreated mice started to become sick (figure 5.17).

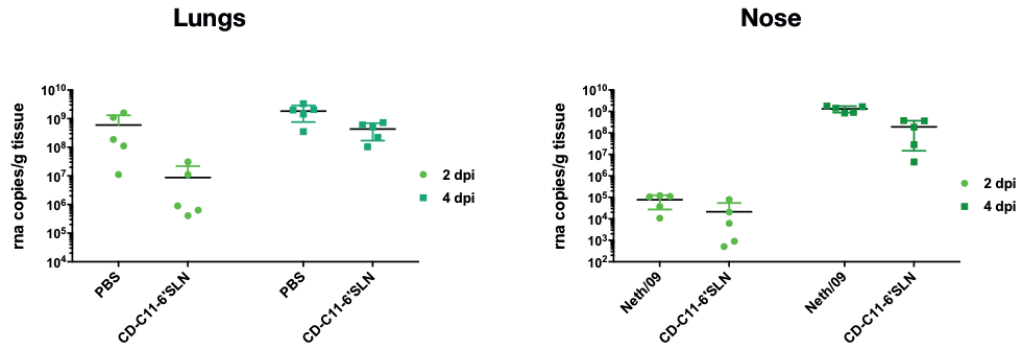

Figure 5.18: The viral concentration in the lungs and nose of the CD-C11-6'SLN treated and non-treated mice. The viral titer was evaluated with qPCR measurements.

The nose mucosa and lung homogenate were then analyzed to calculate the corresponding viral titers. 2 days after the start of the experiment, there was approximately 2-log unit reduction in the lung viral titers of the CD-C11-6'SLN treated mice in comparison to pbs treated ones, whereas the difference was 1 log unit in the nose. 4 days after, the difference between the titers was less than 1 log both in the lungs and in the nose (figure 5.18).

Additionally, bronco alveolar lavage (BAL) was titrated in order to count the number of infective viruses. As figure 5.19 shows, the difference between the CD-C11-6'SLN treated and non-treated tissues is even bigger than qPCR measurements. One mouse has almost 0 infective viruses. It should be noted that the variations in the treated mice is larger than non-treated ones. The variations may have two reasons: Either, the response of the each mouse to the CD-C11-6'SLN is different or the delivery of the CD-C11-6'SLN at the initial stage of the experiment.

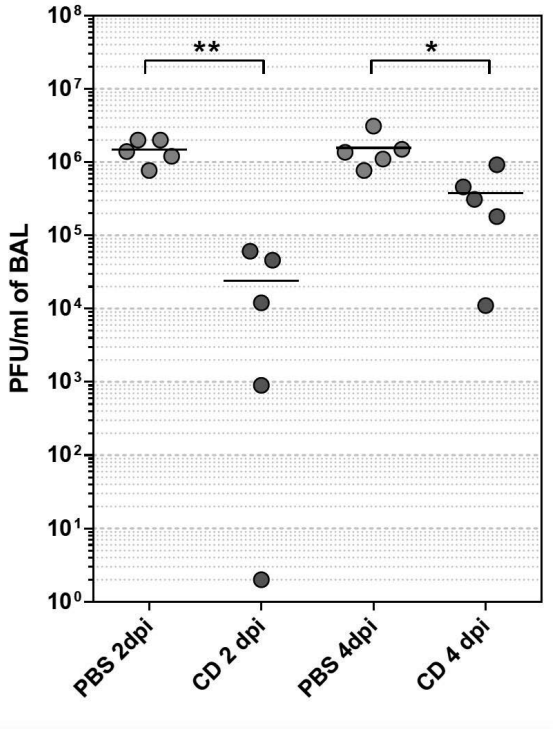

Figure 5.19: The quantity of the active virus was demonstrated with the titration of the bronco alveolar lavage (BAL)

Second treatment of the mice with CD-C11-6'SLN might be unnecessary at this stage of the project. It is possible that the tissues of the mouse were swollen due to infection, and CD-C11-6'SLN could not penetrate deep into tissues. Therefore, second treatment of the mice with CD-C11-6'SLN might be unnecessary at this stage of the project. More elevated methods might be necessary in order to conduct the second treatment.

H1N1 Neth/09 is a very aggressive influenza strain. CD-C11-6'SLN treatment protected the mouse to loose weight and body temperature. Moreover, 99% reduction of the viral titer in the lungs and 90% reduction in the nose are very successful in-vivo results. It is important to note that the CD-C11-6'SLN concentrations used in the experiments are not very high and scalable to humans. If this experiment would be performed on a human, 100 mg of CD-C11-6'SLN would be used.

5.8. Conclusion

Replacing the gold NPs with cyclodextrin did not affect the virucidal inhibition mechanism. Cyclodextrin derivatives successfully inhibited influenza strains with virucidal mechanism. When 6'SLN grafted onto β-Cyclodextrins without any additional spacer ligands, the antiviral activity was poor. Perhaps, these nanomaterials lack the flexibility to interact with the HA trimer.

6'SLN grafted β-Cyclodextrins with 6C and 11C spacers showed a similar inhibitory activity. However, cyclodextrins with 11C spacer were more reproducible. Therefore, in-vivo and ex-vivo experiments were conducted with CD-C11-6'SLN (figure 5.20).

The virucidal activity was further demonstrated with ex-vivo experiments, where the dilution of the inoculum naturally occurs. At the peak of the infection, 72 hours after the treatment, there was 5 log units difference between the viral titers of the CD-C11-6'SLN treated tissues and non-treated tissues. Moreover, in-vivo antiviral activity of CD-C11-6'SLN was demonstrated using a mouse model. CD-C11-6'SLN treatment protected the mice to loose weight and body temperature. There was also a significant

difference between the viral titers in the lungs and the nose. It is worth to mention that ex-vivo and in-vivo experiments were conducted with very aggressive influenza strain (H1N1 Netherlands/09) at a reasonable material concentration. Therefore, CD-C11-6'SLN has a big potential to become a drug against influenza.

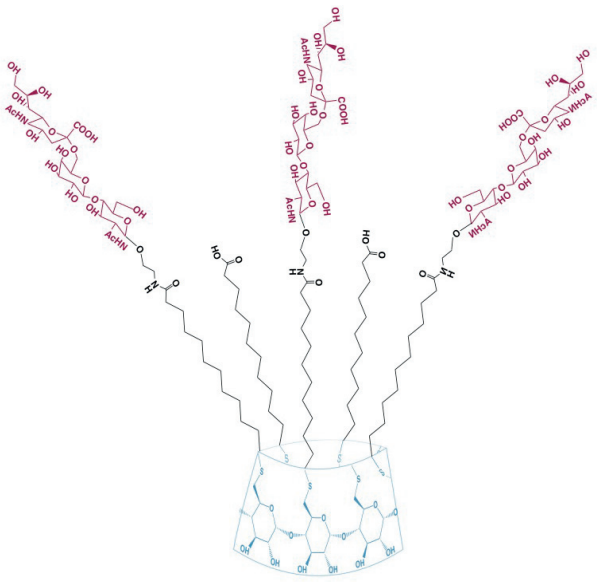

Figure 5.20: Chemical structure of the CD-C11-6'SLN

One reason why 1918 Spanish influenza pandemic was very deadly is that patients had extensive cell damage in the pulmonary tissues. Ex-vivo and in-vivo results demonstrate that CD-C11-6'SLN have big potential to prevent the deformations in the lung tissues which may reduce influenza related deaths.

CHAPTER 6

Conclusion and Outlook

In the previous chapters, antiviral activity of the 6'SLN bearing nanomaterials having a gold or cyclodextrin core was demonstrated. 6'SLN trisaccharide provided high affinity binding between the nanomaterials and the virus, whereas the rigid spacer provided the irreversible inhibition mechanism.

Gold NPs enabled us to conduct a detailed activity-structure relationship. Chemical structure of the spacer ligand as well as the 6'SLN density was demonstrated to be important in order to target influenza virus. Inhibition of the influenza virus was achieved at sub-nanomolar gold NP concentrations and the mechanism was demonstrated to be virucidal. NPs were successful to inhibit both influenza A and B types, including clinical strains. However, certain H3N2 strains could not be inhibited.

Antiviral nanomaterials have to be fully organic and biodegradable in order to become a drug that treats influenza infections. For this reason, the gold core was replaced with β- CD. Similar to gold NPs, β-CD derivatives successfully inhibited influenza virus with virucidal mechanism. The ex-vivo experiments further demonstrated that the inhibition mechanism is virucidal. Moreover, β-CD derivatives successfully inhibited influenza in-vivo (mouse model). Mice did not loose body weight and temperature when treated with β-CD derivatives. Also the viral titers in the nose and lungs were significantly lower. More importantly, the drug concentrations at which the in-vivo experiments were conducted are easily scalable to humans.

6.1. Important Conclusions

The influence of the nanomaterial surface structure on the inhibitory activity

The spacer ligand is one of the most important elements of the nanomaterials targeting influenza. They can significantly enhance the inhibitory activity of the nanomaterials, even though end-group does not have a high binding affinity to HA. For example, NPs with 3'SLN grafted PEG8 spacer showed a very weak inhibitory activity against human influenza viruses, as expected. However, when grafted onto a rigid spacer (C15), the inhibitory activity was significantly enhanced. Similarly, NPs with mono sialic acid grafted onto PEG8 spacer poorly inhibited human influenza strains. On the other hand, when mono sialic acid was grafted onto β-CD core through a rigid spacer (C11), the inhibition of the human influenza strains was successful.

Three sialic acid binding pockets are located on the globular head of the HA trimer. Ideally, the nanomaterials interact with these three pockets for a high affinity binding. However, for virucidal nanomaterials, this may not be needed. For example, targeting two binding pockets may leave more space to the free hydrophobic ligands so that the virucidal activity is enhanced.

One big difference between the gold and cyclodextrin scaffolds is the total number of ligands on the surface. β-CD have ~ 4 ligands whereas the surface of gold NPs is much more crowded, ~140 ligands/NP. Therefore, the results in these two cases did not always correlate although the materials were modified similar spacer ligands. For example, 11C spacer was found to be too short to inhibit certain influenza strains when grafted onto gold NPs. On the other hand, the same linker showed a very strong inhibitory activity against many influenza strains when grafted onto the cyclodextrin core. In the first case, the ligands are densely packed on the NPs surface and perhaps C11 does not have enough freedom to interact with sialic acid binding pockets.

Mechanism of inhibition

Irreversible inhibitory activity of the nanomaterials against influenza virus was demonstrated with in-vitro and ex-vivo experiments. Irreversible inhibition is possible when 1) the inhibition mechanism is virucidal 2) the dissociation constant, K_d, is unexceptionally low. The latter is rarely seen in the nature. One well-known example is the interaction between the streptavidin and the vitamin biotin where $K_d = 10^{-14}$ mol/L. The tight bonding mode between the streptavidin and vitamin biotin makes the interaction close to the covalent interaction.

Irreversible inhibition due to the very low dissociation constant is a possibility in our case, however it is unlikely. First of all, the nanomaterial concentration to inhibit the influenza is not unexceptionally low. In a typical dose-response assay, to achieve 90% inhibition of the virus, the ratio between the number of nanomaterials and the HA trimers is in the range of 10^5-10^8. The inhibitory concentrations should have been much lower if the dissociation constant would be significantly low. Secondly, when the inoculum is diluted thousand times or ten thousand times, the concentration of HA proteins decrease to ~10^{-15}-10^{-16} mol/L. The dissociation constants at this range are very rare. Therefore, the mechanism of inhibition is probably virucidal. Nanomaterials potentially distort the viral proteins so that the virus becomes inert.

Potential of the virucidal nanomaterials to become therapeutics

One reason why 1918 H1N1 Spanish influenza was very deadly is that the virus caused extensive cell damage in the lung tissues. Glycan array studies show that this strain was targeting 6'SLN trisaccharides on the host-cell glycoproteins. Similarly, swine influenza pandemic virus H1N1 CAL/09 was also targeting 6'SLN trisaccharides. Perhaps, an influenza virus that does not target highly expressed sialic acid moieties on the respiratory track cannot lead to pandemics. For humans this sialic acid type is 6'SLN and for avians 3'SLN. Therefore, to decorate the nanomaterials with these glycans is indeed a good strategy to fight against the pandemics.

Previously, several multivalent materials bearing a sialic acid end-group were demonstrated as potential antivirals against influenza. However, most of these studies did not involve in-vivo results or the reported results were not complete. There is only one study in which 6'sialyllactoseamine (6'SL) grafted PAMAM dendrimers were tested against several influenza strains.[45] This study also involves very detailed in-vivo results where the condition of the mice as well as the viral titers in the lung was demonstrated. One big difference between our study and their study is the material concentrations. Our experiments were conducted with ~ 25 μg/mouse of materials whereas their experiments were conducted with ~ 25 mg/mouse of materials. If the concentrations would be scaled to humans, we would do the experiment with ~100 mg/human whereas they would do with 100g/human. Also, the antiviral activity of the cyclodextrin materials seem to be stronger considering the condition of the mouse as well as viral titers. Thus, cyclodextrin based nanomaterials have big potential to become drugs, in particular to fight against influenza pandemics.

6.2. Future Work: Targeting Other Sialic Acid Binding Viruses

6'SLN is a trisachharide that human influenza virus utilizes to attach host-cells receptors. In this thesis, it was demonstrated that 6'SLN grafted onto nanomaterials with a rigid spacer irreversibly inhibited influenza virus. This concept can be adjusted to other sialic acid targeting viruses. In order to do so, it is important to know the glycan sequence that the virus binds to with high affinity. This information can be obtained from glycan array studies. Additionally, crystal structure of the viral ligands should also be taken into account.

The family of sialic acid binding viruses is relatively small. Influenza is the virus affecting the highest number of people in the world. Therefore, in this project the focus was the human influenza virus. The other viruses that can be interesting to target are avian influenza virus, rotavirus and certain types of enterovirus.

Targeting Avian Influenza Strains

Avian influenza is a very dangerous and fatal virus, both for avians and humans. It also has lots of economic consequences since many animals have to be killed once the infection appears.

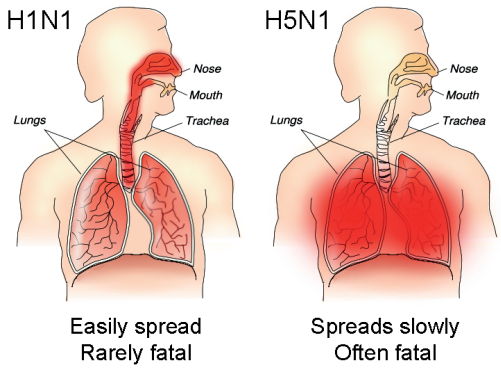

Figure 6.1: Human influenza strains primarily affect the upper respiratory track where the cells are rich with 2,6 linked sialic acid, whereas avian influenza strains affects the lungs where the cells are rich with 2,3 linked sialic acid.

Avian influenza preferentially binds to 3'SLN moieties on the host-cell receptors. Humans have tissues rich with -2,3 linked sialic acid, but deep in lungs (figure 6.1). Therefore, it is more difficult for humans to be infected with avian influenza. However, once the infection starts, it is usually fatal. For this reason, to irreversibly inhibit the avian strains can be even more valuable than inhibiting human influenza strains.

Nanomaterials coated with 3'SLN can irreversibly inhibit avian influenza strains. The next step of this project is to conduct antiviral and virucidal assays against avian influenza strains, particularly against H5N1. H5N1 is a highly pathogenic strain, which causes pandemics. H5N1 pandemics usually result in millions of animal deaths and are also fatal for humans. It is therefore very important to inhibit this strain with virucidal mechanism.

Targeting Rotavirus and Norovirus

Rotavirus causes inflammation of stomach and intestines. It is particularly dangerous for children, as it is the main cause of fatal diarrhea in young children. In 2013, rotavirus caused 215,000 deaths worldwide. Currently vaccination is the only method to protect against many strains of rotavirus. Therefore, to design nanomaterials targeting the rotavirus can be interesting.

Even though rotavirus is known to be a sialic acid targeting virus, many studies showed that some human rotavirus strains changed their binding affinity from sialic acid to the histo-blood group A antigen α-D-GalNAc-(1-3)-(α-L-Fuc-[1-2])-D-Gal.[93–96] Therefore, this trisaccharide can be grafted onto NPs to target the rotavirus. We conducted some preliminary experiments on the rotavirus DS-1 strain. Similar to the experiments against influenza, the gold NPs with blood group A trisaccharide were synthesized and tested against rotavirus DS-1 strain. However, we could not achieve any inhibition. One challenge to target rotavirus is the position of the receptor binding points on the viral ligands (figure 6.2). The binding point is at the side of the viral ligand and therefore, it is difficult to target the virus with multivalent nanomaterials. In this respect, nanomaterials having different sizes, shapes as well as trisaccharide densities should be investigated.

Norovirus is a similar virus to the rotavirus and it is the most common cause of gastroenteritis in humans. Norovirus was also demonstrated to target the histo-blood group antigens.[97,98] Therefore, a similar approach might be followed to target the norovirus.

To target these viruses, collaboration with Functional Glycomics should be established. Different strains of purified Noro and Rotavirus can be then analyzed for their glycan binding affinity. The glycan sequences providing high affinity binding can be then grafted onto nanomaterials to target the viruses. In parallel, crystal structure of the viral ligands should be investigated in order to improve the design of the nanomaterials.

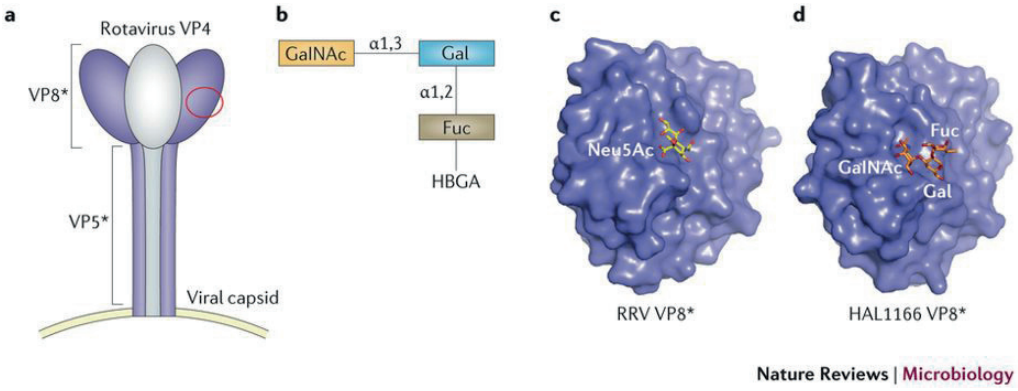

Figure 6.2: Illustration showing rotavirus viral ligand VP4 where the attachment point is shown with red circle (a). Human rotavirus target blood group A trisaccharide α-D-GalNAc-(1-3)-(α-L-Fuc-[1-2])-D-Gal (b and d). On the other hand, rhesus rotavirus target sialic acid (c).

Broad spectrum antivirals against sialic acid targeting viruses

Sialic acid coated gold NPs did not show a good inhibitory activity against the influenza virus. On the other hand, sialic acid grafted cyclodexrin was successfully inhibited influenza H1N1 Netherlands/09, H3N2 Singapore/04 and B/Yamagata at concentrations comparable to 6'SLN grafted cyclodextrins. Probably, the chemical structure and the density of the spacer ligand as well as the scaffold improved the binding in comparison to gold NPs. Therefore, sialic acid grafted cyclodextrins have a potential to become broad-spectrum antivirals against sialic acid targeting viruses.

Bibliography

1. Dimitrov, D. S. Virus entry: molecular mechanisms and biomedical applications. *Nat. Rev. Microbiol.* **2**, 109–122 (2004).
2. Ravindran, M. S. & Tsai, B. Viruses Utilize Cellular Cues in Distinct Combination to Undergo Systematic Priming and Uncoating. *PLOS Pathog* **12**, e1005467 (2016).
3. Chen, L. *et al.* Antiviral activity of peptide inhibitors derived from the protein E stem against Japanese encephalitis and Zika viruses. *Antiviral Res.* **141**, 140–149 (2017).
4. Colpitts, C. C. & Schang, L. M. A small molecule inhibits virion attachment to heparan sulfate- or sialic acid-containing glycans. *J. Virol.* JVI.00896-14 (2014). doi:10.1128/JVI.00896-14
5. Ndeboko, B. *et al.* Developments in Cell-Penetrating Peptides as Antiviral Agents and as Vehicles for Delivery of Peptide Nucleic Acid Targeting Hepadnaviral Replication Pathway. *Biomolecules* **8**, 55 (2018).
6. Warren, T. K. *et al.* Therapeutic efficacy of the small molecule GS-5734 against Ebola virus in rhesus monkeys. *Nature* **531**, 381–385 (2016).
7. Zhang, M.-Z., Chen, Q. & Yang, G.-F. A review on recent developments of indole-containing antiviral agents. *Eur. J. Med. Chem.* **89**, 421–441 (2015).
8. Siddharta, A. *et al.* Virucidal Activity of World Health Organization–Recommended Formulations Against Enveloped Viruses, Including Zika, Ebola, and Emerging Coronaviruses. *J. Infect. Dis.* **215**, 902–906 (2017).

9. Shogan, B., Kruse, L., Mulamba, G. B., Hu, A. & Coen, D. M. Virucidal Activity of a GT-Rich Oligonucleotide against Herpes Simplex Virus Mediated by Glycoprotein B. *J. Virol.* **80**, 4740–4747 (2006).
10. Motakis, D. & Parniak, M. A. A Tight-Binding Mode of Inhibition Is Essential for Anti-Human Immunodeficiency Virus Type 1 Virucidal Activity of Nonnucleoside Reverse Transcriptase Inhibitors. *Antimicrob. Agents Chemother.* **46**, 1851–1856 (2002).
11. Boyd, M. R. *et al.* Discovery of cyanovirin-N, a novel human immunodeficiency virus-inactivating protein that binds viral surface envelope glycoprotein gp120: potential applications to microbicide development. *Antimicrob. Agents Chemother.* **41**, 1521–1530 (1997).
12. Yang, F. *et al.* Crystal structure of cyanovirin-N, a potent HIV-inactivating protein, shows unexpected domain swapping 11Edited by R. Huber. *J. Mol. Biol.* **288**, 403–412 (1999).
13. Kim, S., Shin, K.-R. & Zhang, B.-T. Molecular immunocomputing with application to alphabetical pattern recognition mimics the characterization of ABO blood type. in *2003 Congress on Evolutionary Computation, CEC 2003 - Proceedings* **4**, 2549–2556 Vol.4 (2004).
14. Philp, D. & Stoddart, J. F. Self-Assembly in Natural and Unnatural Systems. *Angew. Chem. Int. Ed. Engl.* **35**, 1154–1196 (1996).
15. Mammen, M., Choi, S.-K. & Whitesides, G. M. Polyvalent Interactions in Biological Systems: Implications for Design and Use of Multivalent Ligands and Inhibitors. *Angew. Chem. Int. Ed.* **37**, 2754–2794 (1998).
16. Fasting, C. *et al.* Multivalency as a Chemical Organization and Action Principle. *Angew. Chem. Int. Ed.* **51**, 10472–10498 (2012).

17. Bhatia, S., Camacho, L. C. & Haag, R. Pathogen Inhibition by Multivalent Ligand Architectures. *J. Am. Chem. Soc.* **138**, 8654–8666 (2016).
18. Cagno, V. *et al.* Broad-spectrum non-toxic antiviral nanoparticles with a virucidal inhibition mechanism. *Nat. Mater.* **17**, 195 (2018).
19. Giner-Casares, J. J., Henriksen-Lacey, M., Coronado-Puchau, M. & Liz-Marzán, L. M. Inorganic nanoparticles for biomedicine: where materials scientists meet medical research. *Mater. Today* **19**, 19–28 (2016).
20. Giljohann, D. A. *et al.* Gold Nanoparticles for Biology and Medicine. *Angew. Chem. Int. Ed.* **49**, 3280–3294 (2010).
21. Baram-Pinto, D., Shukla, S., Perkas, N., Gedanken, A. & Sarid, R. Inhibition of Herpes Simplex Virus Type 1 Infection by Silver Nanoparticles Capped with Mercaptoethane Sulfonate. *Bioconjug. Chem.* **20**, 1497–1502 (2009).
22. Baram-Pinto, D., Shukla, S., Gedanken, A. & Sarid, R. Inhibition of HSV-1 Attachment, Entry, and Cell-to-Cell Spread by Functionalized Multivalent Gold Nanoparticles. *Small* **6**, 1044–1050 (2010).
23. Di Gianvincenzo, P. *et al.* Gold nanoparticles capped with sulfate-ended ligands as anti-HIV agents. *Bioorg. Med. Chem. Lett.* **20**, 2718–2721 (2010).
24. Yang, X. X., Li, C. M. & Huang, C. Z. Curcumin modified silver nanoparticles for highly efficient inhibition of respiratory syncytial virus infection. *Nanoscale* **8**, 3040–3048 (2016).
25. Antoine, T. E. *et al.* Prophylactic, therapeutic and neutralizing effects of zinc oxide tetrapod structures against herpes simplex virus type-2 infection. *Antiviral Res.* **96**, 363–375 (2012).

26. Rosemary Bastian, A. *et al.* Mechanism of Multivalent Nanoparticle Encounter with HIV-1 for Potency Enhancement of Peptide Triazole Virus Inactivation. *J. Biol. Chem.* **290**, 529–543 (2015).
27. Bowman, M.-C. *et al.* Inhibition of HIV Fusion with Multivalent Gold Nanoparticles. *J. Am. Chem. Soc.* **130**, 6896–6897 (2008).
28. Papp, I. *et al.* Inhibition of Influenza Virus Infection by Multivalent Sialic-Acid-Functionalized Gold Nanoparticles. *Small* **6**, (2010).
29. Lin, Z. *et al.* The inhibition of H1N1 influenza virus-induced apoptosis by silver nanoparticles functionalized with zanamivir. *RSC Adv.* **7**, 742–750 (2017).
30. Brem, H. *et al.* Placebo-controlled trial of safety and efficacy of intraoperative controlled delivery by biodegradable polymers of chemotherapy for recurrent gliomas. *The Lancet* **345**, 1008–1012 (1995).
31. Deng, C., Jiang, Y., Cheng, R., Meng, F. & Zhong, Z. Biodegradable polymeric micelles for targeted and controlled anticancer drug delivery: Promises, progress and prospects. *Nano Today* **7**, 467–480 (2012).
32. Jeong, J. H. & Park, T. G. Poly(l-lysine)-g-poly(d,l-lactic-co-glycolic acid) micelles for low cytotoxic biodegradable gene delivery carriers. *J. Controlled Release* **82**, 159–166 (2002).
33. Nair, L. S. & Laurencin, C. T. Biodegradable polymers as biomaterials. *Prog. Polym. Sci.* **32**, 762–798 (2007).
34. Tyssen, D. *et al.* Structure Activity Relationship of Dendrimer Microbicides with Dual Action Antiviral Activity. *PLOS ONE* **5**, e12309 (2010).
35. Ceña-Diez, R. *et al.* G2-S16 dendrimer as a candidate for a microbicide to prevent HIV-1 infection in women. *Nanoscale* **9**, 9732–9742 (2017).

36. Galán, M. *et al.* Dendronized PLGA nanoparticles with anionic carbosilane dendrons as antiviral agents against HIV infection. *RSC Adv.* **6**, 73817–73826 (2016).
37. Dey, P. *et al.* Multivalent Flexible Nanogels Exhibit Broad-Spectrum Antiviral Activity by Blocking Virus Entry. *ACS Nano* **12**, 6429–6442 (2018).
38. Pirrone, V., Wigdahl, B. & Krebs, F. C. The rise and fall of polyanionic inhibitors of the human immunodeficiency virus type 1. *Antiviral Res.* **90**, 168–182 (2011).
39. Barras, A. *et al.* High Efficiency of Functional Carbon Nanodots as Entry Inhibitors of Herpes Simplex Virus Type 1. *ACS Appl. Mater. Interfaces* **8**, 9004–9013 (2016).
40. Pérez-Anes, A. *et al.* Phosphonate terminated PPH dendrimers: influence of pendant alkyl chains on the in vitro anti-HIV-1 properties. *Org. Biomol. Chem.* **7**, 3491–3498 (2009).
41. Reuter, J. D. *et al.* Inhibition of Viral Adhesion and Infection by Sialic-Acid-Conjugated Dendritic Polymers. *Bioconjug. Chem.* **10**, 271–278 (1999).
42. Bhatia, S. *et al.* Linear polysialoside outperforms dendritic analogs for inhibition of influenza virus infection in vitro and in vivo. *Biomaterials* **138**, 22–34 (2017).
43. Papp, I. *et al.* Inhibition of Influenza Virus Activity by Multivalent Glycoarchitectures with Matched Sizes. *ChemBioChem* **12**, 887–895 (2011).
44. Tang, S. *et al.* Antiviral Agents from Multivalent Presentation of Sialyl Oligosaccharides on Brush Polymers. *ACS Macro Lett.* **5**, 413–418 (2016).
45. Kwon, S.-J. *et al.* Nanostructured glycan architecture is important in the inhibition of influenza A virus infection. *Nat. Nanotechnol.* **12**, 48–54 (2017).

46. Lauster, D. *et al.* Multivalent Peptide–Nanoparticle Conjugates for Influenza-Virus Inhibition. *Angew. Chem. Int. Ed.* **56**, 5931–5936 (2017).
47. Morimoto, N. *et al.* Specific Distribution of Sialic Acids in Animal Tissues As Examined by LC–ESI-MS after Derivatization with 1,2-Diamino-4,5-Methylenedioxybenzene. *Anal. Chem.* **73**, 5422–5428 (2001).
48. Dhavale, D. & Henry, J. E. Evaluation of sialic acid-analogs for the attenuation of amyloid-beta toxicity. *Biochim. Biophys. Acta BBA - Gen. Subj.* **1820**, 1475–1480 (2012).
49. Stencel-Baerenwald, J. E., Reiss, K., Reiter, D. M., Stehle, T. & Dermody, T. S. The sweet spot: defining virus-sialic acid interactions. *Nat. Rev. Microbiol.* **12**, 739–749 (2014).
50. Matrosovich, M., Herrler, G. & Klenk, H. D. Sialic Acid Receptors of Viruses. *Top. Curr. Chem.* **367**, 1–28 (2015).
51. WHO | Estimated rotavirus deaths for children under 5 years of age: 2013, 215 000. *WHO* Available at: http://www.who.int/immunization/monitoring_surveillance/burden/estimates/rotavirus/en/. (Accessed: 25th September 2018)
52. Influenza (Seasonal). *World Health Organization* Available at: http://www.who.int/news-room/fact-sheets/detail/influenza-(seasonal). (Accessed: 25th September 2018)
53. Barman, S. *et al.* Role of domestic ducks in the emergence of a new genotype of highly pathogenic H5N1 avian influenza A viruses in Bangladesh. *Emerg. Microbes Infect.* **6**, e72 (2017).

54. Past Pandemics | Pandemic Influenza (Flu) | CDC. (2018). Available at: https://www.cdc.gov/flu/pandemic-resources/basics/past-pandemics.html. (Accessed: 25th September 2018)
55. Jeyanathan, T., Overgaard, C. & McGeer, A. Cardiac complications of influenza infection in 3 adults. *CMAJ Can. Med. Assoc. J.* **185**, 581–584 (2013).
56. Ghebrehewet, S., MacPherson, P. & Ho, A. Influenza. *BMJ* **355**, i6258 (2016).
57. Treanor, J. Influenza Vaccine — Outmaneuvering Antigenic Shift and Drift. *N. Engl. J. Med.* **350**, 218–220 (2004).
58. Ferraro, B. *et al.* Clinical Applications of DNA Vaccines: Current Progress. *Clin. Infect. Dis. Off. Publ. Infect. Dis. Soc. Am.* **53**, 296–302 (2011).
59. Wu, N. C. & Wilson, I. A. Structural insights into the design of novel anti-influenza therapies. *Nat. Struct. Mol. Biol.* **25**, 115–121 (2018).
60. Srinivasan, S., Ghosh, M., Maity, S. & Varadarajan, R. Broadly neutralizing antibodies for therapy of viral infections. *Antibody Technology Journal* (2016). doi:10.2147/ANTI.S92190
61. Bao, J., Marathe, B., Govorkova, E. A. & Zheng, J. J. Drug Repurposing Identifies Inhibitors of Oseltamivir-Resistant Influenza Viruses. *Angew. Chem. Int. Ed.* **55**, 3438–3441 (2016).
62. Trebbien, R., Pedersen, S. S., Vorborg, K., Franck, K. T. & Fischer, T. K. Development of oseltamivir and zanamivir resistance in influenza A(H1N1)pdm09 virus, Denmark, 2014. *Eurosurveillance* **22**, (2017).
63. Clercq, E. D. The design of drugs for HIV and HCV. *Nat. Rev. Drug Discov.* **6**, 1001–1018 (2007).
64. Li, T. *et al.* Clinical Implications of Antiviral Resistance in Influenza. *Viruses* **7**, 4929–4944 (2015).

65. Koszalka, P., Tilmanis, D. & Hurt, A. C. Influenza antivirals currently in late-phase clinical trial. *Influenza Other Respir. Viruses* **11**, 240–246 (2017).
66. Triana-Baltzer, G. B. *et al.* DAS181, a sialidase fusion protein, protects human airway epithelium against influenza virus infection: an in vitro pharmacodynamic analysis. *J. Antimicrob. Chemother.* **65**, 275–284 (2010).
67. Belardo, G., Cenciarelli, O., Frazia, S. L., Rossignol, J. F. & Santoro, M. G. Synergistic Effect of Nitazoxanide with Neuraminidase Inhibitors against Influenza A Viruses In Vitro. *Antimicrob. Agents Chemother.* **59**, 1061–1069 (2015).
68. Sleeman, K. *et al.* In Vitro Antiviral Activity of Favipiravir (T-705) against Drug-Resistant Influenza and 2009 A(H1N1) Viruses. *Antimicrob. Agents Chemother.* **54**, 2517–2524 (2010).
69. Gupta, P. *et al.* Preclinical pharmacokinetics of MHAA4549A, a human monoclonal antibody to influenza A virus, and the prediction of its efficacious clinical dose for the treatment of patients hospitalized with influenza A. *mAbs* **8**, 991–997 (2016).
70. Ekiert, D. C. *et al.* A highly conserved neutralizing epitope on group 2 influenza A viruses. *Science* **333**, 843–850 (2011).
71. Chai, N. *et al.* A broadly protective therapeutic antibody against influenza B virus with two mechanisms of action. *Nat. Commun.* **8**, 14234 (2017).
72. Kallewaard, N. L. *et al.* Structure and Function Analysis of an Antibody Recognizing All Influenza A Subtypes. *Cell* **166**, 596–608 (2016).
73. Blixt, O. *et al.* Printed covalent glycan array for ligand profiling of diverse glycan binding proteins. *Proc. Natl. Acad. Sci. U. S. A.* **101**, 17033–17038 (2004).

74. Smith, D. F. & Cummings, R. D. Chapter 6 - Glycan-Binding Proteins and Glycan Microarrays. in *Handbook of Glycomics* 137–160 (Academic Press, 2010). doi:10.1016/B978-0-12-373600-0.00006-8

75. Venkataraman, M., Sasisekharan, R. & Raman, R. Glycan array data management at Consortium for Functional Glycomics. *Methods Mol. Biol. Clifton NJ* **1273**, 181–190 (2015).

76. Liu, Y. *et al.* Sialic acid-dependent cell entry of human enterovirus D68. *Nat. Commun.* **6**, 8865 (2015).

77. Liu, Y. *et al.* Structure and inhibition of EV-D68, a virus that causes respiratory illness in children. *Science* **347**, 71–74 (2015).

78. Haag, R. & Kratz, F. Polymer Therapeutics: Concepts and Applications. *Angew. Chem. Int. Ed.* **45**, 1198–1215 (2006).

79. Otterstrom, J. J. *et al.* Relating influenza virus membrane fusion kinetics to stoichiometry of neutralizing antibodies at the single-particle level. *Proc. Natl. Acad. Sci. U. S. A.* **111**, E5143–E5148 (2014).

80. Ahmed, S. R. *et al.* In situ self-assembly of gold nanoparticles on hydrophilic and hydrophobic substrates for influenza virus-sensing platform. *Sci. Rep.* **7**, (2017).

81. Zhang, Z. *et al.* Influenza-binding sialylated polymer coated gold nanoparticles prepared via RAFT polymerization and reductive amination. *Chem. Commun.* (2016). doi:10.1039/C6CC00501B

82. Saha, K., Agasti, S. S., Kim, C., Li, X. & Rotello, V. M. Gold Nanoparticles in Chemical and Biological Sensing. *Chem. Rev.* **112**, 2739–2779 (2012).

83. Woehrle, G. H., Brown, L. O. & Hutchison, J. E. Thiol-Functionalized, 1.5-nm Gold Nanoparticles through Ligand Exchange Reactions: Scope and Mechanism of Ligand Exchange. *J. Am. Chem. Soc.* **127**, 2172–2183 (2005).
84. Alymova, I. V. *et al.* Glycosylation changes in the globular head of H3N2 influenza hemagglutinin modulate receptor binding without affecting virus virulence. *Sci. Rep.* **6**, (2016).
85. Gulati, S. *et al.* Human H3N2 Influenza Viruses Isolated from 1968 To 2012 Show Varying Preference for Receptor Substructures with No Apparent Consequences for Disease or Spread. *PLOS ONE* **8**, e66325 (2013).
86. Peng, W. *et al.* Recent H3N2 Viruses Have Evolved Specificity for Extended, Branched Human-type Receptors, Conferring Potential for Increased Avidity. *Cell Host Microbe* **21**, 23–34 (2017).
87. Tiwari, G., Tiwari, R. & Rai, A. K. Cyclodextrins in delivery systems: Applications. *J. Pharm. Bioallied Sci.* **2**, 72–79 (2010).
88. Szejtli, J. Medicinal applications of cyclodextrins. *Med. Res. Rev.* **14**, 353–386 (1994).
89. Davis, M. E. & Brewster, M. E. Cyclodextrin-based pharmaceutics: past, present and future. *Nat. Rev. Drug Discov.* **3**, 1023–1035 (2004).
90. Martinez-Morales, A. A. *et al.* Synthesis and Characterization of Iron Oxide Derivatized Mutant Cowpea Mosaic Virus Hybrid Nanoparticles. *Adv. Mater.* **20**, 4816–4820 (2008).
91. Khan, A. R., Forgo, P., Stine, K. J. & D'Souza, V. T. Methods for Selective Modifications of Cyclodextrins. *Chem. Rev.* **98**, 1977–1996 (1998).
92. Šardzík, R. *et al.* Preparation of aminoethyl glycosides for glycoconjugation. *Beilstein J. Org. Chem.* **6**, 699–703 (2010).

93. Böhm, R. *et al.* Revisiting the role of histo-blood group antigens in rotavirus host-cell invasion. *Nat. Commun.* **6**, ncomms6907 (2015).
94. Haselhorst, T. *et al.* Sialic acid dependence in rotavirus host cell invasion. *Nat. Chem. Biol.* **5**, 91–93 (2009).
95. Hu, L. *et al.* Cell attachment protein VP8* of a human rotavirus specifically interacts with A-type histo-blood group antigen. *Nature* **485**, 256–259 (2012).
96. Jiang, X., Liu, Y. & Tan, M. Histo-blood group antigens as receptors for rotavirus, new understanding on rotavirus epidemiology and vaccine strategy. *Emerg. Microbes Infect.* **6**, e22 (2017).
97. Huang, P. *et al.* Noroviruses Bind to Human ABO, Lewis, and Secretor Histo-Blood Group Antigens: Identification of 4 Distinct Strain-Specific Patterns. *J. Infect. Dis.* **188**, 19–31 (2003).
98. Tan, M. & Jiang, X. Histo-blood group antigens: a common niche for norovirus and rotavirus. *Expert Rev. Mol. Med.* **16**, e5 (2014).

Appendix A

Synthesis Protocols of the group A gold NPs:

Synthesis of PEG(4)-CH_3 NPs: 88.6 mg hyaluronic acid ($HAuCl_4$) in 15 mL of EtOH was stirred with 48 mg of HS-PEG(4)-CH_3 in 5 mL of EtOH for 10 minutes. To the mixture 94.6 mg sodium borohydrate ($NaBH_4$) in 37.5 mL of ethanol (EtOH) was added dropwise within 5 minutes. For complete NP formation, an overnight reaction was performed. Resulting NPs were diluted in H_2O and concentrated using amicon filters (cut-off MW: 30kDa). Once concentrated, NPs were further washed with H_2O.

PEG(4)-CH_3 _PEG(8)-COOH mixed ligand NPs: A ligand exchange reaction was performed with 70 mg of HS-PEG(8)-COOH and 20 mg of PEG(4)-CH_3NPs, in DMF, overnight. The NPs were precipitated from DMF-diethyl ether mixture and further washed three times with the same solvent mixture. A last wash with only diethyl ether was done and NPs dried under vacuum.

PEG(4)-CH_3 _MUA mixed ligand NPs: A ligand exchange reaction was performed with 1.5 mg of 11-mercaptoundecanoic acid and 20 mg of PEG(5) NPs, in DMF, overnight. The NPs were precipitated from DMF-diethyl ether mixture and further washed three times with the same solvent mixture. A last wash with only diethyl ether was done and NPs dried under vacuum.

NHS Activation of of NPs: 15 mg of NPs were activated using 10 mg N-hydroxysuccinimide ester (NHS), 2 mg of ethylcarbodiimide hydrochloride (EDC-hcl) and 0.1 mg of 4-(dimethylamino)-pyridin (DMAP) in DMF, overnight. The NPs were precipitated from DMF-diethyl ether mixture and further washed three times with the same solvent mixture. A last wash with only diethyl ether was done and NPs dried under vacuum.

Synthesis of A-PEG8-6'SLN NPs: 5 mg of NHS-activated NPs were mixed with 1.7 mg of Neu5Acα(2,6)-Galβ(1-4)-GlcNAc-β-ethylamine in 2 mL of DMF. After an

overnight reaction, 6'SLN grafted NPs were precipitated from diethyl ether and washed with H_2O using amicon filters.

Synthesis of A-PEG8-3'SLN NPs: 5 mg of NHS-activated NPs were mixed with 1.7 mg of Neu5Acα(2,3)-Galβ(1-4)-GlcNAc-β-ethylamine in 2 mL of DMF. After an overnight reaction, 3'SLN grafted NPs were precipitated from diethyl ether and washed with H_2O using amicon filters.

Synthesis of A-PEG8-SA NPs: 5 mg of NHS-activated NPs were mixed with 1.7 mg of 6-aminohexyl Neu5Ac in 2 mL of DMF. After an overnight reaction, SA grafted NPs were precipitated from diethyl ether and washed with H_2O using amicon filters.

Synthesis of A-MUA-6'SLN NPs: 5 mg of NHS-activated NPs were mixed with 1.7 mg of Neu5Acα(2,6)-Galβ(1-4)-GlcNAc-β-ethylamine in 2 mL of DMF. After an overnight reaction, 6'SLN grafted NPs were precipitated from diethyl ether and washed with H_2O using amicon filters.

^{1}H NMR Spectrum of the A-PEG(8)-6'SLN NPs

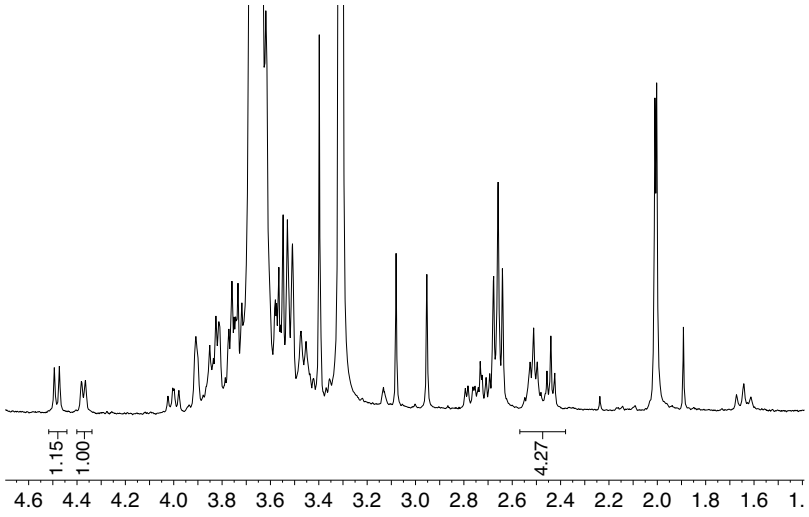

^{1}H NMR Spectrum of the A-PEG(8)-3'SLN NPs

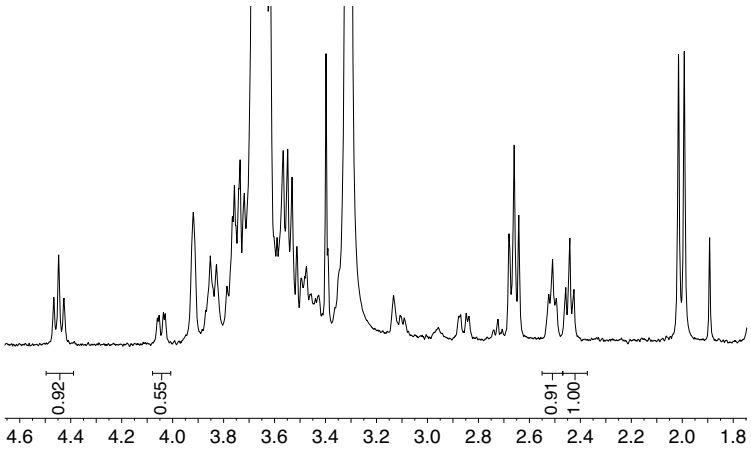

^{1}H NMR Spectrum of the A-PEG(8)-SA NPs

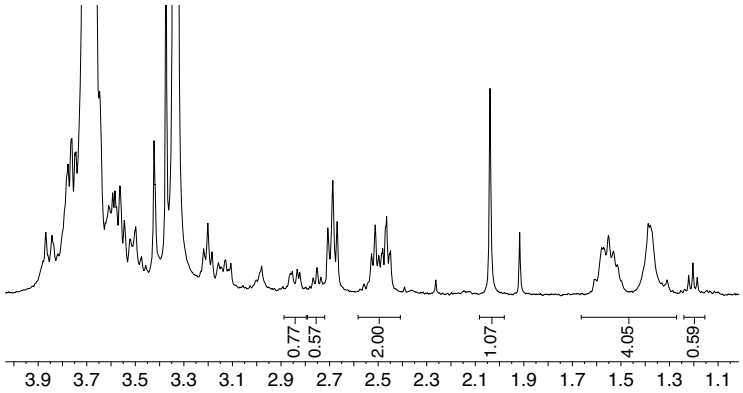

^{1}H NMR Spectrum of the A-MUA-6'SLN NPs

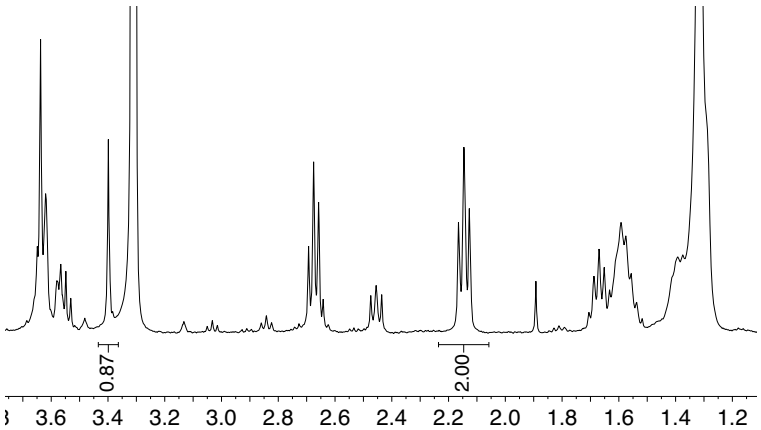

Appendix B

Synthesis of the 6-aminohexyl Neu5Ac:

Carboxylic acid group of *N*-Acetyl neuraminic acid is methylated by using Dowex resin. The hydroxide group adjacent to this acid can then be activated using acetyl chloride. This simultaneously protects the other hydroxyl groups whilst converting the hydroxide adjacent to the protected acid to a chloride. This product (1) can then be purified *via* silica column chromatography and further used to react to the hydroxyl terminus of the molecule 2. This protected-amine modified sialic acid has all of its protecting groups removed readily using sodium methoxide followed by lithium hydroxide and Pd/C. The final product (3), is then capable of being used in the sialic acid modification of the nanomaterials.

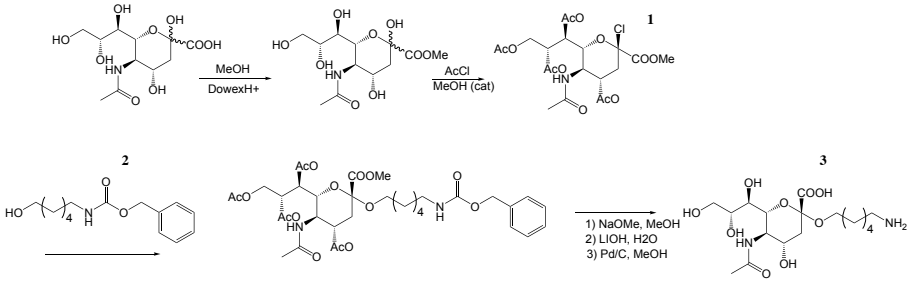

^{1}H NMR Spectrum of the 6-aminohexyl Neu5Ac

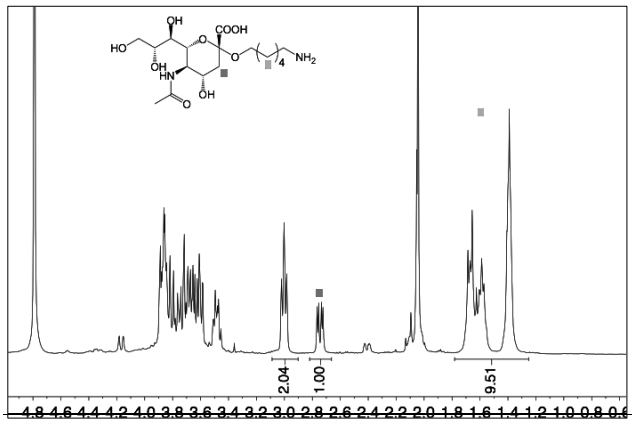

ESI-Mass Spectrum of the 6-aminohexyl Neu5Ac

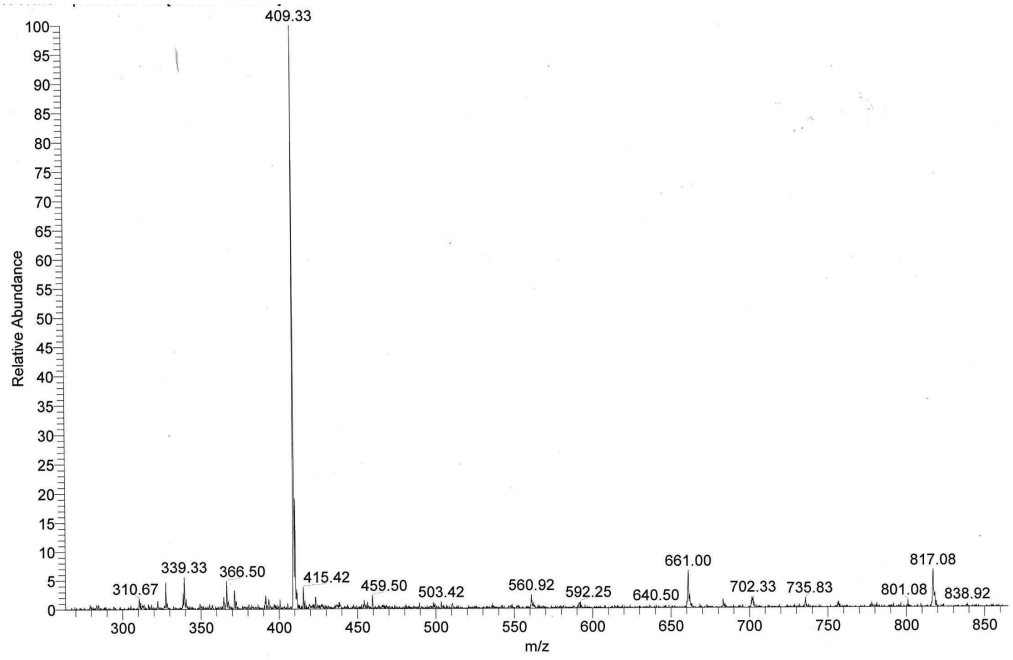

^{1}H NMR Spectrum of the modified CD-C6-6'SLN

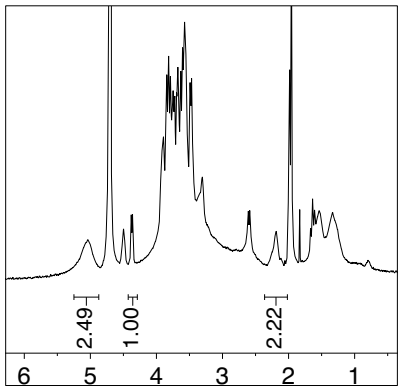

[1]H NMR Spectrum of the modified CD-C1-6'SLN

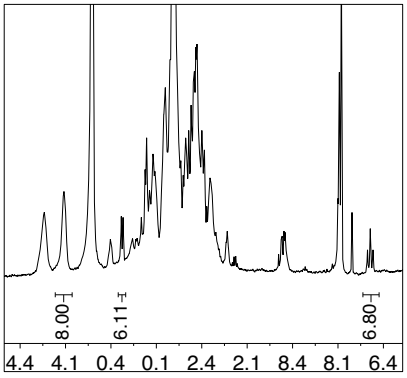

[1]H NMR Spectrum of the modified CD-C15-6'SLN

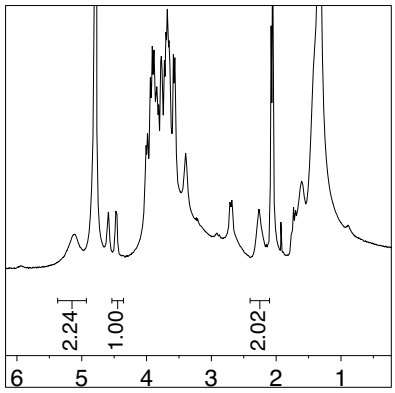

Özgün Kocabiyik

Rue beau séjour 8E 1003 Lausanne Switzerland
+41 76 792 88 65
okocabi@gmail.com

Education

Ecole Polytechnique Fédérale de Lausanne, Switzerland
Phd in Materials Science and Engineering (january 2014- december 2018)
M.Sc. in Materials Science and Egineering (september 2011- july 2013)

Sabanci University, Istanbul, Turkey
B.Sc. in Materials Science and Engineering (september 2005- June 2011)
Minor degree in chemistry

Research Experience

Phd Thesis: Virucidal nanomaterials against influenza
The goal of my project was to synthesize nanomaterials that irreversibly inhibit influenza virus (virucidal inhibition mechanism) while being non-toxic to cells. I synthesized nanomaterials (based on cyclodextrin or gold scaffolds) that target influenza virus and conducted antiviral assays. Cyclodextrin based materials are currently at the in-vivo stage
Supervisor: Prof. Francesco Stellacci

Master Thesis (spring 2013): Polymer grafted Janus gold nanoparticles and their directed self-assembly
Synthesis of polymer grafted Janus gold nanoparticles and studying their self-assembly in different solvent systems
Supervisor: Prof. Francesco Stellacci

Research internship at Swiss Center for Electronics and Microtechnology (CSEM), Neuchatel, Switzerland (fall 2012)
Characterization of polymer nanocomposites with scanning electron microscopy
Supervisor: Dr. Massoud Dadras

Master Semester Project II (spring 2012): Polymer brush modified membranes as glucose responsive systems
Synthesis of polymer brush modified membranes and conducting glucose flux measurements
Supervisor: Dr. Caroline Sugnaux/ Prof. Harm-Anton Klok

Master Semester Project I (fall 2011): Predicting the size related toxicity of metal-oxide nanoparticles
Establishing a theoretical framework to predict the relation between nanoparticle size and toxicity
Supervisor: Prof. Heinrich Hofmann

Summary of Skills

Chemistry Lab Skills:
- Synthesis and purification of glycosides
- Chemical modification of cyclodextrins
- Inorganic nanoparticle synthesis
- Polymerization reactions with atom transfer radical polymerization (ATRP)

Biological Lab Skills:
- Experience with several cell-lines such as MDCK, Vero, MA-104, A549, HEL 92.1.7
- Cell-based antiviral assays against Influenza, rotavirus, herpes simplex virus-2 (HSV-2), adenovirus 37
- Wild-type virus production and purification
- Immunoassays such as ELISA and immunocytochemical assay
- Cell viability assays

Characterization Instruments:
Nuclear magnetic resonance spectroscopy (NMR), Transmission electron microscopy (TEM), scanning electron microscopy (SEM), dynamic light scattering (DLS), ultraviolet-visible spectrescopy (UV-Vis)

Softwares
GraphPad Prism, ChemDraw, PyMol, OriginLab, Adobe Illustrator, MS Office Applications

Languages
English (fluent), French (intermediate), Turkish (native)

Teaching Experience

Teaching assistant in the **trigonometry course** for the first year students (spring 2017)
Assisting students with homework and concepts, exam grading

Master student supervisor for the master thesis titled "Self-assembly behaviour of polymer grafted mixed ligand gold nanoparticles" (spring 2016)

Teaching assistant for the course **surfaces and interfaces** (fall 2015)
Exercise preparation, assisting students with homework and concepts, exam grading

Presentations

O. Kocabiyik, V. Cagno, C. Tapparel, R. Le Goffic, F. Stellacci "Virucidal Nanomaterials Against Influenza", **Gordon Research Conference** "**Physical Virology",** January 2019, Ventura, CA, USA. **Poster Presentation.**

O. Kocabiyik, V. Cagno, C. Tapparel, F. Stellacci, "Antiviral Nanomaterials Against Influenza", **Bioinnovation Day**, november 2018, Geneva, Switzerland. **Pitch Talk**.

O. Kocabiyik, V. Cagno, C. Tapparel, F. Stellacci, "Virucidal Nanomaterials Against Influenza", Beilstein Symposium on Nanomedicine, september 2018, Rüdesheim, Germany. **Poster Presentation.**

O. Kocabiyik, J. Reguera, F. Stellacci, "Pickering emulsions stabilized by polymer grafted Janus nanoparticles", **Gordon Research Conference** "**Noble Metal Nanoparticles"**, June 2015, South Hadley, MA, USA. **Poster Presentation**.

Patents

O. Kocabiyik, F. Stellacci, V. Cagno, C. Tapparel, "**Virucidal Nanoparticles and Use Thereof Against Influenza Virus**", EP18192559.5, Patent Application was field on 04.09.2018.

**Ce document a été imprimé au Centre d'impression EPFL,
imprimerie climatiquement neutre, certifiée myClimate.**